IMPROVED DELIVERY OF PORPHYRIN DERIVATIVES TO IDENTIFIED TARGETS

by

FRANK NINGJUN JIANG

M.D. Nanjing Medical College, China, 1982

A THESIS SUBMITTED IN PARTIAL FULFILMENT OF

THE REQUIREMENTS FOR THE DEGREE OF

DOCTOR OF PHILOSOPHY

IN

THE FACULTY OF GRADUATE STUDIES

DEPARTMENT OF MICROBIOLOGY

We accept this thesis as conforming to the required stand

The University of British Columbia

April, 1992

In presenting this thesis in partial fulfilment of the requirements for an advanced degree at the University of British Columbia, I agree that the Library shall make it freely available for reference and study. I further agree that permission for extensive copying of this thesis for scholarly purposes may be granted by the head of my department or by his or her representatives. It is understood that copying or publication of this thesis for financial gain shall not be allowed without my written permission.

(Signature) _____

Department of Microbiology

The University of British Columbia
Vancouver, Canada

Date May 28, 1992

Abstract

The thesis is in three parts. Initially, work centred on the development of conjugation technology for covalently binding the photosensitizer (PS) benzoporphyrin derivative monoacid ring A (BPD) to monoclonal antibodies (MoAbs) using a water soluble carrier molecule, modified polyvinyl alcohol (M-PVA). This conjugation procedure has been shown to be reliable and reproducible and result in negligible loss of biological activity of both MoAb and PS.

The second part of the thesis was focused on determining the specificity and selectivity of the MoAb-PS conjugate in an in vitro system. The 5E8 MoAb, specific for human squamous cell lung cancer (A549), was used in this study. Extensive studies in which the 5E8-M-PVA-BPD conjugate was tested and compared with an irrelevant control conjugate - T48-M-PVA-BPD under a variety of experimental conditions established that the 5E8 conjugate had specificity in terms of binding to A549 cells, and had significantly ($p < 0.01$) greater efficacy in photodynamic killing in cytotoxicity assays. Further experiments were carried out to determine whether internalization of the BPD enhanced photodynamic killing. The results showed that internalized conjugate had much higher cytotoxicity than did surface associated. This was shown using two different model systems - 5E8 and the C7 antibody which has specificity for human low density lipoprotein (LDL) receptors.

The final part of the thesis was involved in determining the fate of MoAb-PS conjugates

in vivo. Studies were carried out in A549 tumor bearing nude mice comparing the biodistribution of 5E8-M-PVA-BPD and T48-M-PVA-BPD. Both conjugates had biodistribution characteristics which distinguished them from free BPD in that they remained in the circulation and most tissues for significantly ($p < 0.01$) longer times than did free BPD. With the exception of the 5E8-M-PVA-BPD conjugate and A549 tumor tissue, levels in all tissues were highest at the 3 h time point following injection of conjugates. In the case of the A549 tumor and the 5E8-M-PVA-BPD conjugate, the highest concentration of BPD was observed between 14 and 24 h following injection. Since the conjugates tested behaved differently from free BPD it was presumed that the material did not dissociate in vivo and that the specific conjugate demonstrated specificity for the A549 tumor in terms of the kinetics of its accumulation in tumor tissue.

Table of Contents

PAGE

PAGE

PAGE

List of Tables

List of Figures

PAGE

PAGE

PAGE

PAGE

PAGE

List of Abbreviations

BPD	-	benzoporphyrin derivative monoacid ring A
CPM	-	counts per minute
DME	-	Dulbecco's minimum medium
DMF	-	dimethyl formamide
DMSO	-	dimethylsulfoxide
EDCI	-	1-ethyl-3-(3-dimethylaminopropyl)-carbodiimide
ELISA	-	enzyme-linked immunosorbent assay
FCS	-	fetal calf serum
FMP	-	2,2-fluoro-1-methylpyridinium toluene-4-sulfonate
HCG	-	human chorionicgonadotropic hormone
HpD	-	hematoporphyrin derivative
HPLC	-	high performance liquid chromatography
i.v.	-	intravenous
J	-	Joule(s)
kD	-	kilodalton
LDL	-	low density lipoprotein
LPDS	-	lipoprotein deficiency serum
μl	-	microliter
μM	-	micromolar
M-PVA	-	modified polyvinyl alcohol

M	-	molar
MW	-	molecular weight
MEM	-	minimum essential medium
MoAb	-	monoclonal antibody
MTT	-	tetrazolium salt
3-MPA	-	3-mercaptopropionic acid
ηg	-	nanogram
PBS	-	phosphate buffered saline
PGA	-	polyglutamic acid
PDT	-	photodynamic therapy
PS	-	photosensitizer(s)
PEG	-	polyethylene glycol
PDT	-	photodynamic therapy
s.c.	-	subcutaneous
SDS-PAGE	-	sodium dodecyl sulphate-polyacrylamide gel electrophoresis
SMBS	-	sulfo-M-maleimidobenzoyl-N-hydroxysulfosuccinimide ester
TLC	-	thin layer chromatography

Acknowledgements

I am indebted to a great many people for making this project possible and making my stay at UBC so enjoyable and exciting.

I sincerely acknowledge my supervisor Dr. Julia G. Levy for her valuable instruction, support and kind guidance. My sincere thanks also go to Drs. Kilburn, Lentle and Warren for serving on my committee and their advice throughout the course of this work. In addition, I wish to thank Dr. Anna Richter for her advice and experimental assistance. The advice of Dr. John Hobbs is also gratefully acknowledged.

I wish to acknowledge my appreciation of my fellow labmates at Quadra Logic Technologies for their friendship, assistance and in some cases, forbearance. Specifically, I would like to acknowledge Dr. Shiyi Jiang (now at Shanghai Medical University, China) for conjugation work, Herma Neyndorff for in vitro studies, Liz Waterfield and Clair Smits for in vivo studies. I also gratefully acknowledge Gail Rothery and Ruth Burr for their technical assistance in the preparation of this thesis.

I dedicate this Ph.D. thesis to Professor Alan E. Freeland at the University of Mississippi Medical Center, whose professional expertise and bearing have been a great inspiration and a model for me.

CHAPTER I. INTRODUCTION

A. Photodynamic Therapy Background

1. Historical Review

The concept of photodynamic therapy (PDT) for the treatment of patients with malignant tumors dates from 1903, when Jesionek and Tappeiner used eosin and sunlight to treat tumors. In their approach, a 5% aqueous solution of the photosensitizing dye eosin was applied to skin tumors, and the tumor area was exposed to sunlight or radiation from an arc lamp (1). Several years later, Hausmann used hematoporphyrin (Hp) to study PDT, both in vitro and in vivo (2). In 1942, it was observed that injected hematoporphyrin (Hp) accumulated in implanted carcinomas and sarcomas in rats. Subsequent exposure of the porphyrin-saturated tumors to radiation from a quartz lamp caused tumor necrosis (3). During the 20 years that followed, the interest in Hp for clinical treatment continued. In 1961, Lipson introduced the use of hematoporphyrin derivative (HpD) for the fluorescence detection and localization of tumors (4). HpD is a complex mixture of porphyrins produced by the alkaline hydrolysis of acetylated Hp. Later, Lipson used HpD-sensitized photodynamic therapy to treat one case of recurrent breast cancer in a patient (5). In 1975, Dougherty et al. demonstrated the long term photodynamic cure of implanted tumors in mice and rats using red light in conjunction with HpD as the sensitizer (6). Dougherty's group then initiated full-scale clinical studies of tumor

photodynamic therapy using HpD as the sensitizer (7-9). Since then, basic research on, and clinical applications of, the photodynamic approach to tumor treatment has expanded enormously, as is documented in many books and reviews (10-31).

2. Photosensitizers and the Mechanism of Photodynamic Activity

Photosensitizers:

Photodynamic therapy, an experimental cancer treatment modality, involves the administration of a drug from a group of chemicals called photosensitizers (PS) followed by light activation. Although there are a variety of PS, some properties are common to all of them. One of these properties is that, when subjected to light of a characteristic wavelength, the PS will be converted to a high energy triplet state. The triplet state molecule is capable of giving up its energy to molecular oxygen, converting it to a high energy singlet oxygen. In biological systems, this singlet oxygen may then participate in a number of "photodynamic" reactions resulting in the damage of certain cell organelles and eventual cell death. Another property of the PS is that when injected intravenously into the patients with cancer the PS has a tendency to accumulate somewhat selectively in malignant tissue. Therefore, the basis of photodynamic therapy for the cancers is to inject the PS intravenously, allow the PS to circulate in the body for a certain period of time following which the tumor area is exposed to light of a specific wavelength. When the PS is activated by light, it reacts with moleclular oxygen to produce singlet oxygen

which destroys the tumor. The photosensitizer that has generated the greatest interest is hematoporphyrin derivative (HpD). HpD is a synthetic derivative of heme (4, 5, 32) and it has several attractive properties: tumor localization, low toxicity, photodynamic activity and absorption in the red spectrum. In recent years, a more purified version of HpD, known commercially as Photofrin® (33), has been used. Photofrin® is a mixture of Hp oligomers linked by ether bonds and ester bonds. It has enhanced photodynamic cytotoxicity with reduced side effects. It is currently in phase III clinical trials for human PDT studies (34). However, the search for new and better photosensitizers continues (35). Among those new photosensitizers are included, porphyrins and their derivatives (36, 37), modified or expanded porphyrins (38, 39, 40), phthalocyanines (41, 42), purpurins and verdins (43, 44), benzoporphyrin derivative (BPD 46-47), chlorins and their derivatives (48, 49), bacteriochlorophyllin-a and its derivatives (50) and cationic dyes (51). BPD has gained most of the attention. BPD has a number of properties which make it an improved drug over Photofrin®. BPD is a clearly defined and characterizable compound. It is a potent generator of singlet oxygen and has a favourable biodistribution in terms of the accumulation in malignant tissues (52-54). It has also been shown that it is an effective agent for the treatment of tumors in experimental animals (51) and more recently in humans. The optical properties of BPD are a dramatic improvement over Photofrin® since the strong absorption of the band in the red region of the spectrum (688 nm) allows for greater depth of penetration of light and of more effective use of the deeper penetrating photons. This compound is now approved by the FDA for phase I clinical trials. Overall, the ideal properties for the next generation of clinical

photosensitizers include: 1) chemical purity; 2) minimal dark toxicity; 3) significant absorption at wavelengths above 650 nm; 4) high quantum yields for the generation of photochemical reaction; 5) preferential tumor localization; and 6) rapid clearance from normal tissues (56).

Mechanism:

Photosensitizers can interact with visible light by both Type I and Type II photochemical pathways (57). The initial step involves the absorption of light by the PS with the subsequent conversion of the PS to an electronically excited state. The first excited state is normally a singlet state which has an extremely short half-life. Therefore it either decays back to the ground state or undergoes a spin conversion to the more stable and longer lived triplet excited state. PS can undergo Type I and/or Type II photochemical reactions upon reaching excited triplet states. In Type I, the PS interacts directly with the substrate with a resulting hydrogen atom or electron transfer to produce radicals. These radicals can subsequently react with oxygen to produce oxidized products. The sorts of substrates that react in the Type I reaction are those that are electron rich or have easily abstractable hydrogens (58). In Type II, the triplet sensitizer interacts by energy transfer with ground state oxygen to give ground state sensitizer and an electronically excited singlet state of oxygen. Lifetime of singlet oxygen varies from 10^{-6} s in aqueous environments to 10^{-4} to 10^{-5} s in hydrophobic environments (59). The electrophilic nature of singlet oxygen makes it very efficient at producing oxidized forms of biomolecules and this is thought to initiate most damage induced by PDT. The major biological targets for

singlet oxygen are now well known (24, 60). Membranes are peroxidized, leading to fragility and easy lysis. Nucleic acids are also an important target for photooxidation; guanine is the major target of this reaction since the guanine ring is oxidized. Many proteins and enzymes are damaged by photooxidation; the major targets are histidine, methionine, tryptophan.

3. Light Sources

A number of light sources can be used in PDT (61, 62). There are three main requirements for the light sources used for PDT: 1) wavelength which matches the activation spectrum of the PS; 2) sufficient power and density to deliver a tumoricidal light dose in an acceptable time; and 3) a means of directing the light energy to the tumor site with a spatial distribution which matches the size and shape of the tumor. Most pre-clinical and clinical PDT studies utilize laser systems for the generation of photoactivating light combined with microlenses and fiberoptics for tumor detection. An argon-pumped dye laser is the system most often used in PDT (63).

4. Current Status of PDT

Since 1976, more than 3000 patients with a variety of cancers have been treated with PDT (64, 65). Initially, patients with metastatic or recurrent disease were treated with PDT. The results were mixed. The tendency now is to treat superficial (so that light can

penetrate) and earlier stages of primary cancers. Among cancers treated, bladder and lung data appeared most encouraging. In bladder cancers, PDT not only offers patients an alternative to the traditional cystectomy in patients with carcinoma in situ or noninvasive, recurrent papillary disease, but also avoids impotence and the requirement for wearing urostomy pouches (66). The possibility that patients with bladder cancer receiving PDT may develop an immune response to their tumors is currently under investigation (67). In lung cancer, 5-year disease-free survivals have recently been reported for patients treated with PDT alone for early stage, squamous cell lung carcinoma (68). The advances in the development of better drugs and better devices (diode lasers as opposed to argon pumped dye lasers) are considerable and both the drugs and the devices are expected to be available in the near future. Although PS molecules accumulate somewhat selectively in tumor tissue, it is possible that increased selectivity might be obtained by using specific targeting agents linked to PS. The concept of MoAb conjugation to a PS has intellectual appeal because it may allow selective delivery of an efficient but poorly localizing PS to a target tissue. Precise chemistry for MoAb-PS conjugation and in vitro and in vivo analysis of the conjugate of this nature is currently under extensive investigation (69-85).

B. Monoclonal Antibody Mediated Drug Delivery System

1. Therapeutic Targeting

The idea of using antibody with specificity for tumor antigens was conceptualized by Paul Ehrlich at the turn of the century (86). Since that time, many investigators have done extensive work in immunochemistry and radioimmunoassays. With the advent of monoclonal antibodies (87), many investigators have produced "magic bullets" which can be used as tailor-made homing devices for either the localization or the treatment of tumor by conjugating either radionuclides or cytotoxic agents to the appropriate MoAb (88, 89). The obvious advantage of using MoAb as a vector for tumor localization of a drug is attributable to the property of the MoAb to bind specifically to a marker which is more abundant in tumor cells than in normal tissues. MoAb-drug conjugates of this nature continue to be examined extensively (90, 91). Usually, to produce effective immunoconjugates, the following requirements should be considered: 1) the immunoconjugates should be specific and should not react with normal tissues; 2) the linkage of the drug (e.g. toxin) to antibody should not impair the capacity of the antibody to bind antigen; 3) internalized MoAb is a better carrier than noninternalized Ab; 4) the active component of the drug must translocate into the cytoplasm or be at the cell membrane; and 5) for in vivo therapy, the linkage must be sufficiently stable to remain intact while the immunotoxin passes through the tissue of the patient to its cellular site of action.

2. Photoimmunotherapy

About ten years ago, this laboratory first started to investigate a novel anti-cancer treatment - "photoimmunotherapy". In this approach, the photosensitizer Hp, was directly attached to an anti-tumor monoclonal antibody using carbodiimide coupling. The potential advantage of this approach, compared to therapy with MoAb alone or with MoAb coupled to radioisotopes, drugs, or toxins, was thought to be double selectivity. The first level of selectivity is due to the specificity provided by MoAb, while a second level of selectivity comes from the fact that toxicity occurs only at or near the sites that are exposed to light. Conventional immunotoxins carry inherent problems of liver toxicity since conjugates tend to accumulate in that organ. Some immunotoxins are only effective if the complex is internalized into the targeted cell. Additional advantage of the MoAb-PS mediated photoimmunotherapy over conventional MoAb therapy is that the internalization of the MoAb is not a prerequisite for toxicity since active cytotoxic species can act effectively, though they may not be as effective as internalized PS, at the cell membrane level. In 1983, Mew et al. from this laboratory reported the use of MoAb-hematoporphyrin conjugates as anti-cancer agents in vitro and in vivo. In that report, the Ab used was directed against a tumor specific antigen on the DBA/2J rhabdmyosarcoma M-1 (69). Under the experimental conditions used, the antibody-PS conjugate demonstrated high anti-tumor activity without any visible side effects. Controls showed no effect on tumor growth. This early study indicated that 1) MoAb-PS conjugates might have a better anti-cancer effect than drug or MoAb alone, and that 2) the "magic bullet"

technique allowed the lowering of the minimum effective dose of PS required for anti-cancer activity, hence minimizing possible adverse side effects. On the basis of this initial study, it was further showed that conjugates of this nature were also effective in vitro in selectively destroying leukemia cells (70). Furthermore, it was found that another MoAb-PS conjugate was capable of selectively destroying regulatory murine T cells in the circulation using a MoAb with specificity for T suppressor cells (73). Although we were able to show, in these early experiments, that it was possible to conjugate PS covalently to monoclonal antibodies while retaining the photosensitizing activity of the PS and the antigen-binding capacity of the MoAb, we recognized that the process of binding the PS directly to the MoAb was not optimal. Since the conjugation was random, inactivation of the MoAb was a common occurrence if high levels of loading were attempted. Further, PS have a tendency to bind naturally to hydrophobic regions of the MoAb which makes accurate quantification of loading extremely difficult. Because the principal objective in developing a linking technology is directed toward improved delivery of PS to targeted areas in vivo, for both diagnostic and therapeutic purposes, we developed an indirect approach in which high levels of PS loading could be achieved (80, 92). In this approach, we first made a polymer-PS conjugate and then attached it to the MoAb. The polymer used in the study was modified polyvinyl alcohol (M-PVA) and the PS was what promises to be the second generation of the photosensitizers used in humans for PDT, benzoporphyrin derivative (BPD, 52). The MoAb-M-PVA-BPD conjugate was first tested chemically and biologically and we were able to demonstrate that the activities of both BPD and MoAb were retained after the conjugation procedure (80). We then tested this

conjugate in a variety of in vitro experiments in which we showed that it caused a significantly ($p<0.01$) higher photodynamic killing of target cells in comparison to BPD alone or control antibody-BPD conjugate (81). We also showed that internalized MoAb-BPD conjugates caused greater killing of target cells than that of the controls (94). These promising in vitro studies have led us to the most recent in vivo studies in which we again demonstrated the improved delivery of the BPD to the identified target by a specific monoclonal antibody (83).

Several other investigators have also contributed much in this area since the initial report from this laboratory in 1983. Oseroff reported in 1986 (72) the use of a dextran polymer as a carrier. In that study, it was shown that up to 35 photosensitizer molecules (chlorin e_6) could be loaded via a carrier onto an anti-T-cell MoAb while retaining the MoAb binding activity and chlorin e_6 photosensitivity. It was also demonstrated that the conjugate could selectively destroy target T cells by irradiation of cells containing MoAb-PS conjugates bound to their cell surface. However, no proof of covalent bonding between MoAb and PS was provided in that report. In 1988, Hasan reported the preliminary results on using polyglutamic acid (PGA) as a carrier to link the chlorin and latter to attach it to MoAb to form a MoAb-PGA-Chlorin conjugate (94). Complete reports on the nature of this conjugate appeared later (74, 75). Recently, Hasan's group has conjugated chlorin to a MoAb with specificity for a human ovarian carcinoma antigen (84). In their studies, the investigators were able to demonstrate that the conjugate retained significant antigen binding specificity and affinity, and was effective in the

selective photochemical eradication of target cells. Several other investigators have also done similar work with success (77, 78, 95). However, only three published reports (96-98), in addition to an early report from this laboratory (69), described in vivo studies using a MoAb-PS conjugate. In one report (96), the conjugate showed a strong time-dependent localization after intraperitoneal injection in nude mice with subcutaneously implanted human tumors. Distinct cellular localization only appeared 72 h after injection. These observations seemed consistent with the preliminary studies in vivo form this laboratory (69). In the other two reports (97, 98), the peak accumulation of the specific conjugates in the tumor site occurred at 24 h. These results are similar to our recent study with 5E8-M-PVA-BPD conjugate in a tumor bearing nude mouse model (83) where we showed the highest tumor accumulation between 14 and 24 h.

3. Prospects of Photoimmunotherapy

Since the initial work in photoimmunotherapy carried out in this laboratory ten years ago, a large number of papers in this context have been published (69-85). The appealing features of this approach over other methods are:

1. Coupling of PS to MoAb should increase their specificity for the desired target and therefore reduce dose requirements and possible side effects.
2. The MoAb does not have to have intrinsic biologic effector activity, since it is used only as a delivery system.

3. In contrast to most drugs and toxins, the MoAb-PS need not to be internalized, because of the diffusion of singlet oxygen and membranes are a primary target of photodynamic action.
4. PS are small molecules and through a polymer carrier a large number (40 to 60) of them can be linked to MoAb without impairing antibody specificity.
5. Due to the dual selectivity of photoimmunotherapy, its side effects in vivo on normal organs should be minimal since only the area of interest would be exposed to light activation.

Although immunotoxins of various types may be highly efficient in vitro in specifically targeting tumor cells, the ability of such conjugates in vivo to locate and destroy or facilitate imaging of tumor cells represents requirements of much greater complexity. The potential problems associated with the approach are: 1) immunoconjugates concentrate, immediately after adminstration, in organs such as liver, lung and kidney due to the presence of FcR-containing cells, such as alveolar macrophages, dendritic cells, or Kupffer cells; 2) a variety of serum enzymes can degrade the conjugates; 3) vascular barriers may block the macromolecule from reaching the target; and 4) a host anti-MoAb response may neutralize their effectiveness, since the MoAb may be recognized as a foreign protein. In order to overcome these in vivo limitations, the following directions should be considered: 1) the conjugates should be formed via covalent bonds, wherever possible; 2) the levels of denatured or aggregated protein in the preparation should be kept to minimum; 3) the use of low dose external beam X-rays may increase the permeability of the tumor vasculature (99); 4) the use of human or humanized MoAbs may be less

immunogenic than murine products; and 5) to make individuals tolerant of subsequent injections of xenogenic proteins by a relatively simple procedure developed by Sehon and associates (100).

C. Scope of This Study

As described above, PS used in PDT have a tendency to accumulate preferentially in tumor cells, in comparison with many normal tissues. Biodistribution studies with a variety of PS including porphyrins, chlorins and phthalocynaines indicated similar properties for all these molecules. Ratios comparing tumor levels to normal surrounding tissue such as skin and muscle range, usually, between 4:1 and 1:1. While these values are certainly appropriate to effect selective tumor cell killing over normal tissue, using careful light dosimetry, the ability to enhance delivery of PS to the identified target is highly desirable. In this study, a reliable PS delivery system, monoclonal antibody mediated delivery, has been investigated. The work has been completed in several stages described in separate chapters in the thesis. As described in Chapter II, a basic technology was developed whereby a known number of PS molecules, such as benzoporphyrin derivative monoacid ring A (BPD), could be loaded onto a modified intermediate carrier polyvinyl alcohol (M-PVA). The resulting M-PVA-BPD conjugate was tested chemically and biologically. As described in Chapter III, the M-PVA-BPD was further attached to a model monoclonal antibody T48 which reacts specifically with HCG (human choriogonadotropic hormone), using a heterobifunctional reagent (SMBS). The binding between BPD and MoAb was examined. The biological activity of both BPD and MoAb was also tested. Chapter IV describes the conjugation of M-PVA-BPD to the MoAb 5E8 which is specific for human squamous cell carcinoma of the lung. The efficacy of 5E8-M-PVA-BPD in killing A549 cells (positive line for the 5E8 antibody) was determined and

compared to control conjugates and free BPD. Chapter V describes the results of tests determining the effectiveness of surface associated and internalized MoAb-BPD conjugates in photodynamic killing. Two monoclonal antibodies, 5E8 and C7, were used. C7 reacts specifically with human low density lipoprotein (LDL) receptors. Both MoAbs are internalized by target cells at 37°C. The internalization is inhibited at 4°C. Therefore the determination of surface associated vs internalized conjugates could be easily carried out at different temperatures. Chapter VI describes the in vivo studies using MoAb-BPD conjugates. ^{14}C-BPD was linked to MoAbs 5E8 and T48 at a ratio of 50-70:1 (BPD:Ab). Biodistribution of 5E8-M-PVA-BPD in A549 tumor bearing nude mice was determined and compared to that of control conjugates and free BPD. The radioactivity in both normal tissues and tumor was determined at 3, 14, 24 and 48 h after intravenous injection of individual conjugates or free BPD. The tumor accumulation of BPD delivered either in a free form or conjugated to specific or non-specific antibodies was calculated and compared to that of normal tissues.

CHAPTER II. SELECTION AND CHARACTERIZATION OF A CARRIER SYSTEM

Introduction

Benzoporphyrin derivative monoacid ring A (BPD) is a chemically pure porphyrin which has been shown to be a potent photosensitizer in vitro and to have maximum absorbance at 688 nm (52-54). BPD, like many other experimental PS is only poorly soluble in neutral aqueous solutions. It demonstrates better tumor accumulation than Photofrin® which is in phase III clinical trials. However, the selectivity of BPD for the tumor site is not optimal. It is also retained in normal tissues such as skin. The objective of the research reported in this chapter was two fold: first, to enhance the solubility of BPD by linking it to a highly hydrophilic molecule, and second, to develop soluble porphyrin conjugates which could subsequently be linked to monoclonal antibodies to provide enhanced delivery to tumor cells. The carrier molecule with which we have worked was polyvinyl alcohol (PVA). The choice of this molecule was based on the fact that it is relatively easily modified, is easily conjugated to porphyrins, and imparts hydrophilic properties to any subsequent conjugation. In the present study, PVA was reacted with 1,6 hexanediamine in such a way that 30% of its hydroxyl groups (-OH) were replaced by free amino groups ($-NH_2$). This modified PVA (M-PVA) was then conjugated with BPD at different ratios. The subsequent M-PVA-BPD conjugates were extensively tested. The results showed that PVA was covalently bound to BPD and that the chemical linking procedure did not interfere with the PS activity.

Materials and Methods

Chemicals

Polyvinyl alcohol, (PVA, 88% hydrolysed, M.W. 10,000), 2-fluoro-1-methylpyridinium toluene-4-sulfonate (FMP), and dimethyl sulfoxide (DMSO) were all purchased from Aldrich Chemical Co. (Milwaukee, Wis). 1,6-Hexanediamine (98.5%) and sodium borohydride were purchased from BDH Inc. (Vancouver, BC), triethylamine was purchased from Eastman Kodak Co. (Rochester, NY), and 1-ethyl-3-(dimethylaminopropyl) carbodiimide (EDCI) from Sigma Chemical Co. (St. Louis, MO). The BPD was synthesized and purified in Dr. David Dolphin's laboratory, Chemistry Department, University of British Columbia as described elsewhere (101).

Cell Lines and Media

The A549 cell line (obtained from American Type Culture Collection, Rockville, MD), derived from a human squamous cell carcinoma, was maintained in Minimum Essential Medium (Eagle) with Earle's salts, nonessential amino acid and L-glutamine (Terry Fox Laboratory, Vancouver, BC), supplemented with 10% fetal calf serum (FCS, Sigma Chemical Co.). The cells were harvested by trypsinization with 10% trypsin and vigorous shaking. P815 tumor cells (mastocytoma from DBA/2 mice) were cultured in Dulbecco's minimum essential media (DME) supplemented with high glucose, L-glutamine (Terry

Fox Laboratory) and 10% FCS. This tumor cell line has been carried for many years in this laboratory.

Photosensitizer

The photosensitizer BPD was used in this study. This compound has been described in detail elsewhere (52-54, 101). Its structure is shown in Fig. 1. The material used is comprised of two regioisomers in which the monoacid carboxyl group is at either position C or D of the porphyrin ring. This form of BPD was chosen because it has a single reactive group (the COOH on ring C or D) which therefore permits a level of control during conjugation reactions. It has been shown to be a potent photosensitizer, both in vitro and in vivo with a strong absorbance at 688 nm.

Analytical Thin Layer Chromatography (TLC)

Aluminum backed silica plates (0.2 mm silica gel 60 F-254 nm, E. Merck, NJ) were used throughout. Ultra-violet (UV) absorbing species were observed as areas of quenched fluorescence under a UV light. Iodine vapor was used for temporary visualization. Permanent coloration or charring was obtained by heating on a hot plate after spraying (using atomizer) with aqueous ammonium molybdate (75 g ammonium molybdate, 100 ml of conc. H_2SO_4, 900 ml of H_2O).

Preparation of Buffers

A. Acetate buffer (pH 4.21): 3.7 ml of 0.2 M acetic acid solution and 1.3 ml of 0.2 M sodium acetate solution were diluted to a total volume of 100 ml.

B. Phosphate buffer (pH 7.26): 2.8 ml of 0.2 M NaH_2PO_4 solution and 7.2 ml of 0.2 M Na_2HPO_4 solution were diluted to a total volume of 200 ml.

C. Borate buffer (pH 8.42): 5 ml of 0.2 M H_3BO_3 solution and 1.2 ml of 0.05 M NaB_4O_7 solution were diluted to a total volume of 200 ml.

Preparation of Modified PVA

The procedure described here was a modification of Ngo's method for activation of hydrogels (102). A FMP-triethylamine complex was formed by adding 0.5 ml of triethylamine to 1.416 grams (5 mmole, M.W. 283.3) of FMP, and stirring until the FMP was totally dissolved. A minimal amount of DMSO was used to dissolve 500 mg of PVA (M.W. 10,000). The PVA solution was transferred to the reaction flask containing the FMP-triethylamine complex, and the resulting mixture was stirred for another 4 hours at ambient temperature. To the PVA-FMP intermediate, 2.9 grams (M.W. 116.21) of 1,6-hexanediamine was added, and the mixture was stirred overnight. Sodium borohydride (942 mg) was added to the crude product and the mixture was stirred for one hour. The final product was dialysed (M.W. cut off: 6000-8000) against distilled water (4 changes).

Elemental Analysis of Modified PVA

The M-PVA was lyophilized and sent for elemental analysis (Department of Chemistry, University of British Columbia, Vancouver, BC).

Conjugation of Modified PVA to BPD

BPD, 21 mg (26.8 μmole, M.W. 784) and 50 mg (260.8 μmole, M.W. 191.7) of 1-ethyl-3(dimethylaminopropyl) carbodiimide (EDCI) were mixed together in 10.5 ml of anhydrous DMSO, and stirred for 30 min at room temperature under argon. The resulting mixture was divided into 5 portions: 0.5, 1, 2, 3 and 4 ml. To each portion, 1 mg of modified PVA in 1 ml of anhydrous DMSO was added and the mixtures were stirred for 24 h at room temperature under argon. The reactions were monitored by TLC using a solvent system ethylacetate:ethanol:water (2:1:1, v:v:v) and quenched with 2 ml of distilled water at 4°C. After development, the conjugates formed one spot with a R_f value of 0.57. Free BPD moved to solvent front. The concentration of BPD in the M-PVA-BPD conjugates was analyzed spectrophotometrically, and the molar ratios estimated to be 100:1, 75:1, 50:1, 25:1 and 12:1, BPD to M-PVA. All the reactions and handling were performed in a room with low levels of light. The final solutions were lyophilized. The reaction yields were > 95%. The final products were stored over Drierite at 4°C in the dark. The reaction is shown in Fig. 2. The R_f values of M-PVA-BPD are shown in Table I. The molecular weight of the conjugate was estimated to be approximately 30 kD.

HPLC Analysis of M-PVA-BPD Conjugate

Carrier conjugates were analyzed by HPLC. The HPLC system used was as follows: column: ultrasphere 5 μm ODS, 250 × 4.6 mm; solvent system: solution A: 1% $(NH_4)_2SO_4$ 500 ml, CH_3CN 500 ml and CH_3COOH 50 ml, pH 3.0; solution B: 1% $(NH_4)_2SO_4$ 500 ml, C_4H_8O (THF) 500 ml and CH_3COOH (HAc) 50 ml; flow rate: 1.7 ml/min; column temperature: 30°C with pressure between 2600 and 3000 psi; gradient: A:B = 60%:40% for 5 min, then starting gradient flow from 40% B to 70% B in 20 min and staying at 70% B for 5 min, then returning to 40% B. This system resulted in elution of the M-PVA-BPD conjugate at 8-10 minutes whereas the unconjugated BPD isomers eluted at 17 and 19 minutes. The efficiency of the conjugation reaction between M-PVA and BPD was shown to be greater than 90% as determined by spectrophotometric and HPLC analysis. The reactants used and the resulting reactions are outlined in Fig. 2.

Stability Study on M-PVA-BPD

The conjugates (BPD:PVA 25:1) were dissolved in buffers of pH 4.21, 7.26 and 8.42. These solutions (0.064 mM) were stored at different temperatures such as -20°C, 4°C, 20°C and 37°C. The results of decomposition were observed through TLC analysis. The results (Table II) indicate that within four weeks, only BPD-M-PVA maintained in pH 8.42 buffer at 37°C showed some sign of degradation. After one month, all the materials began to show some deterioration, presumably due to hydrolysis of the PVA backbone. All experimental work was undertaken on conjugates which had not undergone hydrolytic

breakdown.

In vitro Cytotoxicity Assay

The adherent cell line, A549, in logarithmic growth was harvested with 10% trypsin and plated in 96-well plates at 10^5 cells/well. Following overnight incubation, BPD or M-PVA-BPD dissolved in medium containing 10% FCS was added to the wells at a range of concentrations (in triplicate). The time of exposure to drugs was 1 h following which the cells were washed with medium containing 5% FCS at 37°C. The washed cells, in 100 μl medium/well, were exposed to fluorescent light for 1 h (5.4 Joules/cm^2) and then returned to the CO_2 incubator. Eighteen hours later cell viability was determined using an MTT assay as described by Mosman (103). The MTT assay, in which a tetrazolium salt (3-(4,5-dimethylthiazol-2-yl)-2,5-diphenyl tetrazolium bromide; Sigma Chemical Co.) is used as a substrate for mitochondrial dehydrogenases, is a convenient colorimetric assay, which measures quantitatively the viability of cells by the production of blue formazan. This assay has been thoroughly tested in our laboratory and proved to correlate absolutely with standard clonogenic assays (104). It has been used in these studies for speed and convenience. The percentage of cells killed was calculated by relating the viability of cells exposed to drug and light to the viability of control cells exposed to light only. The light only controls were included on each plate. The LD_{50} doses of free and conjugated BPD in each cell line were determined.

The cytotoxicity assay in which the suspension-grown P815 cell line was tested has been

described elsewhere (52). Briefly, cells in logarithmic growth were incubated for 1 h at 37°C with a range of concentrations of either BPD alone or conjugated to M-PVA, in the absence of serum. Following incubation, the cells were washed, suspended in DME medium and exposed to fluorescent light for 1 h (5.4 J/cm^2). The cells were then incubated overnight in DME medium containing 5% FCS at 37°C. Survival of cells was assessed by the MTT assay 18 h after their irradiation.

The light source used in all experiments was a bank of 4 fluorescent tubes (General Electric F20T12- Cool White Delux) as described previously (104). The dose of light delivered during 1 h exposure was 5.4 J/cm^2. Except during irradiation, the photosensitizers in solution and in contact with the cells were shielded from light.

Results

The elemental analysis of the modified PVA (M-PVA) showed 6-10% of (nitrogen) N to be present, indicating the probable presence of free amino groups. The conjugation of BPD to the M-PVA did not alter its absorption spectrum and all peaks characteristic of BPD could be observed in the spectrum (Fig. 3). The absorption at 688 nm, which is the most characteristic peak for BPD, was therefore used as a measure of the concentration of BPD in M-PVA-BPD conjugates. For comparison between free and conjugated BPD, the concentrations of conjugates in the assays were adjusted according to their BPD content. An increased loading ratio (BPD to M-PVA) did not change the water solubility of the conjugate at values less than 75:1, beyond which there was a loss of solubility in aqueous solutions.

Preliminary studies of M-PVA-BPD using TLC showed that after conjugation M-PVA-BPD moved as one spot with a R_f value of 0.57 (Table I). Further analysis of the conjugate using reverse phase HPLC showed that 2 species were present as demonstrated by four peaks. The first two major peaks eluted at 8-10 minutes and the others at 17-19 minutes (Fig. 4; BPD consists two regiosiomers present in equal proportion). Since BPD alone is very hydrophobic, it is expected to be eluted later than M-PVA-BPD which is water soluble. The first two major peaks were assigned to the M-PVA-BPD conjugate and the other two major peaks to BPD alone. The HPLC elution property of BPD are well characterized and the peaks eluting at 17-19 minutes have been confirmed as the two

regioisomers of BPD.

The conjugates, in which the molar ratios of BPD to M-PVA varied (from 12:1 to 100:1), were tested at a range of concentrations assumed to provide a titration in the cytotoxicity assay in vitro, in the presence or absence of serum. The LD_{50} values for individual conjugates and for BPD alone were determined and compared. The results obtained using the A549 cell line, in the presence of 5% fetal calf serum, demonstrated similar photosensitizing efficacy between the conjugates and free BPD (Fig. 5). The LD_{50} doses were in the range of 100 to 180 ηg/ml.

In order to determine whether serum proteins had any effect on the targeting of free compared with conjugated BPD, cytotoxicity assays were carried out in serum-free medium. Photosensitizers were added to target cells in medium containing no serum. These cytotoxicity assays utilized the non-adherent murine cell line P815. As seen in Fig. 6, BPD and M-PVA-BPD tested in the absence of serum showed similar phototoxicity, although there was some indication that some of the conjugates might be more effective than free BPD under these conditions. The LD_{50} doses determined for P815 cells were in the range of 6 to 13 ηg/ml.

Discussion

The present work was undertaken to determine whether the photosensitizer BPD could be covalently linked to larger carrier molecules in a reliable and reproducible manner without measurable loss of photosensitizing activity. The reasons for undertaking this were two-fold as stated in the Introduction. The long term goal was to develop technology such that these carrier conjugates could subsequently be covalently linked to molecules such as monoclonal antibodies (MoAbs) to improve the specificity of PDT in applications such as bone marrow purging. Because direct binding of photosensitizers to MoAbs, while possible (69, 70, 73), is difficult to reproduce from batch to batch, it appeared to be advantageous to develop indirect procedures for conjugating large numbers of photosensitizers such as BPD to ligands of interest to render them both macromolecular and hydrophilic. The photosensitizing properties of these conjugates would, in themselves, be of biological interest. It has been possible to assess the biological properties of these conjugates in the context of their in vitro photosensitizing properties.

In preliminary experiments, the potential use of a variety of modified carriers was investigated. Polyvinyl alcohol is a large polymer available in a range of molecular weights. We chose a preparation with a median molecular weight in the region of 10 kD. This molecule is relatively easily modified and is highly hydrophilic. PVA has been studied extensively as a vehicle for drug delivery systems. It is capable of releasing

entrapped drugs in aqueous medium and is able to regulate the release of drugs by swelling (105, 106). The results presented here represent what we consider to be a promising system. The procedure reported here is easily reproducible and efficient. In addition, the conjugate (M-PVA-BPD) remained readily water-soluble even when molar ratios of BPD:M-PVA reached 75:1. A reverse phase HPLC analysis eluted the conjugate into four major peaks. M-PVA-BPD and BPD alone possess different hydrophobicity. BPD is hydrophobic, and becomes hydrophilic when conjugated to water-soluble M-PVA. A reverse phase solvent system elutes the more hydrophilic compound, in this case M-PVA-BPD, first, and the more hydrophobic later. This analysis indicated most of the BPD was covalently bound to the M-PVA. Previous work in this laboratory on linking photosensitizers directly to MoAbs has been hampered not only by the intrinsic difficulties of maintaining the activities of both photosensitizer and MoAb during conjugation, but also by the loss of solubility of the conjugates in aqueous solution. Preliminary spectrophotometric analyses of photosensitizer conjugate M-PVA-BPD showed that the absorption properties of the photosensitizer had not been altered in any detectable manner. That these molecules had not undergone any changes in their photosensitizing properties was confirmed by their unaltered cytotoxic activity in vitro using two different assays and cell lines.

The results of the cytotoxicity assays in vitro showed convincingly that the M-PVA-BPD conjugates (containing BPD conjugated in different molar ratios to M-PVA) were at least as phototoxic as an equivalent number of free BPD molecules in the two test systems

used. The difference between the LD_{50} doses determined for adherent and for suspension-grown cell lines was due partly to the difference in cell sensitivity and partly to the differences between the assay systems (e.g. presence or absence of serum). This indicated that the photosensitizing properties of BPD in the conjugates were unaltered in either condition. We concluded that the accumulation of BPD molecules on a carrier molecule did not interfere with the activation of the photosensitizer by light, and that there was no substantial quenching of the excited state. It appeared that the uptake of conjugates by target cells was comparable to that of unconjugated molecules either in the presence or absence of serum. However, the localization properties of the conjugates on or within target cells have not yet been determined.

The M-PVA-BPD preparations at different ratios were tested for their cytotoxicity in vitro. No significant difference in photodynamic killing was observed. A reasonable ratio of PS to MoAb would be between 20 to 50, since too many PS (greater than 50) would probably increase the possibility of interfering with the antigen binding area of MoAbs and would also increase the molecular weight of the PS-MoAb complex which is not desirable for in vivo administration of the conjugate. However, if only a small number of PS is loaded onto MoAb via a carrier, too much Ab may be required to perform both in vitro and in vivo experiments. We therefore decided to use a preparation of 25:1 (BPD:M-PVA) for our in vitro tests.

In one recent study (107), the biodistribution of BPD and M-PVA-BPD were comparable.

In that study, the tumor system used was the P815 mastocytoma. Following administration of ^{3}H-labelled M-PVA-BPD, high levels of radioactivity were detected in kidney, liver, and spleen. These values were not significantly different from those observed with BPD alone. The only tissues in which concentrations of conjugate were markedly different from those of unconjugated materials were brain, skin and muscle. In each instance, the concentrations of conjugate in these tissues were lower than those of unconjugated drug, although only in brain was the concentration much less. This is probably attributable to blood-brain-barrier kinetics. It was somewhat surprising that the distribution of conjugated materials was so similar to that of BPD, considering the marked structural differences and differences in hydrophobicity between the two preparations.

In summary, we have shown that the conjugation of BPD to M-PVA as a carrier molecule does not reduce its photosensitizing efficiency. On the contrary, in some BPD to M-PVA ratios and under certain conditions, the conjugates were more efficient than free BPD. We have shown that the conjugation of BPD to M-PVA results in formation of a macromolecular photosensitizer, which is soluble in aqueous solutions, fully biologically active in vitro, and which distributes in vivo in a manner analogous to unconjugated BPD (this work was performed by Drs. Anna Richter, Noelle Davis and Ashok Jain). This technology, by which a macromolecular species can be constructed in which a combination of distinct molecules could be aligned within a single carrier, has the potential for increasing the selectivity and efficacy of photosensitizers used in photodynamic therapy.

Chapter Summary

Polyvinyl alcohol was modified with 1,6-hexanediamine to form a carrier molecule, modified polyvinyl alcohol (M-PVA), which contained free amino groups to which porphyrin molecules could be attached. Conjugation was carried out using carbodiimide as the condensing agent in order to form peptide bonds with the free carboxylic acid group present on the porphyrin ring. Benzoporphyrin derivative monoacid ring A (BPD), a chemically pure compound, was conjugated to the carrier molecule. The high efficiency of the coupling reaction permitted the production of a number of conjugates with varying ratios of BPD:M-PVA. The conjugates were readily soluble in aqueous solutions at BPD:M-PVA molar ratios of up to 75:1. In vitro phototoxicity tests utilizing one human and one murine cell lines, showed that the conjugates had phototoxicity equivalent to that of unconjugated BPD.

Table I. R_f values for M-PVA-BPD conjugates at different ratios.

	BPD:M-PVA	R_f	Solvent System
M-PVA-BPD	12.5:1	0.57	EtOAc:EtOH:H_2O 2:1:1 (v:v:v)
	25:1	0.57	
	50:1	0.57	
	75:1	0.57	

Table II. Stability test of M-PVA-BPD through TLC

(solvent system : EtOAc:EtOH:H_2O = 2:1:1; v:v:v)

A. R_f values of M-PVA-BPD in acetate buffer, pH 4.21

	Day 0	Day 1	Day 2	Day 3	Day 7	Day 14	Day21
-20 °C	0.58	0.55	0.59	0.61	0.70	0.76	0.82
4 °C	0.58	0.55	0.59	0.61	0.70	0.76	0.81
20 °C	0.58	0.55	0.59	0.59	0.68	0.76	0.82
37 °C	0.58	0.55	0.59	0.59	0.68	0.75	0.82

B. R_f values of M-PVA-BPD in PBS, pH 7.26

	Day 0	Day 1	Day 2	Day 3	Day 7	Day 14	Day21
-20°C	0.56	0.55	0.59	0.60	0.68	0.75	0.82
4 °C	0.56	0.55	0.59	0.59	0.68	0.75	0.82
20 °C	0.56	0.55	0.59	0.59	0.68	0.75	0.82
37 °C	0.56	0.55	0.59	0.60	0.70	0.75	1.0

C. R_f values of M-PVA-BPD in borate buffer, pH 8.42

	Day 0	Day 1	Day 2	Day 3	Day 7	Day 14	Day21
-20 °C	0.57	0.56	0.59	0.60	0.68	0.75	0.81
4 °C	0.57	0.56	0.60	0.60	0.68	0.75	0.81
20 °C	0.57	0.56	0.59	0.60	0.68	0.75	0.81
37 °C	0.57	0.56	0.59	0.59	0.68	0.75	1.0

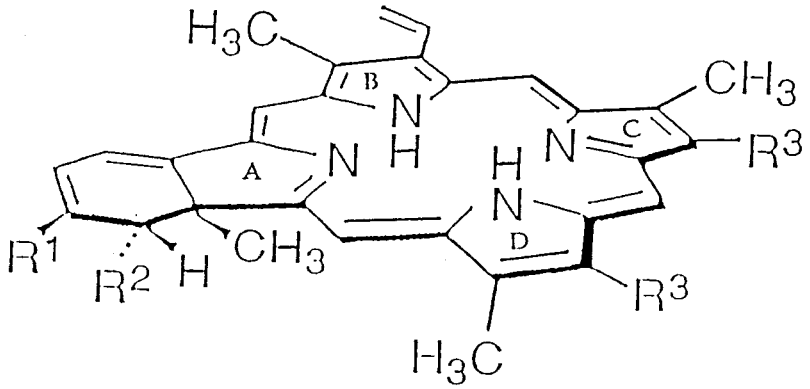

$R^1 = R^2 = CO_2Me$ $R^3 = (CH_2)_2CO_2Me$ or $(CH_2)_2CO_2H$

Figure 1. Structure of benzoporphyrin derivative monoacid ring A (BPD). A and B designate the porphyrin rings at which fusion occurs to yield the ring A, ring B isomers. There is a free carboxyl group (COOH) on either ring C or ring D. R^3 represents the hydrolytic site for formation of mono and diacid derivatives.

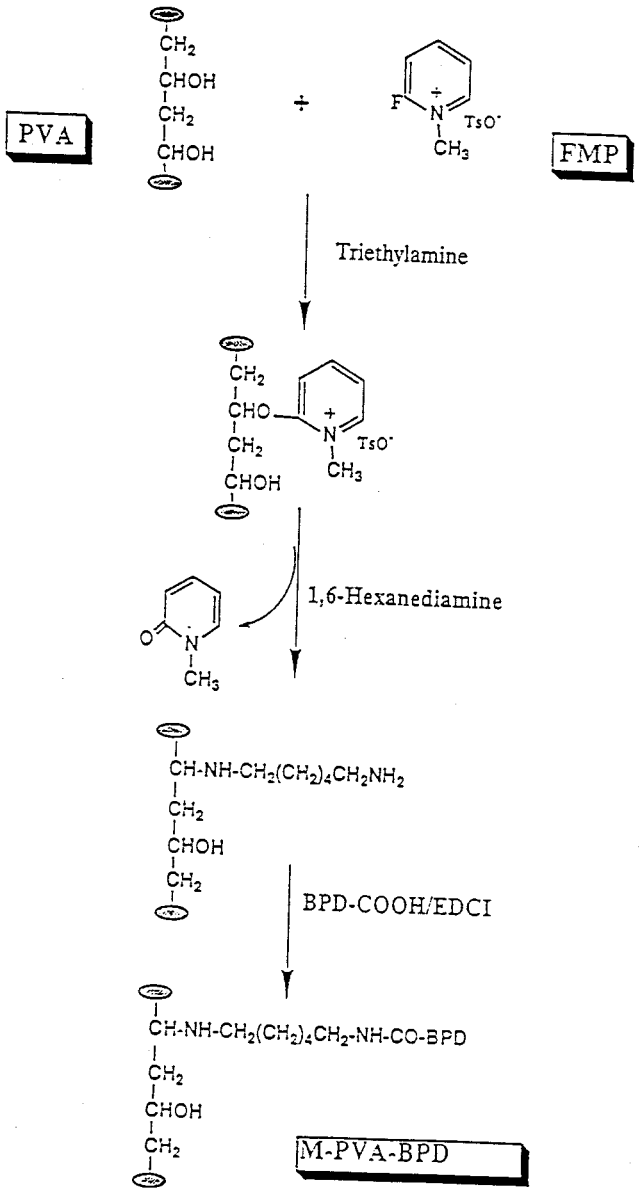

Figure 2. Scheme demonstrating the synthesis of hexanediamine modified PVA and its subsequent conjugation to BPD.

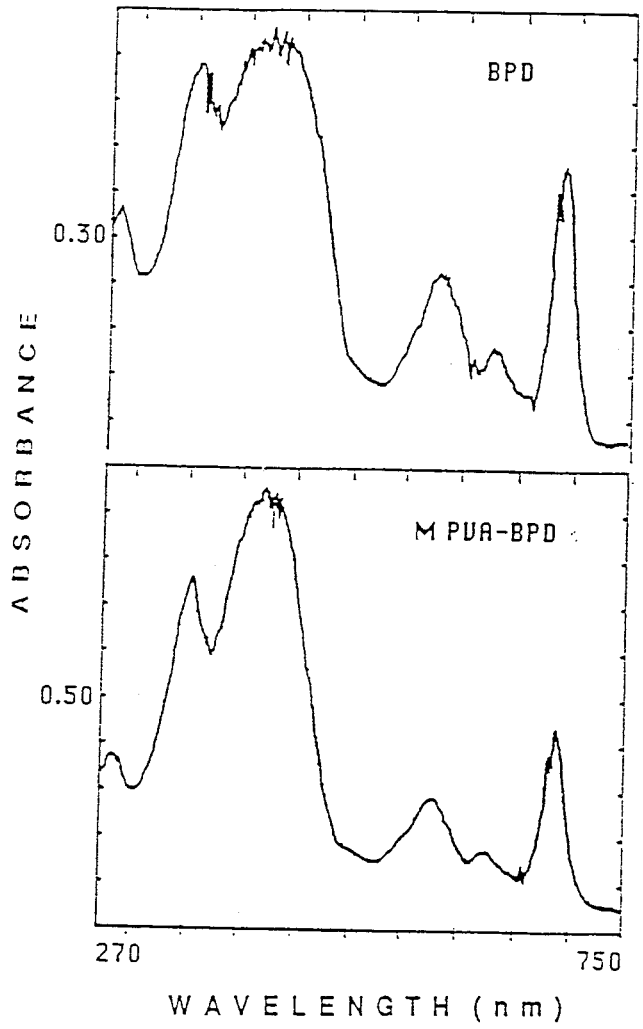

Figure 3. Absorption spectra of BPD and M-PVA-BPD between 270 and 750 nm in 50% ethanol. The concentration of BPD was 20 μg/ml whereas the concentration of the conjugate (calculated as μg BPD) was 17.3 μg/ml.

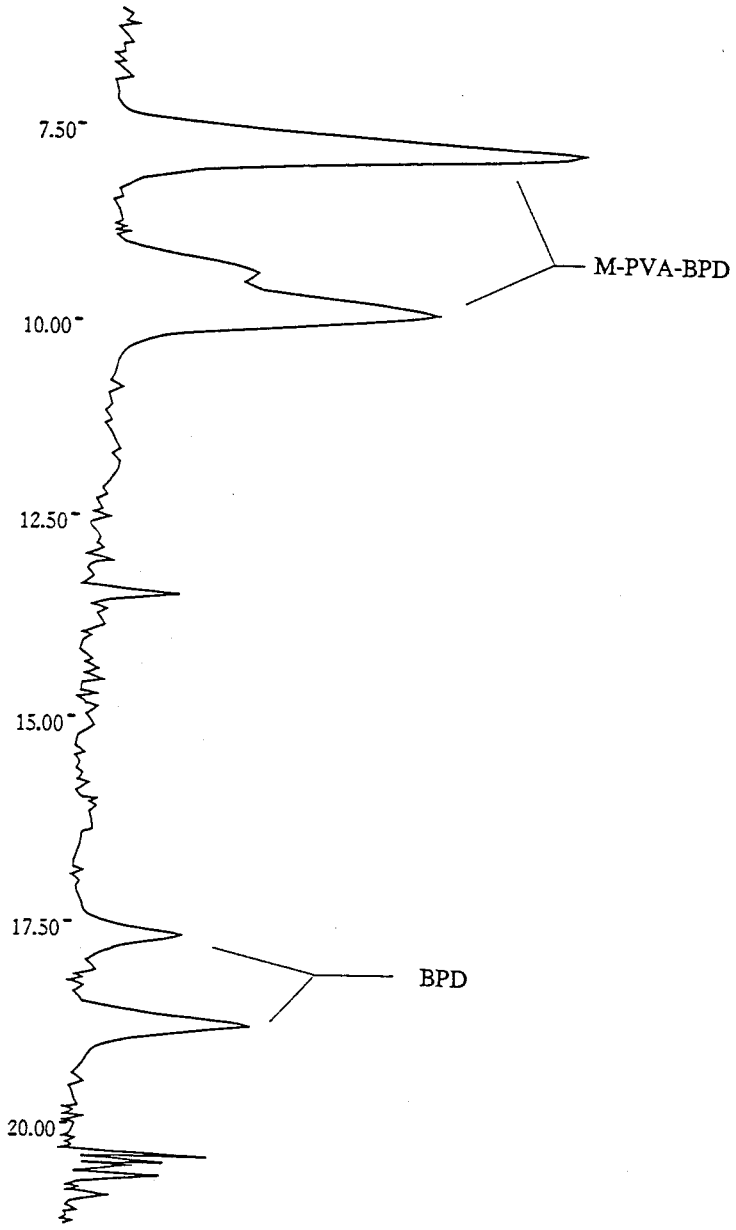

Figure 4. HPLC analysis of M-PVA-BPD. The solvent system used was detailed in the Materials and Methods. M-PVA-BPD was eluted at 8-10 min while BPD was eluted at 17-19 min.

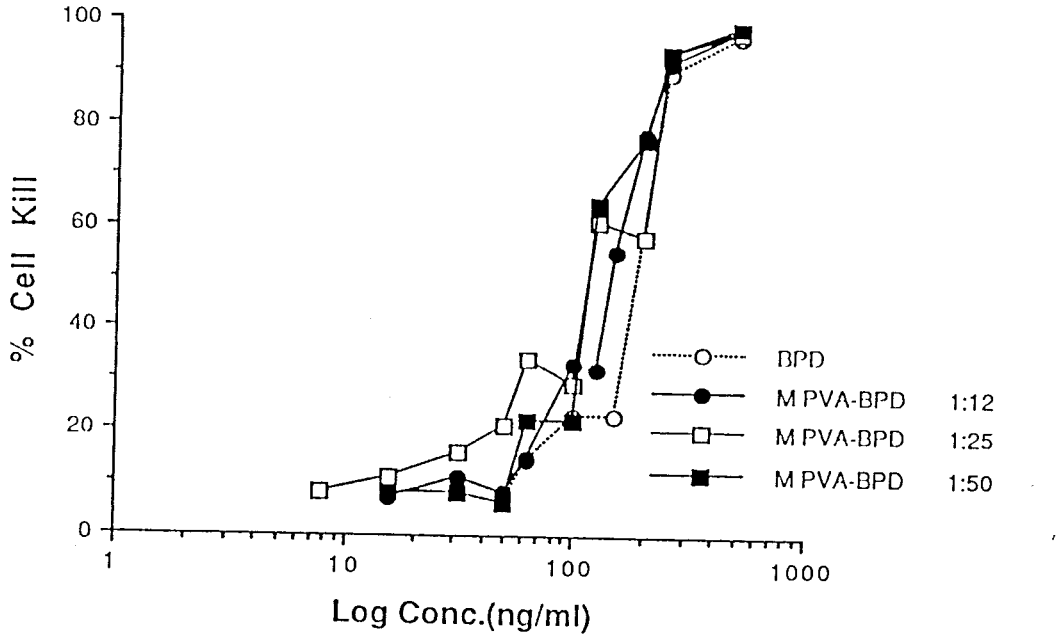

Figure 5. Photodynamic killing of A549 cells with BPD and M-PVA-BPD conjugates in the presence of 10% FCS. Light (fluorescent) dose: 5.4 J/cm^2, 300-750 nm wavelength.

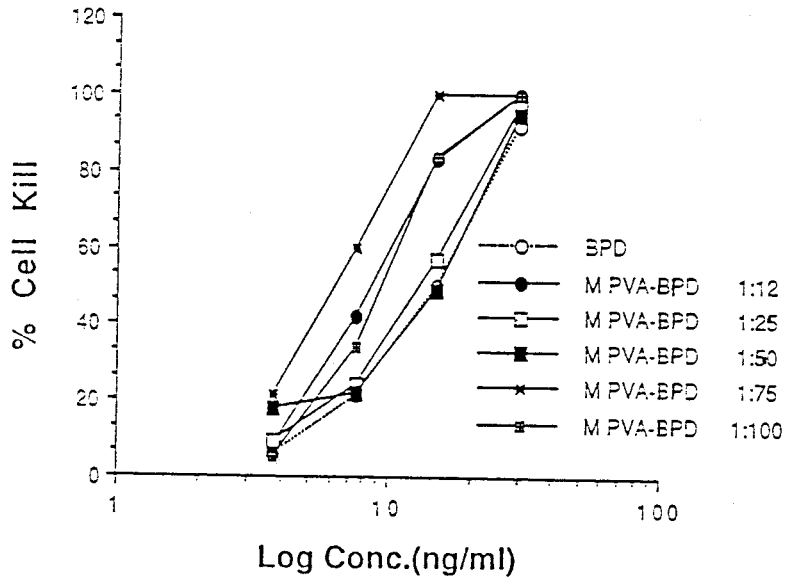

Figure 6. Photodynamic killing of P815 cells with BPD and BPD-PVA conjugates in the absence of serum. Light (fluorescent) dose: 5.4 J/cm^2, 300-750 nm wavelength.

CHAPTER III. DEVELOPMENT OF TECHNOLOGY FOR LINKING PHOTOSENSITIZERS TO A MODEL MONOCLONAL ANTIBODY

Introduction

In Chapter I, a detailed description of how PDT works was provided. In Chapter II, covalent linkage of the photosensitizer BPD to a water soluble carrier M-PVA was described. The objective of the research described in this Chapter was to further link the M-PVA-BPD to a model monoclonal antibody, T48, which reacts specifically with human chorionicgonadotropic hormone (HCG), to form a T48-M-PVA-BPD conjugate. MoAbs which react with antigens associated with malignant cells offer an approach for targeting anti-cancer agents. Preliminary experiments in which photosensitizers were conjugated to MoAbs have established the feasibility of this approach (69, 70, 73). These experiments usually involved conjugation of photosensitizers directly to MoAb molecules. This approach, while successful in many instances, can result in significant losses in biological activity of the antibody, due probably to interference in the antigen-binding region by photosensitizer molecules. In our hands, reproducibility using this approach has been poor, and loss of antibody activity was frequently substantial. The approach described below involves the conjugation of a limited number (one to two) of carrier molecules to T48 MoAb using a heterobifunctional reagent. The carrier molecule (modified polyvinyl alcohol) had been previously loaded with photosensitizer molecules at a ratio of 25:1 (see chapter II). This procedure was found to be reliable and reproducible and resulted in

negligible loss of MoAb specificity and photosensitizer activity. The results are discussed in the context of potential applications of this technology.

Materials and Methods

Preparation of M-PVA-BPD Conjugates

The procedure for this conjugation step has been described in detail in chapter II.

Introduction of Thiol Groups to M-PVA-BPD

The procedures described in this chapter are based on plans to couple M-PVA-BPD to MoAb using heterobifunctional reagents. In order to render the M-PVA-BPD carrier complex reactive with such reagents, it was first treated with 3-mercaptopropionic acid (3-MPA, Aldrich Chemical Co.) in the presence of carbodiimide to introduce free thiol groups (-SH) onto the M-PVA backbone. To obtain appropriate introduction of SH groups, M-PVA-BPD was reacted with 3-MPA at different ratios. Briefly, to 400 μg of M-PVA-BPD in 2 ml DMSO were added 276 μg of 3-MPA (M-PVA:3-MPA=1:5), 552 μg of 3-MPA (1:10) and 1104 μg of 3-MPA (1:20), respectively. The solutions were stirred in the presence of EDCI for 4 h at room temperature under argon. At the end of the reaction, each preparation was transferred to a dialysis bag (M.W. cut-off: 6000-8000) and dialysed against degassed acetate buffer, pH 5.4 at 4°C for 16 h (for 4 changes). Each preparation was then treated with an excess of [2,3-^{14}C] labelled maleic anhydride (New England Nuclear, Boston, MA). Specifically, 133 μl of a stock solution with a concentration of 1 μmol/ml was added to each preparation to give molar ratios of maleic

anhydride to M-PVA-SH of 5:1, 10:1 and 20:1, respectively (SH:maleic anhydride). The reaction (Fig. 8) was allowed to take place for 2 h with stirring at room temperature following which the material was dialysed exhaustively against acetate buffer (0.01M, pH 5.5) at 4°C. The control samples were M-PVA-BPD preparations which had not been substituted with 3-MPA but which were exposed to ^{14}C-maleic anhydride and treated in an identical manner to the substituted material. After dialysis, aliquots were transferred to 20 ml scintillation vials with 15 ml of Aquasol. Samples were counted in a Beckman liquid scintillation counter (Beckman, LS 3801, Beckman Instruments, Fullerton, CA). All the reactions were carried out under argon and all the buffers were degassed with argon before use.

Selection of Heterobifunctional Cross-linking Reagent

Since 3-MPA was chosen as the thiol group to be used in the reaction, it was necessary to determine the reactivity of this molecule with various commercially available cross-linkers. 3-MPA was added to: sulfo-m-maleimidobenzoyl-N-hydroxysulfosuccinimide ester (SMBS, PIERCE, Rockford, Ill), sulfo-succinimidyl 4-(N-maleimidomethyl) cyclohexane-1-carboxylate (S-SMCC, PIERCE) and sulfo-succinimidyl 4-(p-maleimidophenyl) butyrate (S-SMPB, PIERCE) at a molar ratio of 1:1. Reactions were qualitatively analyzed at 0, 15, 30, 60 and 120 min by monitoring the relative intensities of the fluorescent products, measured at 254 nm in a UV light box (Spectrolin, Westbury, NY). SMBS was chosen as the cross-linking agent for further studies because of the efficiency of its reaction with

3-MPA (Fig. 9).

Selection of Model Monoclonal Antibody

The monoclonal antibody (MoAb) selected for this study has a specificity for human chorionicgonadotropic hormone (HCG). This MoAb, T48 (Quadra Logic Technologies Inc. Vancouver, BC) was purified over a protein A column from mouse T48 ascites by M. Chester. T48 was chosen because its binding properties had been well characterized. Also, its activity was easy to monitor by a standard enzyme linked immunosorbent assay (ELISA) making quantitative assessment of binding properties through all steps of the procedures easy to carry out.

Labelling the T48 MoAb by Reaction with SMBS

The T48 MoAb (0.5 mg in 50 μl) was reacted with SMBS at molar ratios of 1:5, 1:10 and 1:30 (MoAb:SMBS) for 45 min at 37°C in 0.01M carbonate buffer, pH 8.5. In order to determine the actual number of SMBS groups bound to the MoAb, the preparations after dialysis against carbonate buffer exhaustively at 4°C were mixed with ^{14}C-labelled cysteine at a molar ratio of 1:100 (MoAb:Cysteine) (Fig. 10). The mixtures as well as controls (MoAb:cysteine mixtures which had not been previously reacted with SMBS) were subjected to 3 rounds of dialysis with a Centricon-30 (Amicon, MA) using 0.01 M acetate buffer, pH 5.5, and further dialysed against the same buffer. After dialysis, aliquots were

transferred to 20 ml scintillation vials with 15 ml fluid. Samples were counted in a Beckman liquid scintillation counter.

Preparation of M-PVA-BPD-MoAb Conjugates

A. Introduction of thiol groups onto the M-PVA-BPD:

It was established that molar ratios of 1:10 (M-PVA-BPD:3-MPA) introduced between 3 and 4 thiol groups per carrier molecule, and that higher ratios of 3-MPA did not significantly improve this. Therefore, material to be conjugated to MoAb was reacted with 3-MPA at this molar ratio in the presence of 0.8 mM EDCI in DMSO. Specifically, 280 μg of M-PVA-BPD was dissolved in 1 ml of DMSO with stirring for 30 min at room temperature. 130 mg EDCI was dissolved in 1 ml of DMSO. 10 μl of 3-MPA (114.8 μmol/ml) was diluted to 1 ml in DMSO. 2.0 μl of EDCI and 2.0 μl of 3-MPA were then added to the M-PVA-BPD solution (M-PVA:3-MPA=1:10). The reaction (Fig. 7) was stirred for 4 h at room temperature under argon, after which it was dialysed also under argon against 0.01 M acetate buffer (pH 5.5) at 4°C for 16 h (4 changes).

B. Reaction of T48 with SMBS:

A molar ratio of 1:30 (MoAb:SMBS) was used since this procedure was found to introduce between 2 and 3 SMBS groups to the MoAb with no loss of MoAb activity (see

below). The concentration of T48 was determined by measuring the antibody solution spectrophotometrically at 280 nm. T48 at a concentration of 9.615 mg/ml was dialysed overnight against 0.01 M carbonate buffer, pH 8.5 at 4°C. SMBS was added to this in the same buffer at a 30 fold molar excess. The mixture was stirred for 2 h after which it was washed through a centricon-30 and the buffer was changed to 0.01 M acetate (pH 5.5).

C. Conjugation of M-PVA-BPD-SH to MoAb-SMBS:

The final reaction (Fig. 7) between the carrier and T48 was carried out by mixing the two materials at equimolar concentrations in acetate buffer (0.01 M, pH 5.5) and stirring gently for 18 h at 4°C. Materials were concentrated by dialysis against polyethylene glycol (PEG) at room temperature.

Thin Layer Chromatography (TLC)

In order to monitor rapidly whether the anticipated reactions had taken place, aliquots of test materials were routinely run in a silica TLC system using a solvent of ethyl acetate:ethanol:H_2O (2:1:1, v:v:v). Controls consisted of free M-PVA-BPD and free MoAb, as well as mixtures of the various reactants. Plates were observed in a UV light box (254 nm).

Separation of Conjugates by Gel Filtration

A Sepharose CL-4B (Pharmacia LKB, Uppsala, Sweden) was used to separate conjugated from unconjugated materials. The column had a bed volume of 68.4 ml and was equilibrated with acetate buffer (0.01 M, pH 5.5). In early studies we experienced some difficulties in developing a chromatographic procedure for separating M-PVA-BPD conjugated materials, since M-PVA and M-PVA-BPD conjugates (including MoAb-PVA conjugates) have a marked tendency to bind to essentially all cross-linked dextran-type column materials. Subsequently we found that the addition of 0.5% (final concentration) low molecular weight (2000) PVA to the materials to be chromatographed successfully blocked this reaction and permitted appropriate elution of the desired product. Therefore all samples to be chromatographed were made up to 0.5% (W/V) PVA before addition to the column. Samples to be run were added to the column in volumes of 1.0 ml or less and eluted at room temperature at a flow rate of 0.43 ml/min. Fractions of 2 ml were collected and analyzed at both 280 nm and 688 nm using a spectrophotometer (LKB ultrospectrophotometer 4050).

Analysis of Materials by Gel Electrophoresis (SDS-PAGE)

In order to determine definitively whether the heterobifunctional cross linkers had actually formed covalent bonds between the MoAb and carrier system, materials eluting from the Sepharose column were subjected to analysis by reducing SDS-PAGE according to

standard procedures using a 7.5% minigel (80). Gels were run at 30 mA for 45 min and silver stained as described (108).

ELISA

The specific activity of the MoAb was monitored at every step in order to determine whether any of the procedures resulted in loss of activity. A standard ELISA was used for this purpose. Immulon II ELISA plates were coated with the antigen (HCG) at a concentration of 5 μg/ml in a volume of 100 μl per well in bicarbonate buffer (0.1 M, pH 9.6) at 4°C overnight. Test MoAb preparations and controls were titrated over these plates at 37°C for 1 h. Plates were developed with alkaline phosphatase labelled rabbit anti-mouse Ig (Jackson Immunoresearch Lab, Inc) and p-nitrophenyl phosphate as substrate. Plates were read at 405 nm on a Titertek Multiskan plate reader (Flow Lab). Plates were always run with a standard preparation of T48 so that quantification of test materials could be carried out.

In vitro Tests of Photosensitizing Activity

M-1 tumor cells were obtained directly from the M-1 tumor (a methylcholanthrene-induced rhabdomyosarcoma of DBA/2 mice), grown subcutaneously in mature, male DBA/2 mice as described elsewhere (52). The cells, in single cell suspension, obtained from a freshly excised, subcutaneously grown tumors, were plated in 96-well Falcon plates

in 200 μl DME containing 10% FCS at a concentration of 10^5 cells/well. After 24 hours the culture medium was changed, and at 48 hours the cytotoxicity test was performed as described in detail earlier (52). Briefly, the cells were washed and then incubated with various concentrations of BPD, M-PVA-BPD or MoAb-M-PVA-BPD conjugate for 1 h at 37°C in the dark in the absence of serum. Following incubation, the cells were washed and exposed to light for 1 h (21.6 Joules/cm^2) and then incubated further in DME-5% FCS at 37°C in the dark, in a 5% CO_2 humidified incubator for 18 h. At that time the viability of the cells was tested using MTT (103), and % killing was calculated for each tested material. The LD_{50} of the cell line was determined in this manner. Care was taken throughout the procedure to shield the porphyrin solutions and microtiter wells containing porphyrins from light, except as described. The light source used in this set of experiments consisted of 16 100 W tungsten bulbs (General Electric; Spectrum 400 to 1200 nm). The light was filtered through a 4 cm thick water filter with circulating cool water. The temperature at the plane of exposure did not exceed 22°C. The incident light density was 6 mW/cm^2 as measured by YSI Kettering Model 65 radiometer, and the dose delivered was 21.6 J/cm^2.

Ab Activity in Conjugates

To determine the antibody activity in the final conjugates, it was essential to know the Ab concentration so that the amount in the conjugate could be directly compared with standard Ab. However, the Ab concentration could not be accurately measured by

analyzing the conjugation product spectrophotometrically at 280 nm since PVA also absorbs at 280 nm (PVA is not a pure compound. It contains some structure absorbing at 280 nm). Similar interference was also expected in protein determination by the Lowry method (109). In order to assess this interference, a range (125-3.91 μg/ml; BPD concentration in the conjugate) of M-PVA-BPD conjugate concentrations was prepared and tested by the Lowry method. It was found that M-PVA-BPD at 63 μg/ml, PVA would give a reading which was below the level of sensitivity for the assay (0.088). If MoAb-M-PVA-BPD conjugates were diluted to the point where the antibody concentration was below 800 μg/ml; then for 1:1 conjugates the M-PVA-BPD component concentrations would be expected to be below 62 μg/ml. Therefore the interference in the Lowry assay was negligible. A standard curve was generated using Ab and M-PVA-BPD mixed at a molar ratio of 1:1, as in the conjugation mixture. The final conjugation product (50 μl) was measured by the Lowry method and the Ab concentration was determined from the standard curve.

Results

Testing the M-PVA-BPD-SH Conjugates

The M-PVA-BPD conjugate used in this work constituted material which had been substituted at a molar ratio of 1:25 (M-PVA:BPD) (Chapter II, 92, 93) and was shown to have coupled at greater than 90% efficiency. Further modification of the PVA backbone was effected by reaction with 3-mercaptopropionic acid (3-MPA) in order to introduce thiol groups on the conjugate. The M-PVA-BPD molecules were reacted at molar ratios of 1:5, 1:10 and 1:20 (M-PVA:3-MPA). The number of free -SH groups available for disulfide bond formation on the carrier molecules was determined by reacting the completed conjugate with ^{14}C-maleic anhydride under mild acidic conditions. The number of ^{14}C-maleic anhydride residues associated with the M-PVA on a molar basis was determined. The results showed that reaction with 10 fold molar excesses of 3-MPA produced a carrier system with 3 to 4 -SH groups available per molecule (Table III). This ratio was used subsequently in conjugate preparations.

Testing the MoAb-SMBS Conjugate

T48 was reacted with SMBS at molar ratios of 1:5, 1:10 ,1:30 and 1:50(MoAb:SMBS). The efficiency of derivatization was tested by reacting the MoAb-SMBS conjugates with ^{14}C-cysteine under conditions favouring alkylation. The ratios 1:5 and 1:10 yielded

conjugates in which between 0 and 2 SMBS residues were associated per MoAb molecule, whereas between 2 to 3 were present when SMBS was reacted at a 30 fold molar excess. A further increase in the SMBS:MoAb ratio did not increase the degree of substitution (Table IV). The ratio 1:30 was chosen. It was felt that this limited number of residues would probably be suitable for conjugation with the carrier. The reactivity of T48 with HCG was monitored throughout these procedures. As shown in Fig. 11, none of the steps involved had any measurable effect on the activity of the MoAb.

Heterobifunctional Linkage Between the M-PVA Carrier and T48

The M-PVA-BPD-SH carrier molecules to be reacted with T48 were prepared by reacting the M-PVA-BPD molecules with a 10 fold molar excess of 3-MPA. The T48 material had been reacted with a 30 fold molar excess of SMBS. The two reactants were mixed together at molar equivalence and tested subsequently for the effectiveness of this conjugation step. Preliminary TLC runs on conjugated M-PVA-MoAb indicated that no free M-PVA-BPD-SH was present since, in the system used, the M-PVA-BPD-SH conjugate migrates with an R_f of 0.57. All detectable M-PVA-BPD-SH after reaction with T48-SMBS remained at the origin with the MoAb.

Testing MoAb-M-PVA-BPD Conjugates

The conjugated materials were run over a Sepharose CL-4B column. Absorption of

fractions was recorded at both 280 and 688 nm (a wavelength at which BPD absorbs strongly). The results (Fig. 12) showed clearly that essentially all the 688 nm absorbing material eluted with a protein peak which had a molecular mass distinctly higher than free antibody (predicted M.W. of the conjugates is about 180 KD). There was some material absorbing at 280 nm in the conjugation mixture which co-eluted with the antibody standard and was thought to be free antibody. The material eluting from the column contain limited free BPD-M-PVA because this material binds strongly to Sepharose and is therefore retained on the column. This procedure therefore permits isolation of the three molecular species predicted in the reaction mixture.

It was of interest to determine the specific activity of the antibody in the various peaks. A representative set of results is shown in Fig. 13 in which it can be seen that the specific activity of the conjugated antibody was equivalent to that of free antibody. Further experiments showed that the BPD associated with the antibody had retained essentially all of its photosensitizing capability (Fig. 14). SDS-PAGE analysis of material presumed to be the conjugate showed the presence of 2 additional bands running at approximately 105 and 75 kD (Fig. 15) along with standard 50 and 25 kD materials. These findings are discussed below.

Discussion

Earlier studies carried out in this laboratory showed that it was possible to link photosensitizer molecules to MoAb covalently without substantial loss of either photosensitizer activity or antibody specificity (69, 70, 73). This early work involved direct interaction of the MoAb with hematoporphyrin (Hp) mediated by random peptide bond formation catalysed by a carbodiimide reaction. These procedures, however, were not optimal, since the conjugation occurred randomly and at high frequency (when high loading was attempted) throughout the MoAb molecule which often resulted in significant losses of the antigen-binding capability of the Ab. In our hands, wide variation was experienced in the efficacy and success of these reactions. Another feature of this type of reaction, which rendered quantification of conjugation difficult, was the propensity of hydrophobic photosensitizer molecules (like BPD) to bind spontaneously to hydrophobic sites on protein molecules such as MoAb in which the Fc region tends to be highly hydrophobic. More recently a number of investigators have successfully bound photosensitizer molecules to MoAbs using carrier molecules such as polyglutamic acid to which photosensitizers were previously bound (74, 94).

In the present study, we have shown that M-PVA can act as a suitable carrier to load photosensitizer molecules onto MoAbs. In Chapter II, we showed that the photosensitizer BPD (52, 53) could be linked to M-PVA in a reproducible and essentially quantitative manner. This kind of carrier system has the added advantage of increasing

the solubility of conjugates in aqueous solution, since M-PVA is extremely hydrophilic. The use of carbodiimide as a reagent for the linking of BPD to M-PVA ensured no cross-linking between photosensitizers and carrier molecules would occur since M-PVA has only free amino groups and BPD has only a single free carboxyl group. Although higher numbers of BPD molecules can be bound to M-PVA than were used here, we used the 1:25 ratio system for this work in order to ensure that sufficient free amino groups remained available for introduction of thiol groups via 3-MPA. The goal of further substituting the M-PVA-BPD carrier was to introduce a limited number of thiol groups which would act as linkers with the reactive derivatized MoAb. Again this reaction was straightforward and easily reproducible. The efficacy of this reaction was monitored using ^{14}C maleic anhydride (Table III), and indicated that optimal conjugation of 3-MPA could be achieved at a molar ratio of 1:10 (PVA carrier:3-MPA).

The decision to use the T48 MoAb as the model system for the development of the conjugation technology was made because this MoAb was well characterized, available in large amounts and easy to test for activity, so that individual steps in the conjugation reaction could be readily monitored. Its reaction with SMBS at pH 8.5 resulted in the successful production of MoAb-SMBS derivatives which contained approximately 3 SMBS moieties per MoAb molecule and retained essentially all antigen-binding activity (Fig. 13).

The final conjugation reaction between the MoAb-SMBS and the M-PVA-BPD-SH carrier appeared to be successful on the basis of further analysis of the reactants. Firstly, on

TLC, M-PVA-BPD conjugates have good mobility with an R_f value of 0.57; MoAb-M-PVA-BPD conjugates on the other hand, remain at the origin. Secondly, gel filtration of the reactants enabled us to separate the MoAb-carrier conjugate from unreacted MoAb, as indicated by the fact that the major peak, eluting first, contained material which absorbed strongly at 688 nm (i.e. BPD) and 280 nm, whereas the second peak eluted in the same volume as the free MoAb standard, and had essentially no 688 nm absorbance. These observations were compatible with the expectation that successfully conjugated material would be of higher molecular weight than free antibody, and contain photosensitizer. However, this step permits only enrichment for conjugated MoAb, and it was recognized that the first peak would certainly contain some free MoAb.

Finally, SDS-PAGE analysis of the conjugated material demonstrated 2 bands with apparent molecular weights of 75 and 105 KD, which were not present in control preparations of T48. These molecular weight values were derived on the basic assumption that the M-PVA-BPD-MoAb conjugate would behave on SDS-PAGE analogously to an unconjugated protein. This assumption may be subject to error since the M-PVA-BPD component is likely to differ from a polypeptide chain in its capacity for binding SDS. However, assuming the figures derived are valid, an H chain cross-linked with the PVA carrier would yield the observed 75 KD band. While the major 105 KD band is possibly the PVA carrier cross-linked between a H chain and a L chain, indicating that this might be a preferential site of conjugation of M-PVA-BPD-MoAb in this system. Furthermore, the SDS-PAGE results provide conclusive proof that all the reactions involving the

establishment of covalent bonds (carbodiimide catalysed reactions, SMBS binding to the MoAb, and the final alkylation between 3-MPA and SMBS) had successfully taken place, since the conditions used to run the gels would have dissociated non-covalent interactions such as hydrophobic bonding. Studies involving the standard cytotoxicity assay and ELISA established that both the sensitizer activity of BPD and antigen binding properties of the MoAb had been retained during the conjugation. No problems have been encountered with the MoAb conjugate, probably due to the aqueous solubility provided by the PVA carrier. The one bonding procedure which was not proven by this SDS-PAGE analysis was the binding of BPD to M-PVA, since it was possible that BPD could have become dissociated on the gel. This aspect will be addressed in Chapter IV in which we traced BPD by preparing conjugates with ^{3}H labelled BPD.

In summary, we have demonstrated a relatively easy and reproducible procedure whereby photosensitizer can be covalently bound to MoAb with retention of biological activity and solubility. Further studies address the properties of such conjugates in their capacity to selectively bind to and kill target cells, as well as their in vivo biodistribution properties, so as to evaluate their potential use as enhancers of selective delivery of photosensitizers.

Chapter Summary

A procedure is described whereby the photosensitizer, BPD was covalently linked to a model monoclonal antibody in a manner which is reproducible, quantifiable, and retains both the biological activity of the antibody and the cytotoxicity of the photosensitizer. The conjugation of BPD to M-PVA has been described in detail in Chapter II. The linkage of the M-PVA-BPD to a model monoclonal antibody involved further substitution of the carrier with 3-mercaptopropionic acid and carbodiimide to introduce 2-3 sulfhydryl residues per carrier molecule, and introduction of sulfo-m-maleimidobenzoyl-N-hydroxysulfosuccinimide ester residues to the monoclonal antibody (3-4 residues/molecule). Conjugation was effected by reaction of the two species at pH 5.5 for 18 h. The subsequent conjugates (MoAb-M-PVA-BPD) were examined both chemically and biologically. Chemically, it was shown that after purification via a sizing column, the PVA conjugate was covalently bound to the MoAb. Biologically, the activity of both BPD and MoAb was retained.

Table III. Results of experiments to determine the presence of available thiol groups on M-PVA-BPD-SH conjugates. M-PVA-BPD conjugates were reacted with 3-mercaptopropionic acid (3-MPA) in the presence of carbodiimide at molar ratio of 1:5, 1:10 and 1:20 (PVA:3-MPA). At the end of reaction, excess maleic anhydride was removed by dialysis against appropriate buffer exhaustively. These -SH substituted conjugates were labeled with ^{14}C-maleic anhydride (-SH:maleic anhydride) to determine the actual number of thiol groups present on carrier molecules. Unsubstituted M-PVA-BPD served as control. The actual readings for each preparation are presented.

Molar ratios M-PVA-BPD:3-MPA	CPM of product	Calculated substitutions
1:5	109,410	1.0769
1:10	253,760	3.830
1:20	457,020	7.501
1:0 (control)	51,017	0

Table IV. Results of experiments to determine the presence of available SMBS groups on MoAb-SMBS conjugates. MoAb T48 was reacted with SMBS at molar ratios of 1:5, 1:30 and 1:50 (MoAb:SMBS). These resulting mixtures were tested for the efficiency of binding by reacting the MoAb-SMBS conjugates with an excess of ^{14}C-labeled cystein (MoAb;cysteine = 1:100) under conditions favoring alkylation. For MoAb-SMBS 1:5 and 1:10 preparations, experiment 1, ^{14}C-labeled cysteine only was used. In experiment 2, (MoAb-SMBS 1:30 and 1:50) 20% of the cysteine added was ^{14}C-labeled and 80% was unlabeled.

Experiment 1.

Molar ratios Ab:SMBS	CPM of product	Calculated substitutions
1:5	37,554	o
1:10	65,136	1.11
MoAb control	1,711	-

Experiment 2.

Molar ratios Ab:SMBS	CPM of product	Calculated substitutions
1:30	13,006	2.4736
1:50	10,419	1.536
MoAb control	6,077	-

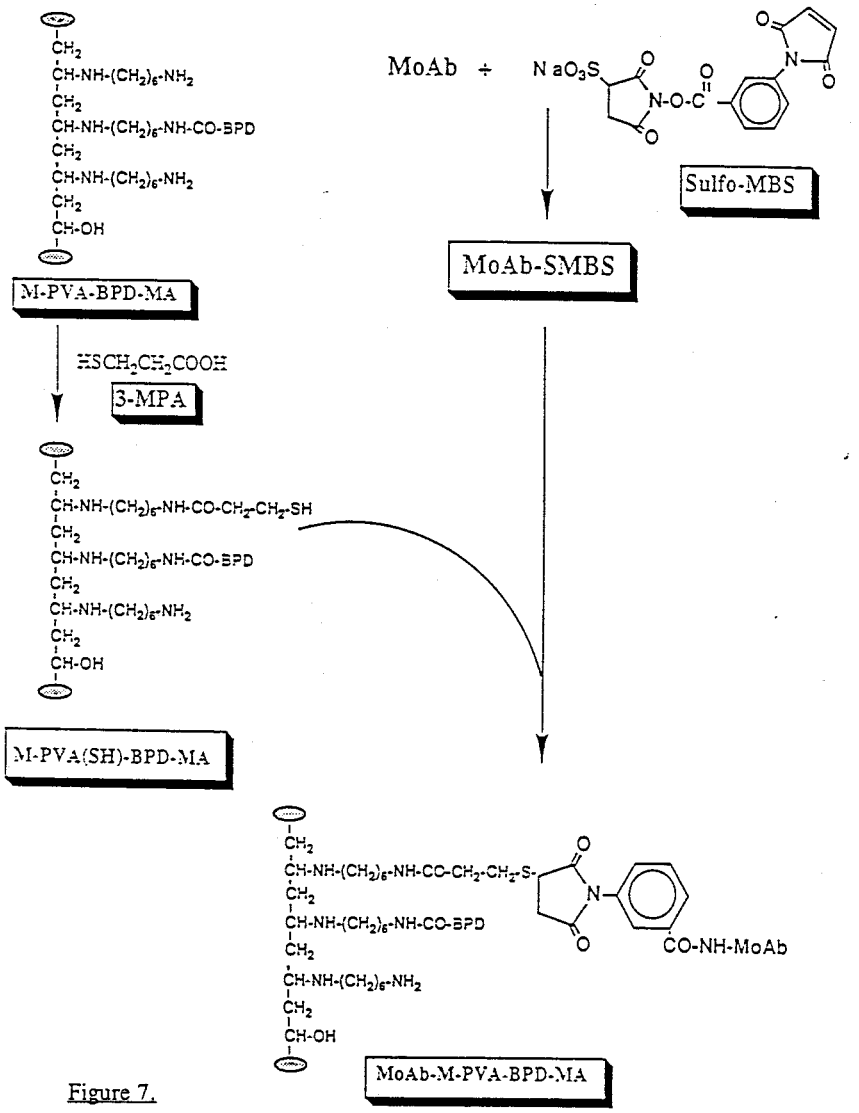

Figure 7.

Figure 7. Scheme for conjugation of MoAb-SMBS with the M-PVA-BPD-SH carrier system.

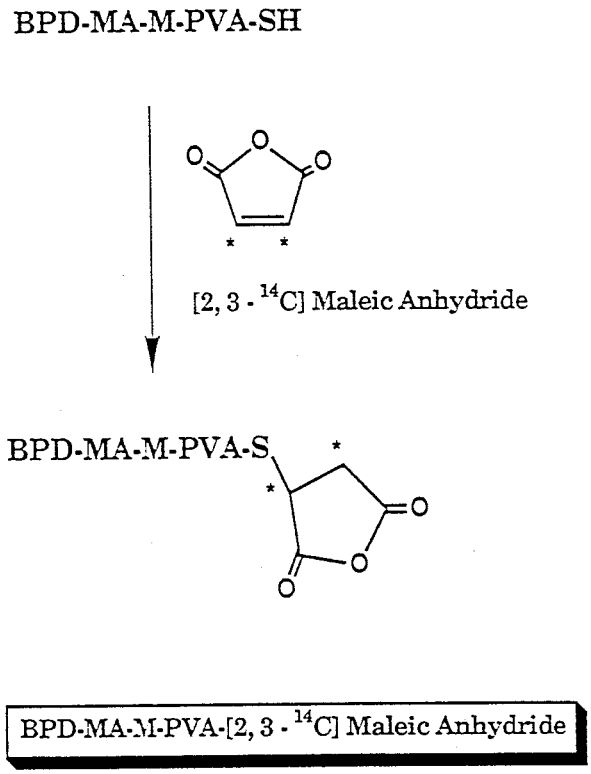

Figure 8. Scheme by which availability of SMBS residues was tested in the MoAb-SMBS conjugate. ^{14}C-labelled cysteine was reacted with the conjugate in a 100 fold molar excess. Bound cysteine was determined following reaction and dialysis.

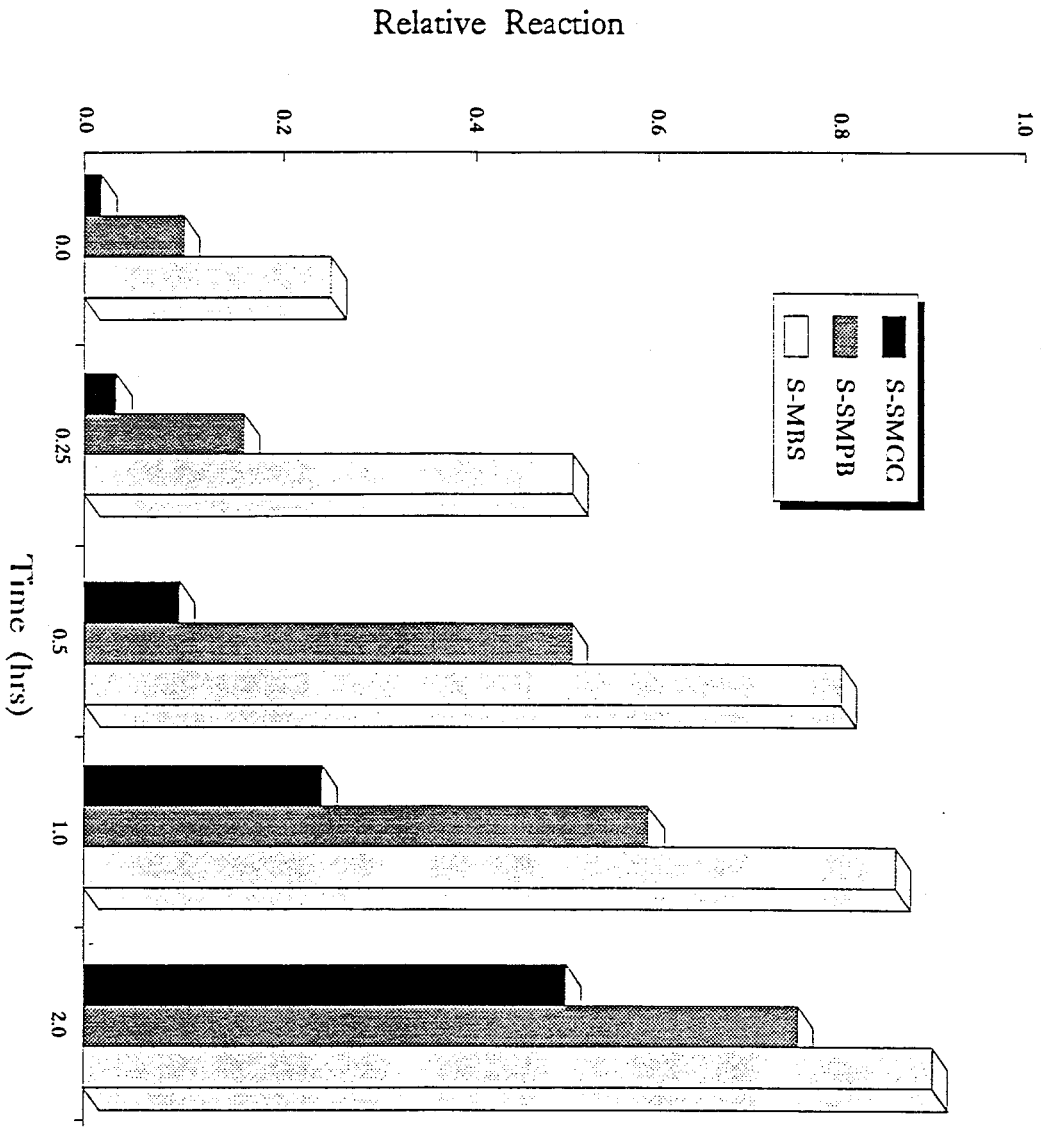

Figure 9. Selection of a heterobifunctional reagent. 3-MPA was reacted with SMBS, S-SMCC or S-SMPB at molar ratio of 1:1. Reactions were qualitatively analyzed at 0, 15, 30 60 and 120 min by monitoring the relative intensities of the fluorescent products, measured at 254 nm in a UV light box.

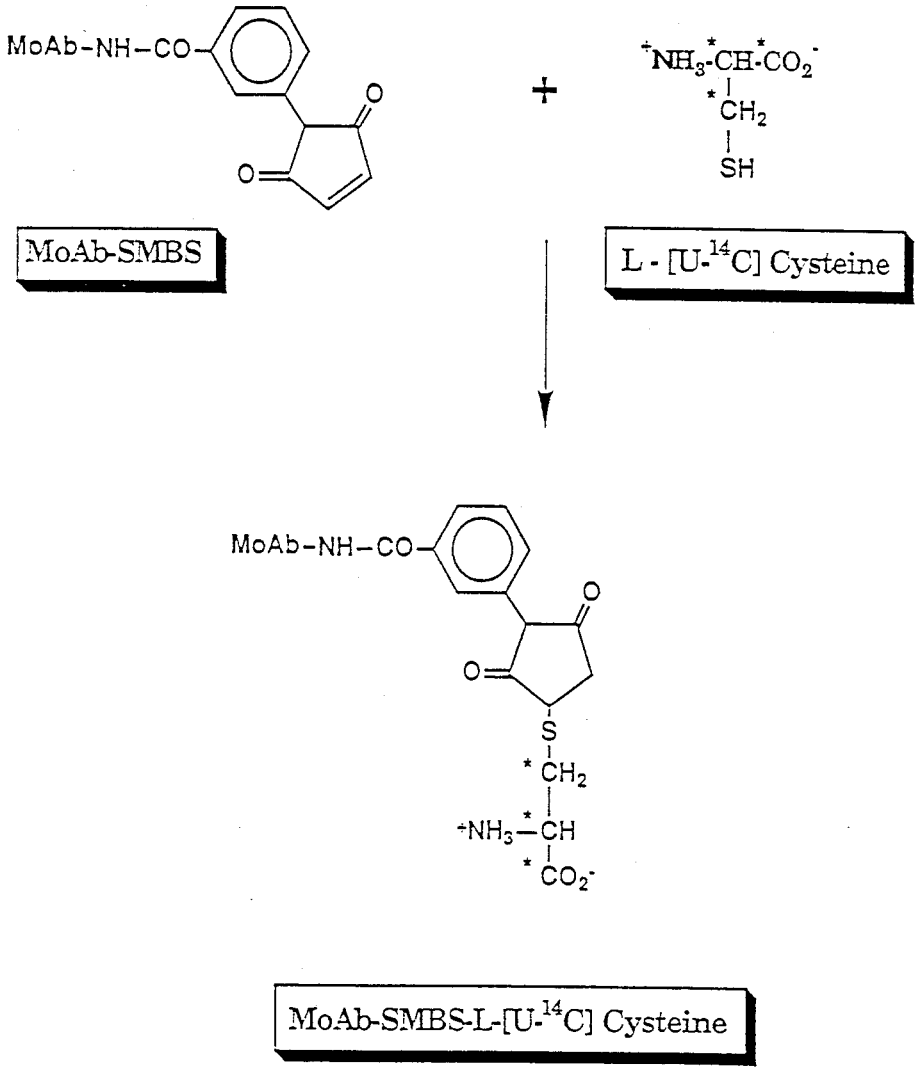

Figure 10. Scheme by which availability of reactive -SH residues were tested in the M-PVA-BPD-SH carrier. ^{14}C-labelled maleic anhydride was reacted with the carrier following which it was dialysed and tested for bound ^{14}C.

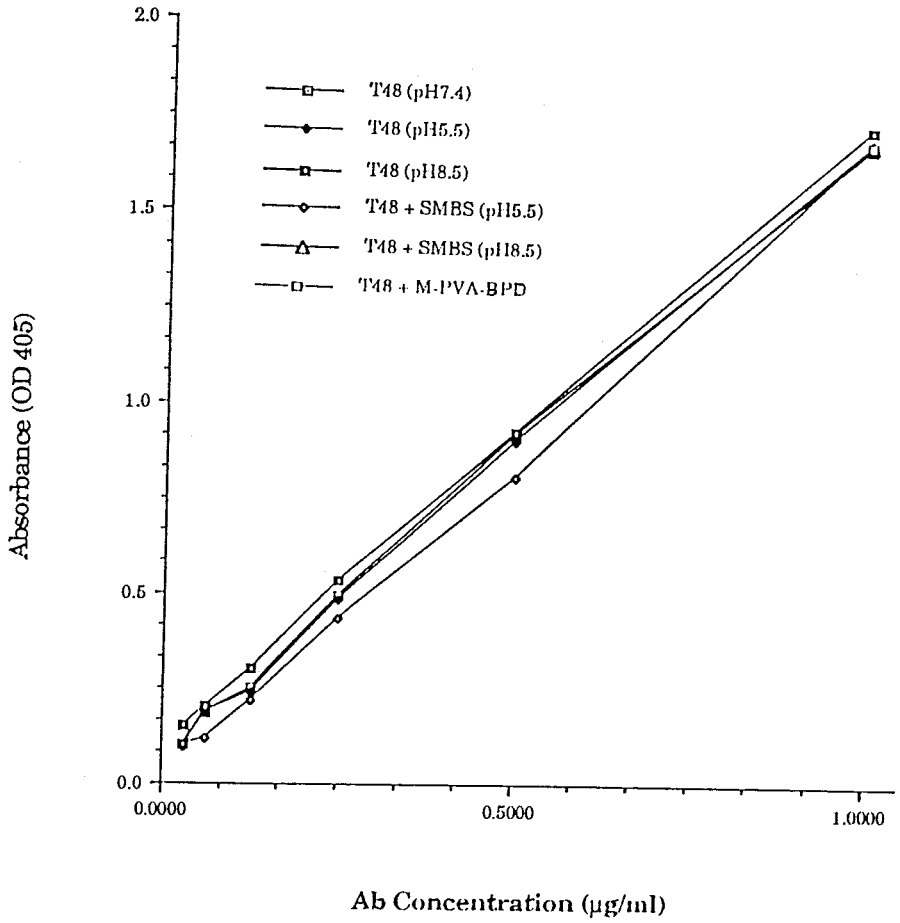

Figure 11. Monitoring T48 specific activity at every step in the conjugation procedure. Antigen binding activity of T48 was measured when T48 was in different pH buffers, mixing with SMBS or M-PVA-BPD.

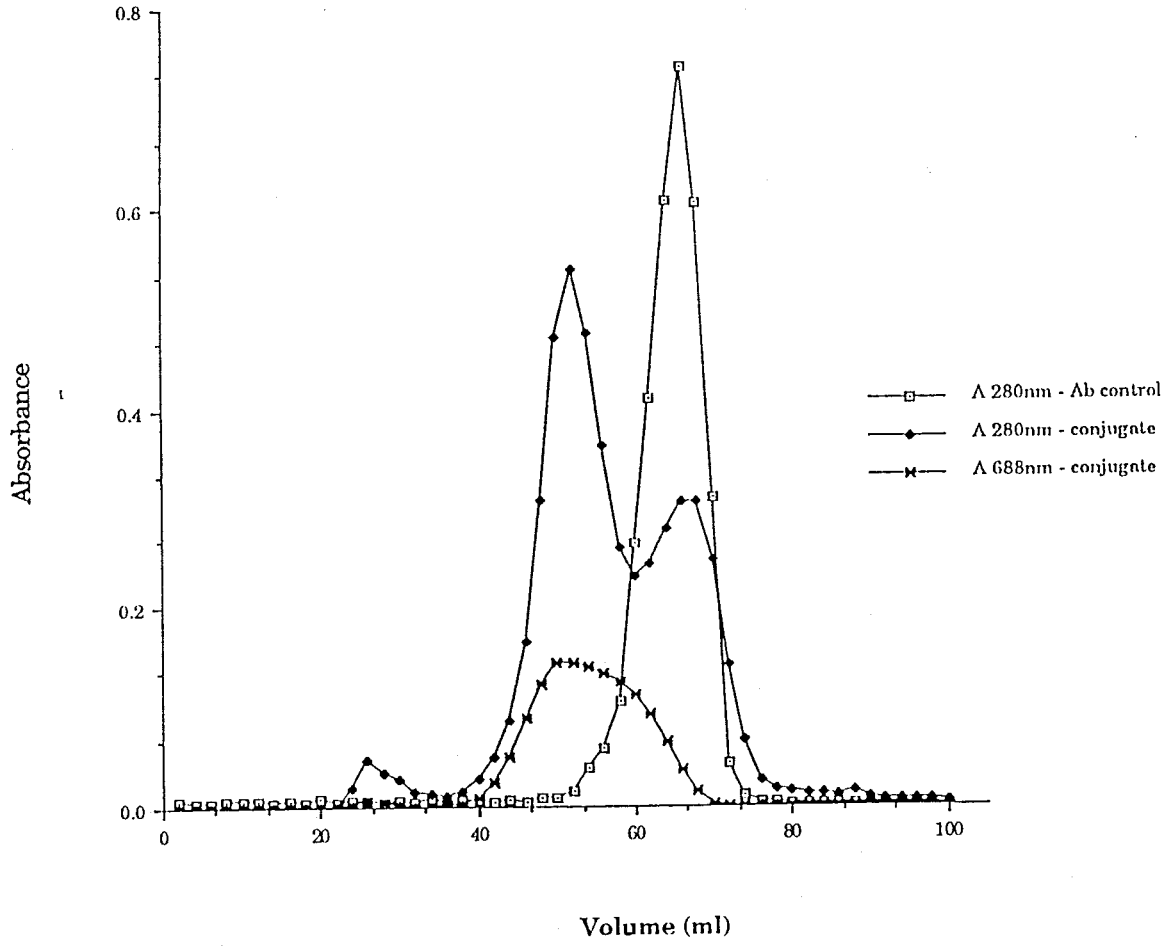

Figure 12. Elution profile of M-PVA-BPD-T48 conjugate on a 1.5 × 45 cm Sepharose CL-4B column equilibrated with acetate buffer at pH 5.5. The flow rate was 0.43 ml/min and each fraction was 2 ml.

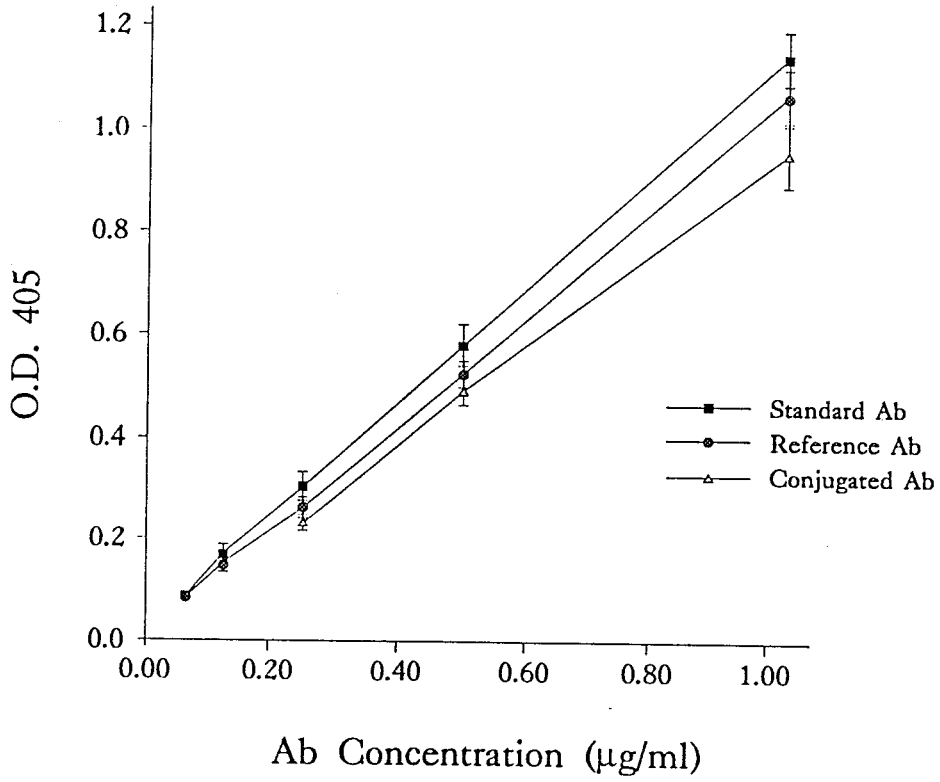

Figure 13. The comparison of specific activity of conjugated Ab with either standard Ab and reference Ab (T48 alone eluted from column with acetate buffer). Starting concentration for 3 preparations was from 1 μg/ml and 2 fold dilutions were used. Results are expressed as the mean ± SD (bar).

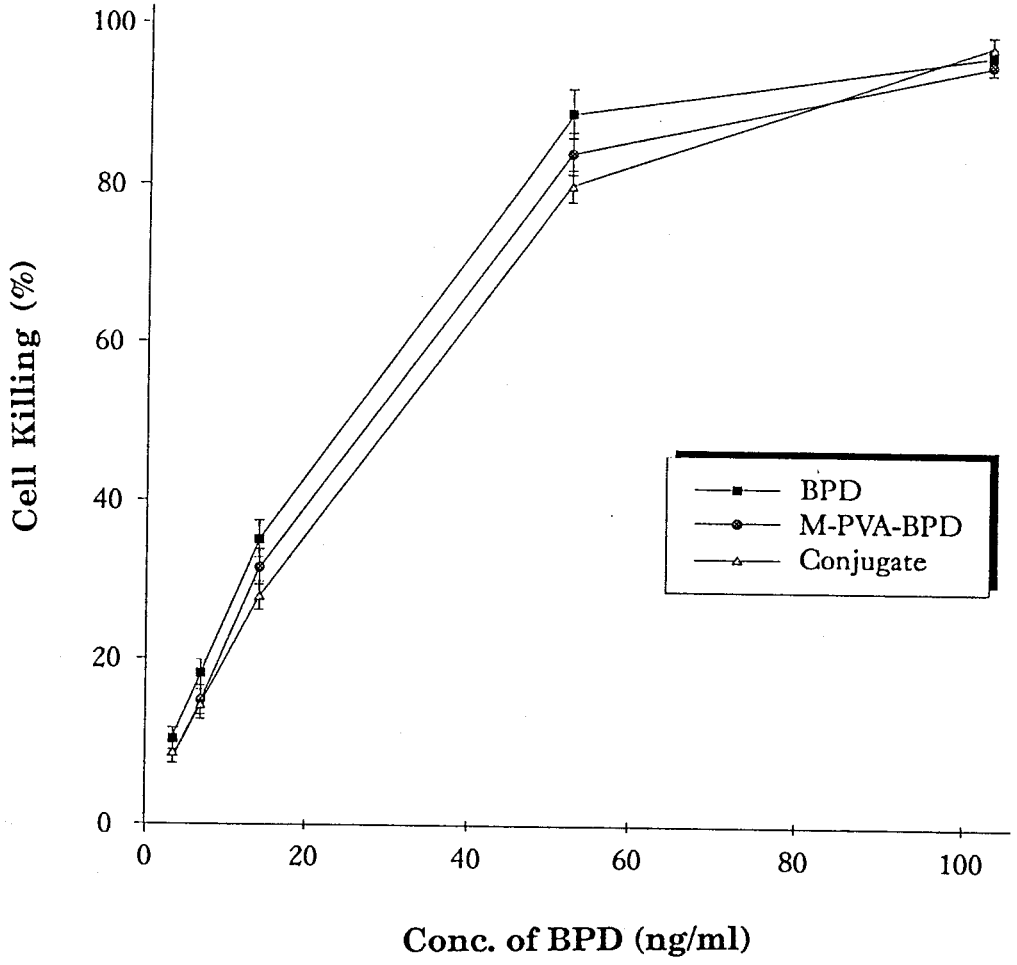

Figure 14. Phototoxic killing of M-1 cells with M-PVA-BPD-T48 conjugate, M-PVA-BPD and BPD in the absence of FCS. Light dose: 21.6 J/cm^2, 300-750 nm wave length. Results are expressed as the mean ± SD (bar).

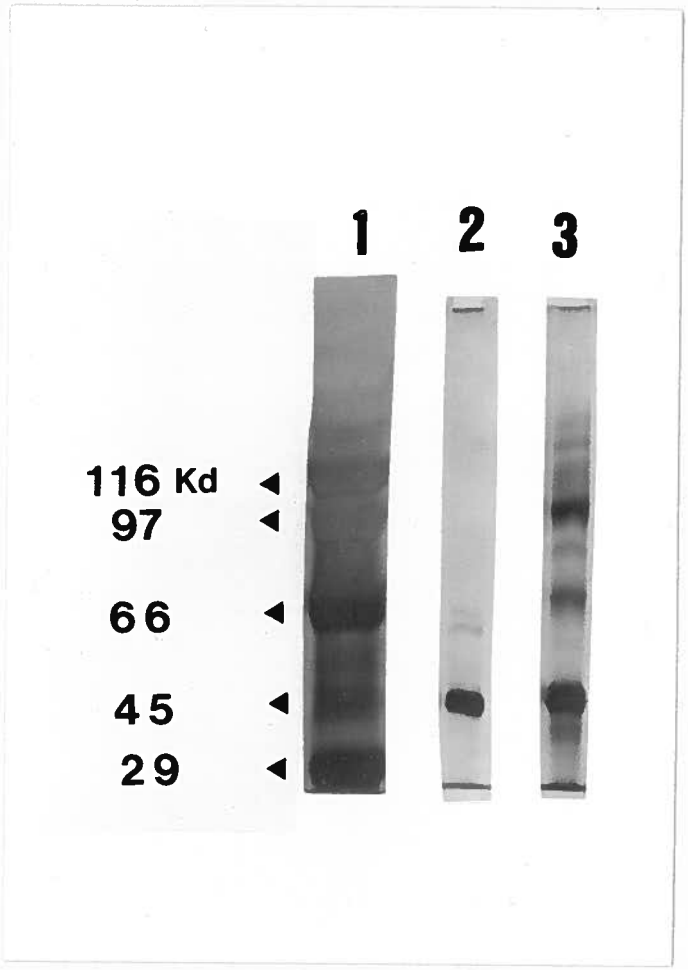

Figure 15. SDS-PAGE analysis of M-PVA-BPD-T48 conjugate eluted from Sepharose CL-4B column. Lane 1, MW markers; Lane 2, T48 (control); Lane 3, M-PVA-BPD-T48 conjugates.

CHAPTER IV. EFFICACY OF A TARGETED MONOCLONAL ANTIBODY-BPD CONJUGATE IN VITRO

Introduction

In Chapter III, we described a novel technology whereby a large number of PS molecules could be covalently bound to the model MoAb T48. Subsequent examination of the conjugate showed that the antigen binding activity of the T48 and the photocytotoxicity of BPD were retained. This led us to further examine the selectivity of MoAb-PS conjugates of this nature on target cells in vitro. The 5E8 MoAb, used in the present study, has been extensively characterized (110, 111). It was derived from a hybrid clone that was produced using spleen cells of mice immunized with a human lung squamous cell carcinoma. It is directed towards an antigenic determinant contained within a M.W. 160,000 non-sulfide bonded glycoprotein (gp160). 5E8 is an IgG_1 and binds little or not at all to normal lung tissue. The MoAb is internalized when it reacts with the glycoprotein at the cell surface at 37°C (112). The gp160 has been identified as a plasma membrane-associated glycoprotein that is found on both human lung tumor cell lines and on surgically excised fresh lung tumor tissue. It is one of the largest cell surface antigens reported, and it is expressed by a large percentage of primary lung tumor types. Its very limited expression in normal human tissues and the lack of any observable molecular heterogeneity make this a suitable target for one of several immunospecific targeting protocols (113, 114). We have used the 5E8 MoAb to assess the specificity and

selectivity of M-PVA-BPD-MoAb conjugates, with the consideration that such conjugates could be used for localization and treatment of early lung cancers through photodynamic therapy.

Materials and Methods

Monoclonal Antibodies

The 5E8 MoAb was kindly provided by Dr. R. Bankert (Roswell Park Memorial Institute, Buffalo, NY). This antibody is an IgG_1 and is internalized when binds to target cells at 37°C. It has been well characterized and described elsewhere (110, 111). It reacts with a cell surface glycoprotein (gp160) associated with human squamous cell carcinomas of the lung but not with normal lung tissue. The MoAb was purified from ascitic fluid by standard procedures before use (111). The control MoAb used in this study, T48, has specificity for an irrelevant antigen, HCG and was chosen because it too has been well characterized and served us in these studies as a model antibody (80).

Tritiated BPD

Tritiated BPD was obtained from New England Nuclear. The labeled product was dissolved in DMSO and stored at -20°C at a concentration of 8 mg/ml. The specific activity was 5.9 mCi/mg.

Cell Lines

The A549 cell line, derived from a human squamous cell carcinoma, was obtained from

the ATCC, maintained according to recommended procedures as described in Chapter II, and was used as the target cell in experiments described below. The M-1 cell line is a rhabdomyosarcoma from DBA/2 mice. It has been maintained, both in vitro and in vivo for the past decade in this laboratory. It is used as a standard cell line for assessing phototoxicity and was used as a specificity control in these experiments. It has been described in detail elsewhere (52). Both cell lines form adherent monolayers in vitro. A549 cells were maintained in MEM containing nonessential amino acids in Eagle's balanced salt solution. M-1 cells were maintained in DME. Both media were supplemented with L-glutamine and 10% FCS. Both cell lines were grown in a humidified 37°C, 5% CO_2 incubator.

Conjugation Procedures

The procedures for producing immunoconjugates, using either ^{3}H-labeled or unlabeled BPD, were described in detail in Chapters II and III and are depicted in Figures 2 and 7. The molar ratio of M-PVA:BPD was 1:25 in all cases.

Separation of Conjugates by Gel Filtration

The conjugated product was separated from unconjugated reactants by passage of the material over a Sepharose CL-4B (Pharmacia LKB) column as described in Chapter III. Eluted material was monitored for absorbance at 688 (to detect BPD) and 280 nm (to

detect protein), as shown in Fig. 16. The peak eluting at 30 - 55 ml contained both 688 and 280 nm absorbing material and preceded a peak which absorbed strongly only at 280 nm and eluted at 55 - 70 ml. This latter was shown to elute in the same position as free antibody. The material eluting at 30 - 55 ml was assumed to be conjugated and was collected and used for further testing. Spectrophotometric analysis of this material at 280 and 688 nm indicated that the molar ratio of M-PVA-BPD:MoAb was essentially 1:1 (BPD:MoAb ratio was about 26:1).

SDS-PAGE Analysis of Unlabeled and Tritiated Conjugates

Conditions for gel analyses were as follows: Sepharose CL-4B column-purified conjugated materials were subjected to SDS-PAGE analysis to determine whether material containing protein and BPD were really covalently linked. Samples containing either ^{3}H-BPD-M-PVA-5E8 or unlabeled BPD-M-PVA-5E8 were run in parallel on a 7.5% polyacrylamide reducing gel. The gel was run at 30 mA (constant current). After electrophoresis, gels were either silver stained (108) or cut into 2 mm slices and transferred into scintillation vials containing 10 ml of 3% Protosol in Econofluor (New England Nuclear) (116). Gel slices were allowed to soak in the above solution at 37°C for 16-18 hours. Radioactivity was determined using a Beckman liquid scintillation counter (Beckman Instruments, Fullerton, CA).

Absorption Properties of Conjugates

The conjugates were characterized using absorption spectra. The conjugate as well as BPD (control) were dissolved in PBS and adjusted so that they were comparable. The effect of conjugation on absorption was established by measuring the absorption spectrum on a Beckman spectrophotometer (Beckman).

Cytotoxicity Assays

A. Photodynamic killing using MoAb-M-PVA-BPD conjugates in the absence of serum: Standard assays, described previously (52), were used to determine the phototoxicity of BPD following the conjugation procedure. Briefly, A549 and M-1 cells were grown to log phase and were harvested with 10% trypsin and vigorous agitation. Cells were then plated in 96-well Falcon plates in 200 μl media containing 10% FCS at a concentration of 10^5 cells/well. Culture medium was changed after 24 hours. On the next day, cells were washed and incubated with various concentrations of PS in serum free medium for 2 h (both A549 and M-1) or 24 h (only A549) at 37°C in the dark. After drug incubation, cells were washed with PBS and replaced with fresh medium. The treated cells were exposed to light for 1 h. After light activation, cells were incubated for a further 18 h in medium-5%FCS at 37°C in the dark. At that time the viability of the cells was tested using MTT as described in previous chapters, and % killing was calculated for each tested material. As mentioned earlier, in our hands, the MTT assay has been found to be

quantitatively comparable to the clonogenicity assay (104), and while the 100% kill level must be extrapolated with the MTT assay (owing to background), rate of kill can be accurately determined.

B. Photodynamic killing of MoAb-BPD conjugates in the presence of serum:

The assay conditions used in these experiments were exactly the same as described above except that both cell lines were incubated with various PS preparations for 1 h in the presence of 10% FCS. This modified experimental condition was designed to more closely resemble the in vivo environment and therefore may have greater relevance in assessing the efficacy of a MoAb mediated delivery system in vivo.

Dark controls were run coincident with all experiments reported here. At all the concentrations used, no dark effects were ever noted. It has been determined in vitro that BPD levels greater than 1.0 μg/ml are required before any intrinsic cell toxicity is seen. The light source and dose were the same as described in Chapter III.

ELISA Assays

The 5E8 antibody reacts in a standard cellular ELISA with A549 cells. The procedure has been described previously (117). Briefly, A549 cells were grown to confluence in 96-well Falcon plates. Plates was then washed with PBS and the cells were fixed to the bottom of the wells with 0.25% glutaraldehyde in PBS for 2 h at 37°C. At that time the plate was quenched with PBS containing 1% BSA. After quenching, 5E8 and BPD-M-PVA-5E8 were titrated over these plates. Plates were developed with alkaline phosphatase labeled rabbit anti-mouse Ig (Jackson Immuno Research Lab, Inc.) and developed with the p-nitrophenyl phosphate substrate. Plates were read at 405 nm on a Titertek Multiskan plate reader (Flow Lab). BPD-M-PVA-T48, at comparable concentrations, was used as a control for specificity of 5E8-M-PVA-BPD conjugates.

Statistical Analysis

The standard Student's t-test was used to establish significance (118, 119).

Results

M-PVA-BPD carrier molecules were conjugated to the 5E8 MoAb at a 1:1 molar ratio according to procedures described earlier. The conjugated material was then passed over a Sepharose CL-4B column. Fractions eluting from the column were monitored for absorbance at 280 and 688 nm. The results (Fig. 17) show that the first major peak eluting from the column absorbed strongly at both wavelengths indicating the presence of both protein and BPD. The second peak absorbed only at 280 nm and eluted in the same column volume as free MoAb. Fractions representing the first peak were pooled and used for further testing. The absorption spectrum of material from this peak is shown in Fig. 18 in which it can be seen that the absorption properties of BPD are not changed as a result of conjugation.

SDS-PAGE (7.5%) was run on the above material and compared to control 5E8 MoAb. The results (Fig. 19) show that the control antibody has a major band at about 50 kD, which was assumed to be H chain. The 25 kD light chain is not visible on these gels since the 29 kD molecular weight standard was run off the bottom of the gel. The conjugated material showed the presence of a number of bands in addition to the 50 kD moiety. Four additional bands with molecular weights between 75 and 150 kD were clearly visible. Since the M-PVA-BPD carrier molecule has a molecular weight in the region of 30 kD, these bands could constitute H or L chains conjugated to one or two M-PVA-BPD molecules. These analyses established successful covalent binding of M-PVA to the

MoAb molecule but did not establish that BPD was still associated with the conjugates. In order to establish this, M-PVA-BPD carriers were prepared using tritiated BPD (^{3}H-BPD) and this ^{3}H-BPD-M-PVA was then used to prepare MoAb conjugates. Duplicate PAGE was run on this material and either silver stained or sliced, eluted and counted. The results (Fig. 19) showed clearly that significant counts were only found to be associated with these higher molecular weight moieties, establishing the presence in them of BPD. Specifically, radiolabeled bands were located at approximately 75, 100, 120 and 150 kD. The 120 and 100 kD bands were located in fractions 10 and 11, respectively (Fig. 19). While it is difficult to be precise, because determination of the amount of protein in each band is not quantifiable, it can be seen that the 100 and 150 kD bands stain more strongly than do the others. Counts in these two bands are roughly equivalent. It is possible to postulate that if a 1:1 molar ratio between the MoAb and M-PVA-BPD was predominant, these bands could be constituted of the following combinations; 75 kD: H_1: M-PVA-BPD_1, or L_1:M-PVA-BPD_2, 100 kD: L_1:M-PVA-BPD_1:H_1 (in which L & H chains are linked via the M-PVA-BPD), 120 kD: H:M-PVA-BPD:H (linked via M-PVA-BPD) and 150 kD: H_2:M-PVA-BPD:L (cross-linked via M-PVA-BPD). While we have no way of verifying these structures, these products are certainly possible considering the number of free thiol groups on the carrier and the reactive SMBS residues on the MoAb (2-3 in each case). The counts at the bottom of the gel (Fig. 19) are thought to be contributed mainly by non-covalently bound M-PVA:BPD which, on control runs, was found to migrate with the gel front (data not shown).

The characterization of the BPD-M-PVA-5E8 conjugate showed that the conjugate has a similar absorption spectrum to that of free BPD (Fig. 17) indicating that its photosensitizing properties have not been changed. Specific activity of the 5E8 conjugate was tested using a cellular ELISA and the results showed that at least 80% of activity was retained (Fig. 20). The control conjugate, while showing some non-specific stickiness at elevated concentrations was well below levels of reactivity seen with 5E8.

Preliminary experiments were performed to determine whether 5E8-M-PVA-BPD conjugates would improve delivery of photosensitizer to the targeted cell line. The irrelevant MoAb-BPD conjugate, T48-M-PVA-BPD was used as a control for these experiments. Initially, cytotoxicity for the A549 cell line was tested, using BPD alone, M-PVA-BPD or 5E8-M-PVA-BPD. Cells and photosensitizer preparations were mixed in the absence of serum and incubated for 2 h in the dark prior to exposure to light. The results (Fig. 21) showed that under these conditions, the MoAb conjugate was taken up less efficiently by the cells than either BPD on its own or M-PVA-BPD. This experiment was repeated, except that preincubation was continued for 24 h. This alteration enhanced phototoxic killing in all preparations but did not improve selectivity with the MoAb conjugate in comparison to other BPD preparations (Fig. 22). However, in M-1 cells, all three preparations showed equal cytotoxicity (Fig. 23). This suggested that there was a difference in susceptibility in terms of photodynamic killing among different cell lines. The M-1 cell line was obviously more sensitive to photodynamic damage than was the A549 cell line. It was felt that the strong affinity of free BPD under serum free conditions

for lipophilic membrane structures could be influencing results and lead to further experiments more closely resembling an in vivo situation. These experiments were carried out in the presence of 10% FCS. In one series (Fig. 24), A549 cells in 10% FCS were incubated in the dark for 1 h with BPD, the 5E8 MoAb conjugate or the control T48 MoAb conjugate. Under these conditions it appeared that significant ($p < 0.01$) selectivity was shown by the 5E8 conjugate in comparison to control materials. In order to establish specificity, a further experiment was carried out using M-1 cells in 10% FCS as targets (both 5E8 MoAb and T48 MoAb do not react with this murine cell line). The results (Fig. 25) show that there is no difference ($p < 0.3$) in phototoxicity between the two MoAb conjugates indicating that the enhanced killing of 5E8-MoAb on A549 cells was specific.

Discussion

In previous chapters (II and III) we demonstrated the feasibility of conjugating BPD to MoAbs using the heterobifunctional linker SMBS. This procedure in which BPD was covalently bound to hexanediamine-modified PVA via a carbodiimide mediated reaction at a molar ratio of about 25:1 (BPD:PVA), permits loading of 25-50 (1 or 2 carrier molecules) BPD residues to the MoAb molecule. PVA was chosen as the carrier of choice because it bestows water solubility to the carrier-conjugate system. The work described here has shown that this procedure is applicable to other MoAb systems and produces conjugates which can be readily purified and retain both antigen-binding specificity and photosensitizer activity. BPD on its own is a highly phototoxic agent and has, because of its hydrophobicity, a strong affinity for cell membranes. The aim in this study was to determine whether in vitro conditions could be set up in which selectivity of MoAb-BPD conjugates could be demonstrated with specified target cells in spite of the high intrinsic cytotoxicity and hydrophobicity of BPD.

Because BPD is a highly hydrophobic molecule, it was essential to establish that it was covalently bound to the carrier conjugate rather than associated through hydrophobic interactions. The reducing SDS-PAGE analysis of material eluting in the first peak from the Sepharose CL-4B column which absorbed strongly at both 688 and 280 nm indicated that the M-PVA carrier had been covalently bound to the 5E8 MoAb since bands at 75-150 kD were visible in the conjugated material which were not present in the control

MoAb. Since the PVA carrier is estimated to have a molecular weight in the region of 30 kD, these higher molecular weight bands could represent H or L chain-PVA conjugates. However, SDS-PAGE analysis did not establish the presence of BPD in the higher molecular weight entities. In order to establish this, a M-PVA-BPD conjugate was produced with ^{3}H-labeled BPD and reacted under identical conditions with the MoAb. This material, when run on SDS-PAGE, eluted, and counted, showed clearly that the only significant counts were associated with these higher molecular weight bands. Additional counts, located at the dye front, constituted low molecular weight material which was thought to be unconjugated M-PVA-BPD or residual free BPD. We consider this to constitute proof that the reactions carried out in this conjugation procedure resulted in the formation of covalent bonds both between BPD and M-PVA as well as between the M-PVA-BPD carrier and MoAb.

Characterization of the 5E8-M-PVA-BPD conjugate showed that absorption properties of the conjugate were similar to those of free BPD, and that biologically most of the antibody activity and essentially all of the photosensitizer activity was retained. Since there was no loss of 688 absorbing activity in relation to other absorption peaks (this occurs when BPD is photobleached) and because, when the 688 absorption properties were used to quantify available BPD in conjugates, it appeared that the photodynamic properties were virtually the same as control materials.

When cytotoxicity was performed in the absence of serum on either control or target cells,

no significant ($p<0.3$) difference among the specific conjugates, control conjugates and free BPD was observed. However, in the presence of 10% FCS the MoAb conjugates (both 5E8 and T48) were found to have a greater affinity for target cells than did BPD on its own. This finding that serum lowers the affinity of free BPD for cell membranes is not surprising since it has been shown that free BPD has a strong affinity for serum proteins, particularly lipoproteins, which provides competition for cell membrane association (120). During the washing steps, most of free the BPD would be washed out along with serum proteins. The conjugated material, on the other hand, probably does not have equivalent affinity for serum proteins. However, when the A549 cell line was used as a target, in the presence of serum, the 5E8 conjugate was far more effective in cell killing than was the T48 control. Table V clearly establishes that the M-1 cell line is almost twice as sensitive as A549 cells to photodynamic damage and yet 5E8-M-PVA-BPD exhibits much higher killing in the target cell line. Specifically, the 5E8-M-PVA-BPD conjugate was 10 fold more effective than the control conjugate and 15 times more cytotoxic than BPD toward the A549 cell line on the basis of the LD_{50} (Table V) in the presence of 10% FCS. In the case of the control cell line (M-1) both conjugates had similar LD_{50} values which were approximately two thirds to one half of that of BPD alone. These data provide evidence that the 5E8 conjugate can, under the parameters described here, deliver photosensitizer in both a selective and specific manner, to the designated target cell.

The long term goal of this work was to establish the use of this conjugate in the detection

and photodynamic treatment of early squamous cell carcinomas of the head and neck or lung. Conditions for its use in vivo will be considerably different from those described here. The fact that in serum levels of 10%, we see adequate levels of selectivity encourages us to believe that this approach is feasible and should be pursued. In relating these observations to an in vivo situation, where plasma concentrations would be much higher, one would predict that selectivity with MoAb conjugates would be further enhanced.

Chapter Summary

We have developed procedures in which the photosensitizer BPD can be covalently linked to carrier molecules of modified polyvinyl alcohol (M-PVA) to produce water soluble M-PVA-BPD conjugates with molecular weights in the range of 30 kD. These carriers can subsequently be covalently linked to monoclonal antibodies (MoAbs) using heterobifunctional linking agents. We have describe here such a conjugate in which the MoAb (5E8) has specificity for a glycoprotein detected on human squamous cell carcinomas of the lung. We provided evidence that the conjugates produced were covalently linked and have retained both their photosensitizing and antigen binding activities. We have shown further that the MoAb-M-PVA-BPD conjugate, in the presence of 10% fetal calf serum exhibited highly enhanced phototoxic killing of the target cell line (A549) in comparison to free BPD or a control MoAb-M-PVA-BPD conjugate. These results therefore demonstrate both the selectivity and specificity of this MoAb conjugate.

Table V. LD_{50} values for the phototoxic activity of BPD alone or conjugated to monoclonal antibodies. The 5E8-M-PVA-BPD has specificity for an antigen expressed on the A549 cells.

	LD_{50} (ηg/ml)	
Treatment	A549 cell line	M-1 cell line
BPD	150	85
T48-BPD	100	58
5E8-BPD	10	45

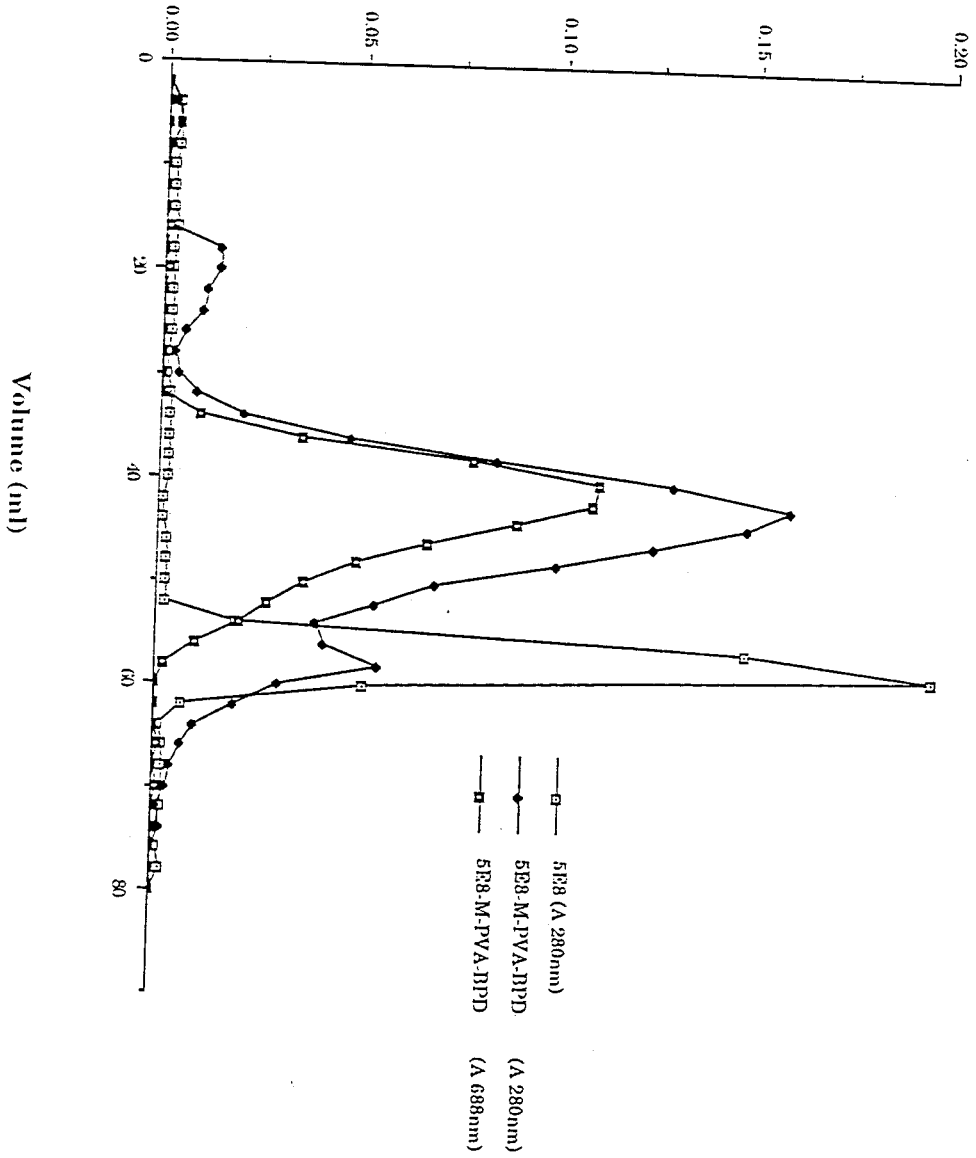

Figure 16. Elution profile of 5E8-M-PVA-BPD conjugate on a 1.5 × 45 cm Sepharose CL-4B column equilibrated with acetate buffer at pH 5.5. The flow rate was 0.43 ml/min and each fraction was 2 ml.

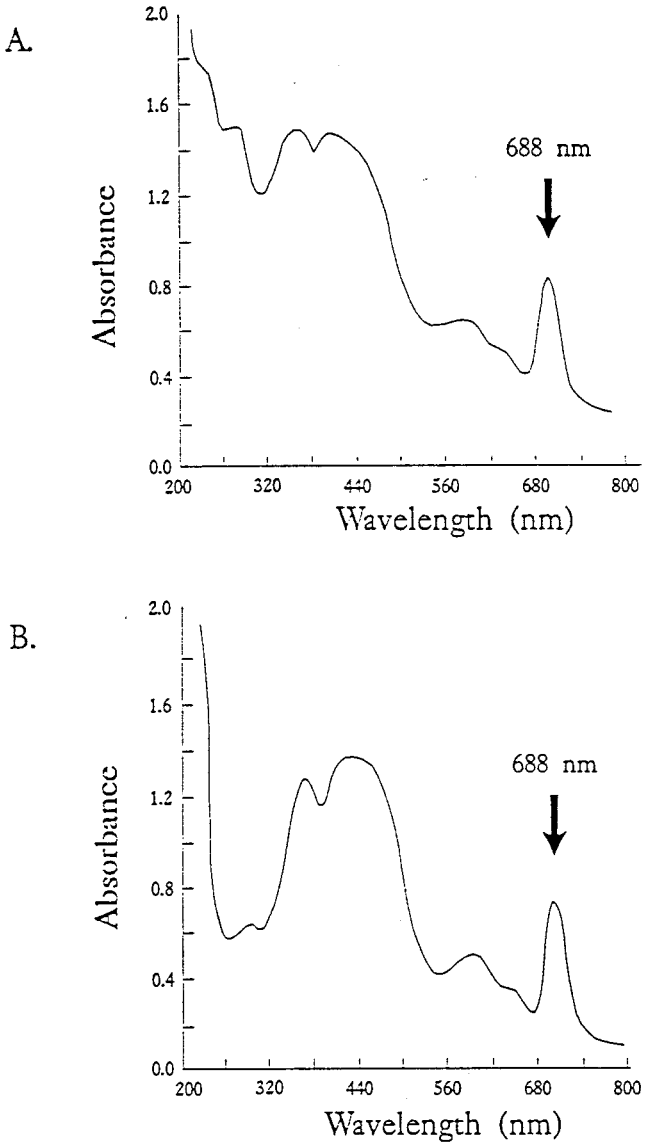

Figure 17. The absorption spectrum of 5E8-M-PVA-BPD conjugate (A) and BPD (B) in the range from 200 to 800 nm. Both materials were dissolved in PBS. Concentration of each material was adjusted to the comparable level.

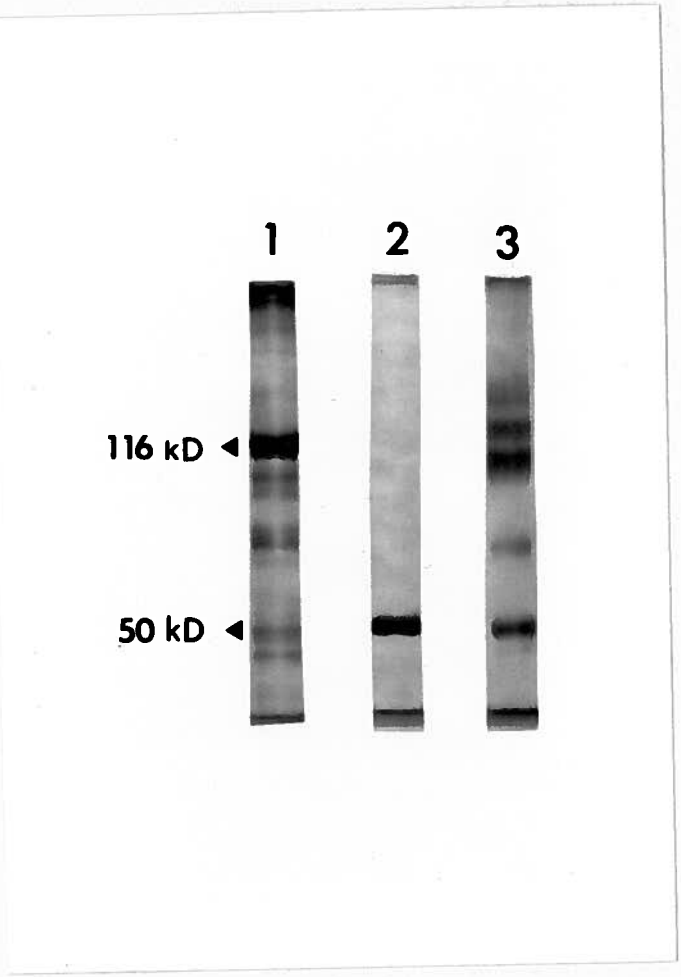

Figure 18. SDS-PAGE analysis of 5E8-M-PVA-BPD conjugate eluted from a Sepharose CL-4B column. Lane 1, MW markers; Lane 2, 5E8; Lane 3, 5E8-M-PVA-BPD conjugate.

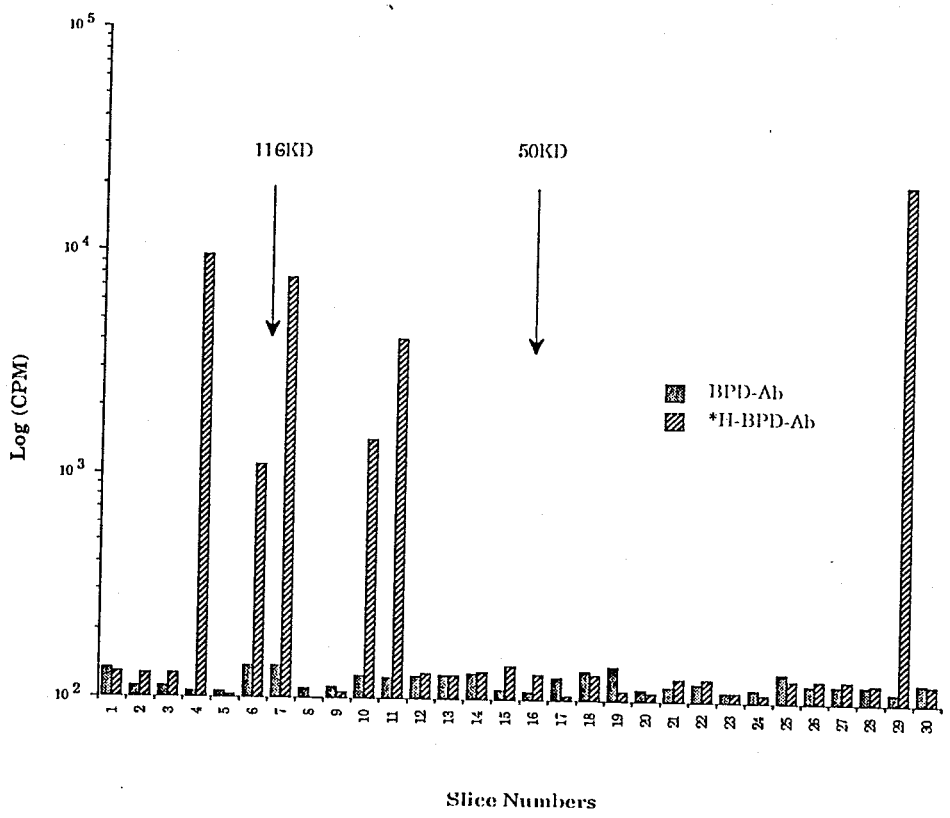

Figure 19. Radioactivity in gel slices. Samples containing either ^{3}H-BPD-PVA-5E8 or BPD-PVA-5E8 were run on a 7.5% reducing gel. After electrophoresis, gels were cut into 2 mm slices from the top and transferred to scintillation vials containing 10 ml of 3% protosol in econofluor. After soaking and eluting, radioactivity was measured. The results showed that the high counts were only found to be associated with the 75 kD, 100 kD, 120 kD and 150 kD bands in the ^{3}H-BPD-M-PVA-5E8 lane. BPD-M-PVA-5E8 lane gave only background readings. The efficiency was 45.3%.

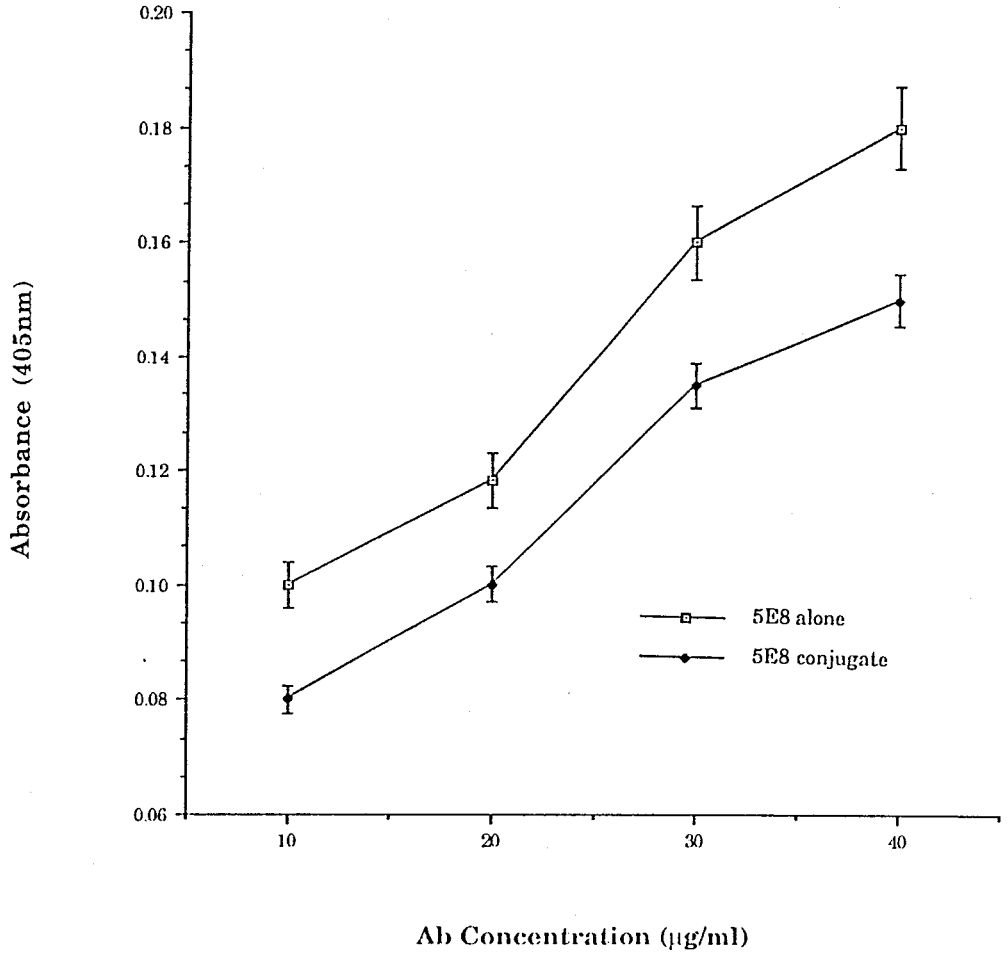

Figure 20. The comparison of specific activity of conjugated Ab with non-conjugated Ab on A549 using ELISA. Results are expressed as mean ± SD (bar).

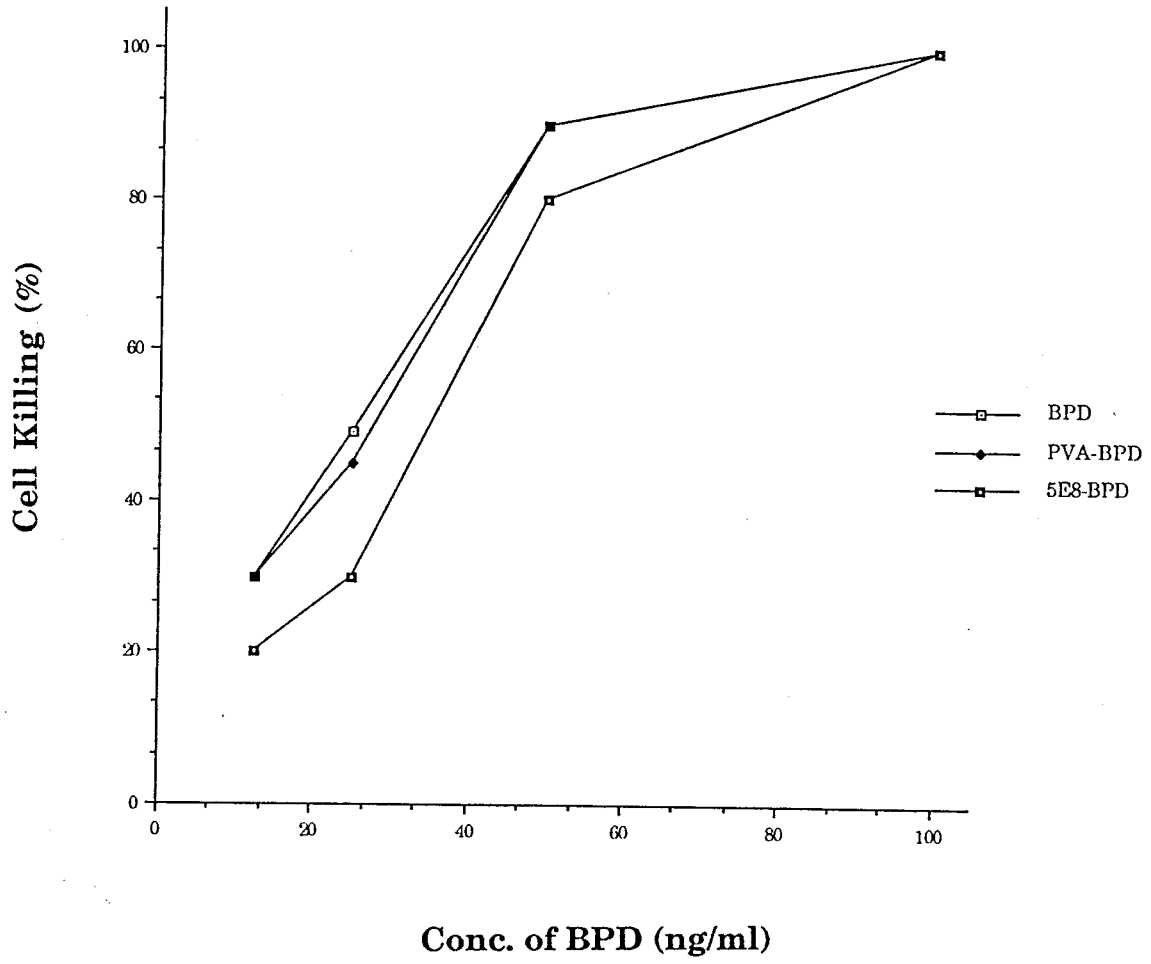

Figure 21. Phototoxic killing of A549 cells with the 5E8-M-PVA-BPD conjugate, M-PVA-BPD and BPD following 2 h incubation with photosensitizer preparations in the absence of serum. Light : 21.6 J/cm^2, 300-750 nm wavelength.

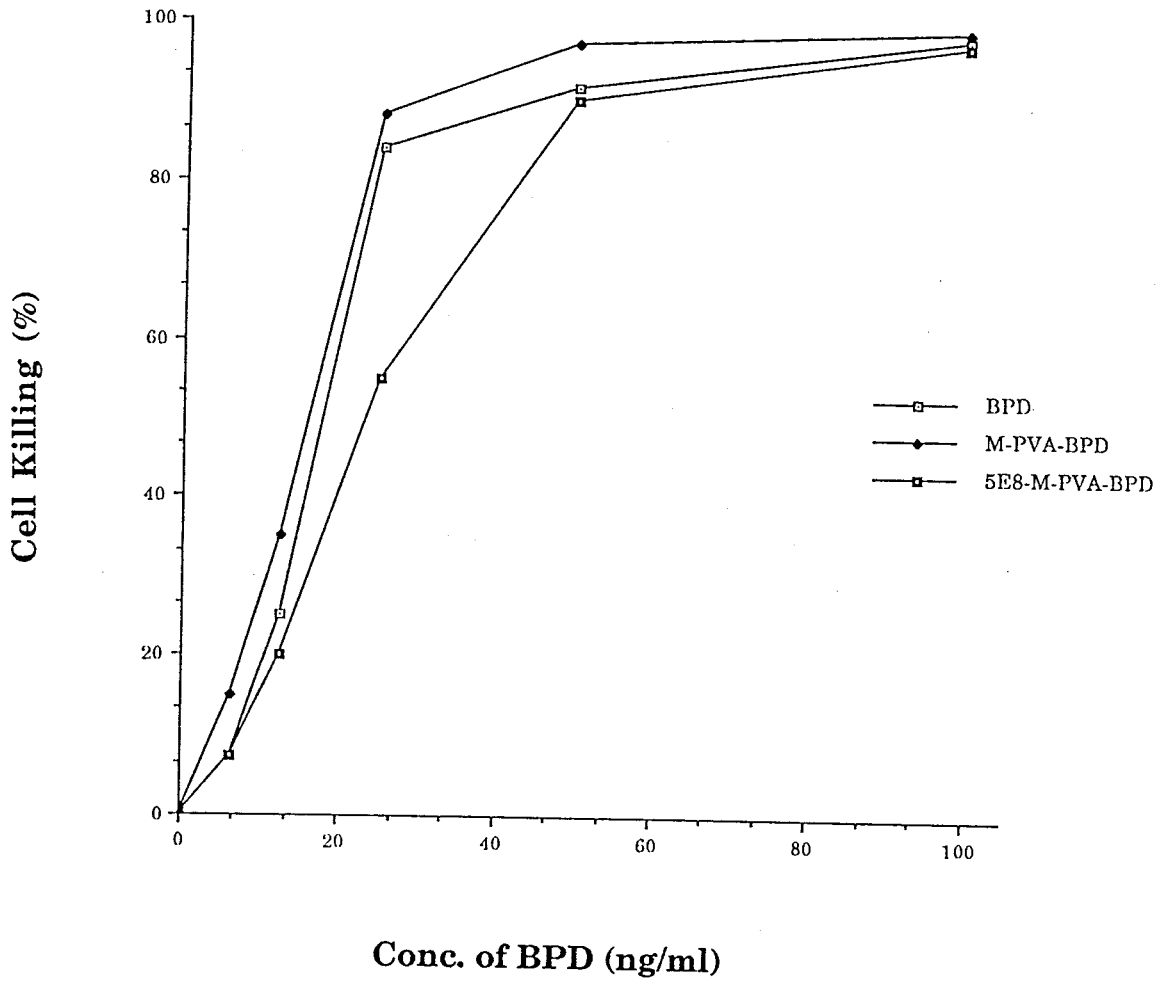

Figure 22. Phototoxic killing of A549 cells with 5E8-M-PVA-BPD conjugate, M-PVA-BPD and BPD following 24 h incubation with photosensitizer preparations in the absence of serum. Light dose : 21.6 J/cm^2, 300-750 nm wavelength.

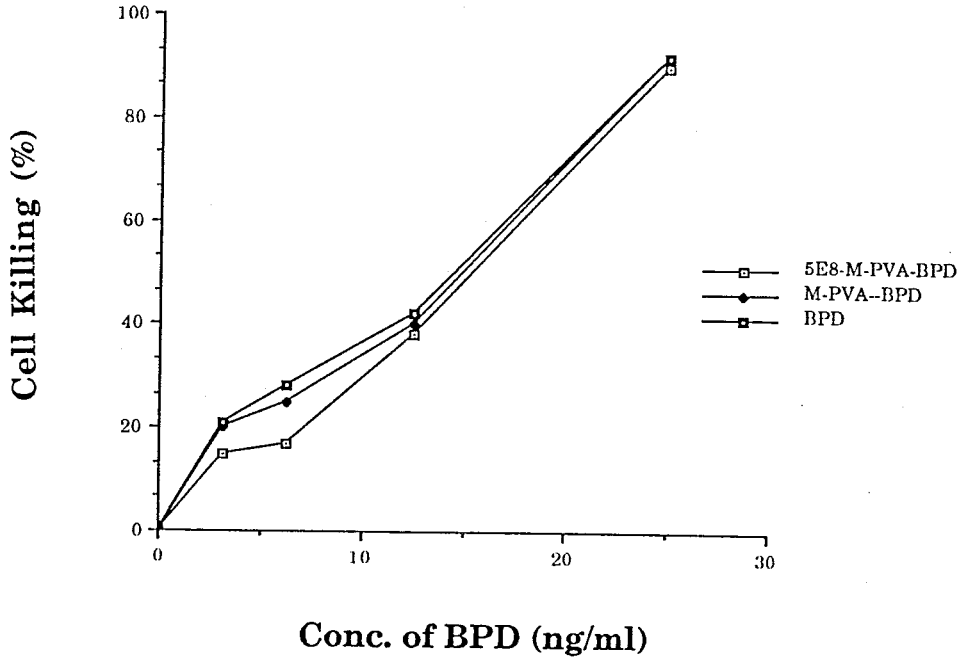

Figure 23. Phototoxic killing of M-1 cells with the 5E8-M-PVA-BPD conjugate, M-PVA-BPD and BPD in the absence of serum. Light dose : 21.6 J/cm^2, 300-750 nm wavelength.

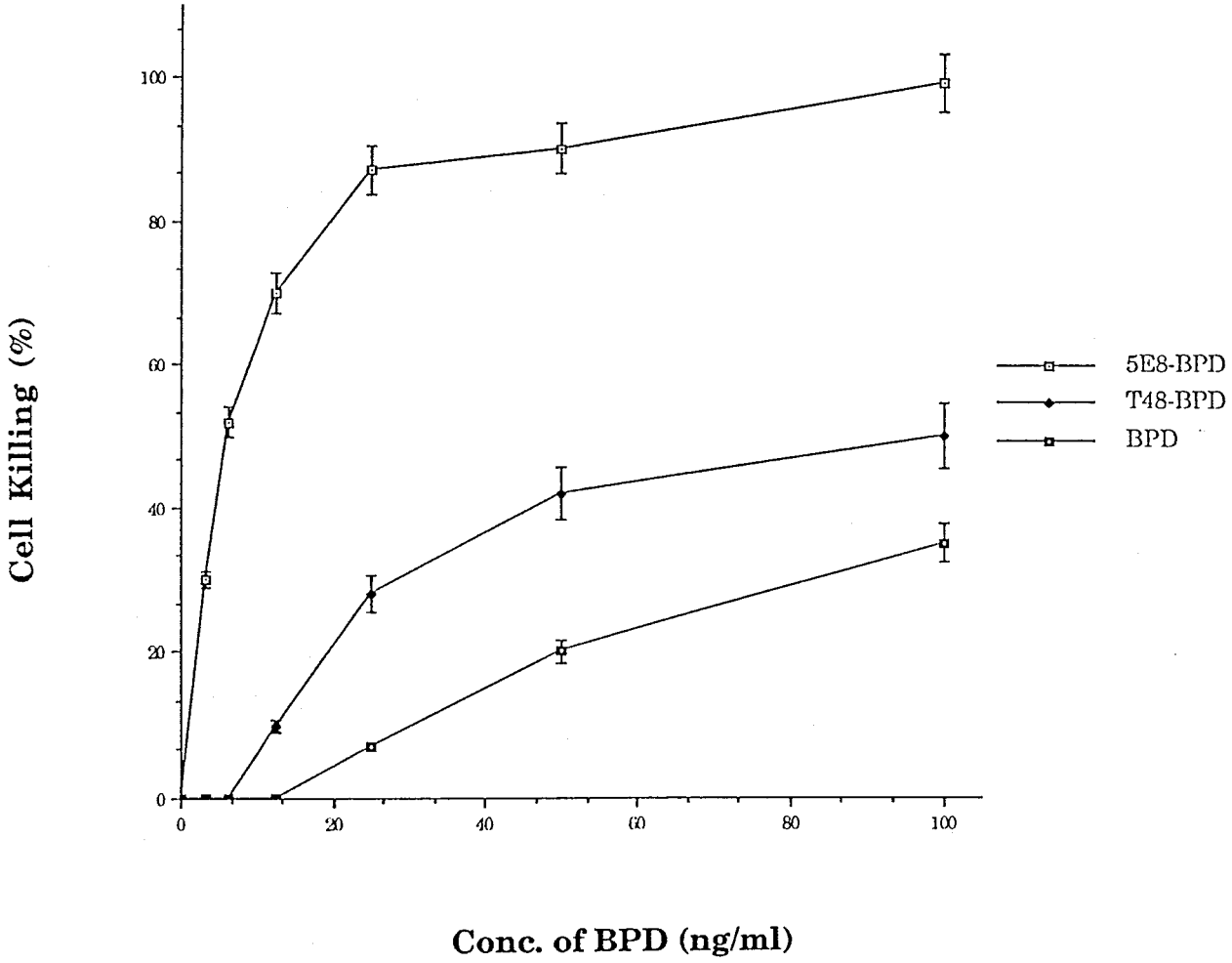

Figure 24. Phototoxic killing of A549 cells with the 5E8-M-PVA-BPD conjugate, T48-M-PVA-BPD and BPD in the presence of 10% FCS. Light dose: 21.6 J/cm^2, 300-750 nm wavelength. Results are expressed as mean ± SD (bar).

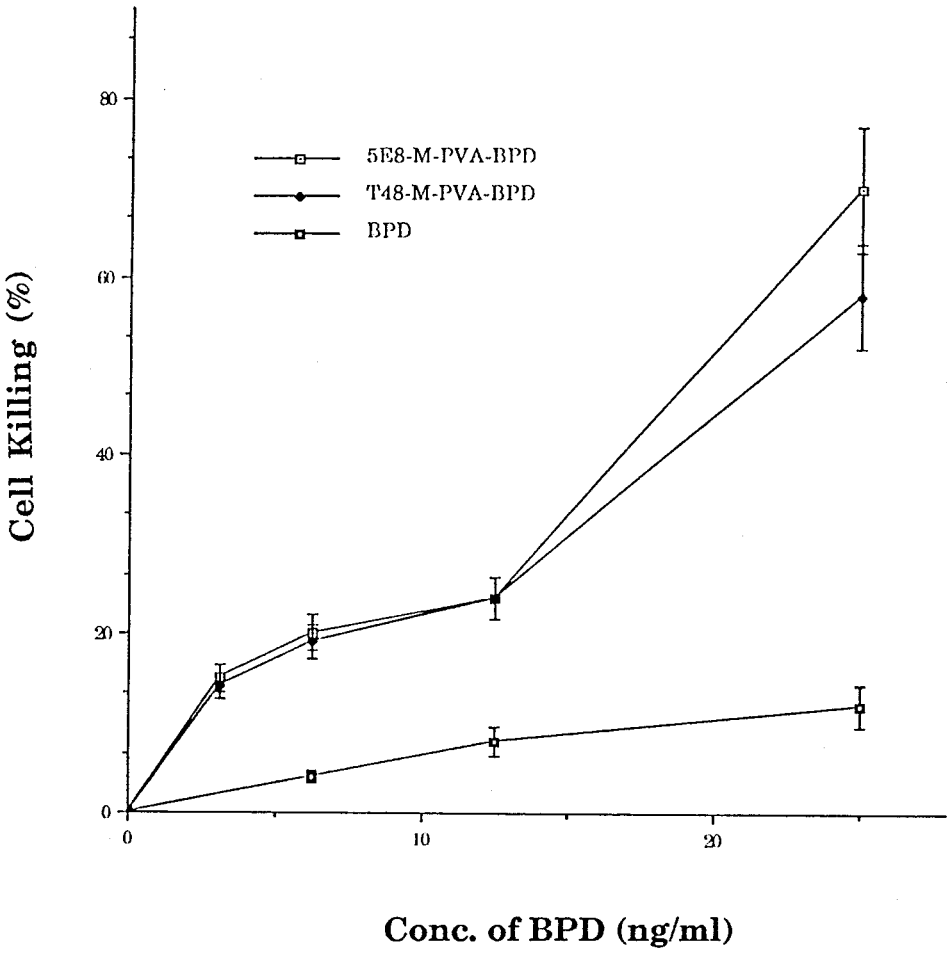

Figure 25. Phototoxic killing of the M-1 cell line with the 5E8-M-PVA-BPD conjugate, T48-M-PVA-BPD and BPD in the presence of 10% FCS. Light dose: 21.6 J/cm^2, 300-750 nm wavelength. Results are expressed as mean ± SD (bar).

CHAPTER V. MEMBRANE ASSOCIATED VS INTERNALIZED MOAB-BPD CONJUGATE IN PHOTODYNAMIC KILLING

Introduction

Previous chapters (I-IV) have described a novel therapy for cancer - Photodynamic therapy (PDT). We demonstrated that it is possible to enhance the efficacy of PDT by way of an improved drug delivery system - monoclonal antibody mediated drug delivery. In studies on the mechanism of the PDT, one interesting, yet unanswered question addresses whether PS molecules delivered to the surface of the target cell are as effective as those which are internalized into the cell prior to light activation. In the case of most immunotoxins, it is known that in order to initiate a cytotoxic action, they have to bind effectively to the target cell antigens via the antibody moiety (121) following which bound conjugates are endocytosed by the cells. After internalization, immunotoxins may be directed to lysosomes where they are degraded. However, a small portion of the immunotoxins escapes into the cytosol where its targets are located. There, the toxin may inhibit protein synthesis either by inactivating elongation-factor-2(diphtheria toxin, PE) or ribosomes (ricin, abrin etc. 122-124). Although the density of the target antigen on the cell membrane influences the effectiveness of immunotoxins, the cytotoxicity in many instances depends on the amount of internalized immunoconjugates (125). PS, unlike most conventional anti-cancer drugs, initiate their action by inducing the formation of singlet oxygens when they are activated by light. Singlet oxygen can then participate in

a number of photodynamic reactions which damage or kill cells. Although the actual site for MoAb-targeted singlet oxygen damage is not defined, the observation that the singlet oxygen can diffuse 0.2 micron suggested that the membrane may be a major target (126, 127). Therefore, the question of internalization becomes more interesting to determine. To address this question will not only help us to understand the mechanism of how the conjugates work in PDT, but also to provide important information on designing the formulation of the PS.

In this chapter, two monoclonal antibody-BPD conjugates (5E8-M-PVA-BPD and C7-M-PVA-BPD) were used to assess the efficacy of photodynamic killing outside or inside the target cells. MoAb 5E8 is specific for a M.W. 160,000 glycoprotein (gp160) on the surface of human lung cancer. Approximately 40% of the 5E8 bound to target cells (A549) is internalized 30 minutes after binding at 37°C (112). MoAb C7 reacts with the human low density lipoprotein (LDL) receptor. This antibody is also internalized by the target cells (GM3348B) at a rapid rate at 37°C. The results of our experiments suggest that cytotoxicity is enhanced by the internalization of conjugates in comparison to conjugates associated primarily with the cell membrane.

Materials and Methods

Monoclonal Antibodies

5E8 has been described in detail in Chapter IV. C7 is an IgG_1 a monoclonal antibody directed against the human and bovine low density lipoprotein (LDL) receptor. This antibody has been well characterized and described in detail elsewhere (128). In normal fibroblasts, the receptor-bound monoclonal antibody (C7) was taken up and degraded at 37°C at a rapid rate similar to that for LDL (128). The antibody was purified from ascites over protein A column and was stored at -20°C.

Cell Lines

Three fibroblast cell lines were used in these experiments. GM3348B is a normal fibroblast cell line. GM2408B is a mutant cell line which has LDL receptors but is internalization-defective (2-25% of normal LDL receptor activity). GM2000E is a mutant cell line which has no LDL receptors (<2% of normal LDL receptor activity) (Human Genetic Mutant Cell Repository, Camden, New Jersey). Fibroblast cells were maintained in the DME medium with 20% FCS.

Conjugation of C7 to BPD

C7 was linked to M-PVA-BPD through SMBS. The procedure used here was exactly the same as that of T48 or 5E8 (see chapter III).

Characterization of C7-M-PVA-BPD Conjugates

C7-M-PVA-BPD was purified through the Sepharose CL-4B column as described earlier for T48 and 5E8 (Chapter III). The elution profile was very similar to that of the T48 or 5E8.

Membrane Associated versus Internalized MoAb-BPD Conjugates

A. 5E8-M-PVA-BPD:

5E8 is rapidly internalized by target cells (A549) at 37°C (112). The internalization of 5E8 is inhibited when cells are incubated at 4°C. This feature was used to assess the surface associated vs internalized 5E8-M-PVA-BPD conjugate in the photodynamic killing of target cells by carrying out the experiments at different temperatures (i.e. either at 4 or 37°C). In brief, 96-well plates, in which both A549 (target) and M-1 (control) cell lines were grown, were cooled to 4°C for 30 min before addition of different BPD preparations pre-chilled to 4°C (5E8-M-PVA-BPD, T48-M-PVA-BPD and BPD). One set of plates was

incubated with the various conjugates at 37°C and the other at 4°C for 1 h. Both sets were washed with PBS 3 times and replaced with plain medium. Both sets were then exposed to laser light at a wavelength of 688 nm at a power density of 2 mW/cm^2. Laser light was produced by an argon-ion (Series 2000, Spectra-Physics, Mountain View, CA) pumped dye laser (model 590, Coherent Laser Products Division, Palo Alto, CA) containing DCM dye (Eastman Kodak, Exciton Chemical Co. Dayton, OH). Light treatment of all plates was carried out on ice. After light exposure, both plates were returned to the 37°C incubator. Thus, the only difference in treatment was the temperature at which cells were exposed to the immunoconjugates. The MTT test was performed on the next day as described in previous chapters (II and III).

B. C7-M-PVA-BPD:

5×10^3 cells/well of GM3348B, 1×10^4 cells/well of GM2408B or 5×10^4 cells/well of GM2000E were seeded into 96-well plates. Fibroblasts were grown in lipoprotein deficient serum (LPDS) medium for 48 hours before use. This procedure causes an increase in the number of LDL receptors on the cells (126). C7-M-PVA-BPD or T48-M-PVA-BPD was added to the cells at various concentrations and incubated at either 4 or 37°C. The remaining steps of the cytotoxicity experiment were the same as described above.

Immunofluorescent Patterns of 5E8-M-PVA-BPD on A549 and M-1 Cell Lines

Immunofluorescence experiments were performed using A549 and M-1 cell lines and 5E8-M-PVA-BPD, T48-BPD and BPD. The method has been described in detail elsewhere (126). Briefly, monolayers of A549 and M-1 cells were grown on cover slips. When confluent, the coverslips were chilled at 4°C for 30 min. Each coverslip was transferred to a fresh petri dish and then overlaid with 200 μl cold PBS containing the different photosensitizer preparations. Coverslips were incubated at either 4°C or 37°C for 1 h followed by 3 washes with PBS/BSA. Cells were fixed for 15 min in 3% paraformaldehyde in buffer D (10 mM sodium phosphate and 50 mM NaCl at pH 7.4) at room temperature. Cells were rinsed once with 2 ml of 50 mM NH_4Cl_2 and twice with buffer D. For the slides incubated initially at 37°C, 3 ml of buffer D containing 0.05% Triton X-100 was added and the slides were placed on ice. Both sets of coverslips were placed in new petri dishes and incubated for 1 h at 37°C with fluorescein-coupled goat anti-mouse IgG that recognized the mouse MoAbs. Coverslips were washed with PBS/BSA and mounted on glass slides with 90% glycerol in 0.1 M Tris/chloride and observed under the fluorescent microscope. The slides were viewed with a Zeiss photomicroscope equipped with a 100-Watt mercury epifluorescence light source and the appropriate filter package. Since BPD emits red fluorescence when excited, its location can be easily visualized. Photographs were taken on Kodak Tri-X film at an ASA of 400 using the automatic photometer of the Zeiss instrument.

Results

Effects of Internalization on the Cytotoxicity of the 5E8-M-PVA-BPD Conjugate on A549 Cells

When incubation was carried out at 37°C, the 5E8-M-PVA-BPD conjugate, specific for A549 cells, produced significantly greater cytotoxicity than that of the control conjugate (T48-BPD) or free BPD (Fig. 24). The LD_{50} for the 5E8-M-PVA-BPD conjugate at 37°C was 10 ηg/ml. However, it required at least 100 ηg/ml of the control conjugate or free BPD to achieve the same cytotoxicity (Table VI). This represents a ten fold difference in the LD_{50} between the specific and non-specific MoAb conjugates. When the two MoAb-BPD conjugates (5E8-M-PVA-BPD and T48-BPD) were incubated with the control M-1 cells at 37°C, no enhanced killing was observed with the 5E8 conjugate (Fig. 25). Both MoAb conjugates produced a similar level of cytotoxicity which was slightly higher than free BPD (Table VI). When the cytotoxicity assay was performed at 4°C with A549 cells, the 5E8-M-PVA-BPD conjugate was less effective than at 37°C (Fig. 26). The LD_{50} of the 5E8-M-PVA-BPD conjugate was 100 ηg/ml as opposed to 200 ηg/ml for free BPD (Table VI). Comparing the cytotoxicity of 5E8-M-PVA-BPD on target cells at 37 and 4°C, one sees a ten-fold difference ($p < 0.01$) indicating that the internalized conjugate can produce greater killing effects than that of surface associated materials. Using the same treatments, killing of a control cell line (M-1) at 4°C was less efficient (Fig. 27). The LD_{50} for 5E8-M-PVA-BPD and T48-BPD was 50 ηg/ml and 75 ηg/ml, respectively. Comparing

the cytotoxicity of 5E8-M-PVA-BPD and T48-M-PVA-BPD on this control cell line at 4 and 37°C, only a 1-2 fold increase in cytotoxicity was observed which is thought to be solely due to the temperature difference.

Effects of Internalization of C7-M-PVA-BPD Conjugates on Cytotoxicity

C7 is a MoAb which reacts specifically with the LDL receptor. This MoAb is internalized by the target cells through a receptor mediated process which occurs at 37°C. At 4°C, C7 will bind with high avidity to receptors but will not be internalized (128). Efficacy of C7-M-PVA-BPD complexes at killing fibroblasts (GM3348B, GM2204B or GM2000E) cells at both 37 and 4°C was determined in order to evaluate the role of internalization on photodynamic killing. In one experiment, performed at 37°C, C7-M-PVA-BPD showed greater killing than that of control conjugate (Fig. 28). When a similar experiment was performed at 4°C, the cytotoxicity of both drug preparations decreased (Fig. 29). The LD_{50} for C7-M-PVA-BPD and T48-M-PVA-BPD was 8 and 25 ηg/ml respectively (Table VII). Comparing the cytotoxicity of C7-M-PVA-BPD at 4 and 37°C, one observes almost a four-fold difference. Using the internalization defective GM2408B as the target cells, the cytotoxicity between 37 and 4°C of any drugs tested here was similar (Fig. 30, 31). The lack of internalization of this particular cell line could explain why there is no difference of killing between 37 and 4°C. This further supports the notion that internalization plays an important role in cytotoxicity of photosensitizers. When GM2000E cells (which have no LDL receptors) were incubated with the drugs at two

different temperatures, the difference in photodynamic killing was not distinct (Fig. 32, 33). The LD_{50} for all the drugs at either 37 or 4°C was greater than 25 ηg/ml.

Immunofluorescence Experiments

To actually visualize the difference between membrane associated and internalized conjugates, a series of immunofluorescence experiments were carried out. In A549 cells, significant levels of red fluorescence was observed in 5E8-M-PVA-BPD treated cells at 4 and 37°C (Fig. 34, 35). A different staining pattern, however, was observed between surface associated and internalized 5E8-M-PVA-BPD. The former seemed to stain more faintly and sporadically whereas the staining of the latter cells was brighter and more concentrated. In comparison, very faint nonspecific staining was seen in A549 cells incubated with T48-M-PVA-BPD or BPD (Fig. 36, 37). Little fluorescence could be seen in M-1 cells with any of the three drugs (data not shown).

Discussion

Many PS molecules under investigation for possible use in PDT share the property of selective accumulation in abnormal tissues, such as malignant tissues. However, the mechanisms by which this occurs is not understood, as is not the role of specific localization. The studies described in this chapter attempted to investigate these issues at a preliminary level. The main question addressed here was whether PS molecules delivered to the surface of the target cell were as effective as those which are internalized prior to light activation. Delivery of BPD via a MoAb conjugate (5E8-M-PVA-BPD) produced very selective killing to the target cell line (A549). For most immunotoxins the internalization of cell-bound complexes and appropriate intracellular processing, to allow drugs to reach certain organelles, is essential to produce cell death (121-123). Adequate amounts of immunoconjugates must first react with the cell surface membrane antigens. Such immunotoxins must then undergo internalization and appropriate intercellular trafficking for cytotoxicity to be elaborated. Some studies indicate that the amount of internalized immunoconjugate parallels the cytotoxicity of the drug. In this study, we compared the cytotoxicity of surface associated versus internalized conjugates on the target and control cell lines. Our principal objective was to determine the effect of internalization on photodynamic killing.

Since both 5E8 and C7 monoclonal antibodies bind to the membrane of the target cells at 4°C and are internalized at 37°C, we used these two MoAbs to assess the cytotoxicity

of surface associated and internalized conjugates. We designed experiments in such a way that we could determine the cytotoxicity of either cell surface or internalized PS (see Materials and Methods). We found that internalization of the conjugate could enhance cell killing by four to ten times. Specifically, the internalized 5E8-M-PVA-BPD conjugate showed 10-fold higher killing on A549 cells than that of membrane bound materials. It is known that the 5E8 MoAb is internalized by the target cells at a relatively fast rate. About 30 minutes after incubation of 5E8 with A549 cells at 37°C, up to 40% of membrane bound antibody is internalized. This high accumulation of 5E8-M-PVA-BPD inside the cells within a short period of time was thought to result in a higher cytotoxicity than seen with cells incubated at 4°C. Since it is assumed that the conditions of the experiment were saturating for the conjugates, it was assumed that the same number of molecules of conjugate were involved at both 4°C and 37°C. Therefore differences observed in cell killing should be attributable to the location of the PS and not the amount associated with each cell.

In the case of C7-M-PVA-BPD, when killing experiments were performed using normal fibroblasts (GM3348B) the internalized conjugate had only 4-fold higher killing than that of surface associated materials. At 4°C the activity of C7-M-PVA-BPD was relatively high (LD_{50} = 8 ηg/ml) and the conjugate produced greater killing than BPD alone in the presence of FCS. The LD_{50} for C7-M-PVA-BPD was only 8 ηg/ml. This relatively high cytotoxicity caused by membrane associated C7 conjugate decreased the difference of internalized vs membrane bound conjugates in cell killing. The following factor may

contribute to this increased cytotoxicity of C7-M-PVA-BPD at 4°C. That is, that although internalization of C7 via the LDL receptor is reduced 90% at 4°C, the avidity of the receptor is higher (128). Therefore, there may actually be more of the C7-M-PVA-BPD present on the surface of these cells at 4°C than that at 37°C. Given the high level of cytotoxicity of C7-M-PVA-BPD at 4°C, the 4-fold greater killing observed at 37°C may indicate that internalization of BPD exposed particularly sensitive intracellular targets to the action of the PS.

When an internalization defective cell line (GM2408B) was used to test the difference of cytotoxicity between 37 and 4°C, one would not expect any significant difference, since these cells cannot internalize the conjugate regardless of incubation temperature. The results of these experiments indeed showed very similar cytotoxicity at the different temperatures on this cell line. These results support the above findings that internalization of the conjugate is very important. These findings would suggest that either internalized MoAb-PS delivers the cytotoxic signal more readily than that of surface associated conjugate, or that intracellular organelles are more susceptible to photodynamic damage than are membranes. The cytotoxcity results on GM2000E cells indicated that the absence of LDL receptors on these cells made them more resistant to photodynamic killing by either PS alone or conjugated to MoAbs. The temperature did not seem to affect the efficacy of cytotoxicity of PS either.

The immunofluorescence experiments were designed to visualize the difference between

surface associated versus internalized conjugates on target and control cells. It was observed that the internalized conjugates and the surface associated materials exhibited different staining patterns. Internalized conjugates stained more brightly and abundantly indicating cytoplasmic localization whereas the surface associated staining was weaker and more sporadic which is characteristic of membrane straining. These results showed distinct qualitative differences between internalized as opposed to surface associated BPD, and are compatible with predictions made regarding location of the PS at 37°C vs 4°C. These procedures did not permit quantitation of BPD under the experimental conditions, nor were intracellular targets identifiable. Further studies using radiolabeled conjugates and confocal microscopy would clarify these issues.

Chapter Summary

The experiments designed in this chapter were designed to determine whether internalized MoAb-PS conjugates would cause higher phototoxicity than that of membrane bound materials. Two MoAb-PS conjugates, 5E8-M-PVA-BPD and C7-M-PVA-BPD, were tested. The 5E8 MoAb reacts specifically with a cell surface glycoprotein associated with human squamous cell carcinomas of the lung. C7 has specificity for human LDL receptors. Both 5E8 and C7 are internalized by target cells at 37°C. This internalization is inhibited when cells are incubated at 4°C. The cytotoxicity assays were therefore performed at both 37°C and 4°C to compare the efficacy of membrane bound and internalized conjugates. In one series of experiments, 5E8 conjugates were tested on target cells (A549) at both temperatures. It was shown that the internalized 5E8 conjugates had much higher cytotoxicity than that of membrane bound materials. The difference was 10-fold. In another series of experiments, C7 conjugates were examined on target cells (GM3488B) at both temperatures. The results showed that the internalized conjugates caused greater cytotoxicity than that of membrane bound conjugates. These preliminary experiments suggest that both internalized MoAb-PS conjugates deliver cytotoxic signals more readily than do membrane bound materials or that certain intracellular organelles are more susceptible to photodynamic killing.

Table VI. BPD concentration (ηg/ml) required to kill 50% of cells (LD_{50}) under various conditions.

Cell Line	M-1		A549	
Treatment	37°C	4°C	37°C	4°C
5E8-BPD	45	50	10	100
T48-BPD	58	75	100	200
BPD	85	140	>100	200

Table VII. BPD concentration (ηg/ml) required to kill 50% (LD_{50}) of GM 3348B (normal human fibroblast) cells under various conditions.

Treatment	37°C	4°C
C7-M-PVA-BPD	2.6	8
T48-M-PVA-BPD	11	>25

Table VIII. BPD concentration (ηg/ml) required to kill 50% (LD_{50}) of GM2408B (have LDL receptors but no internalization) cells under various conditions.

Treatment	37°C	4°C
C7-M-PVA-BPD	5	7.5
T48-M-PVA-BPD	>12.5	>25

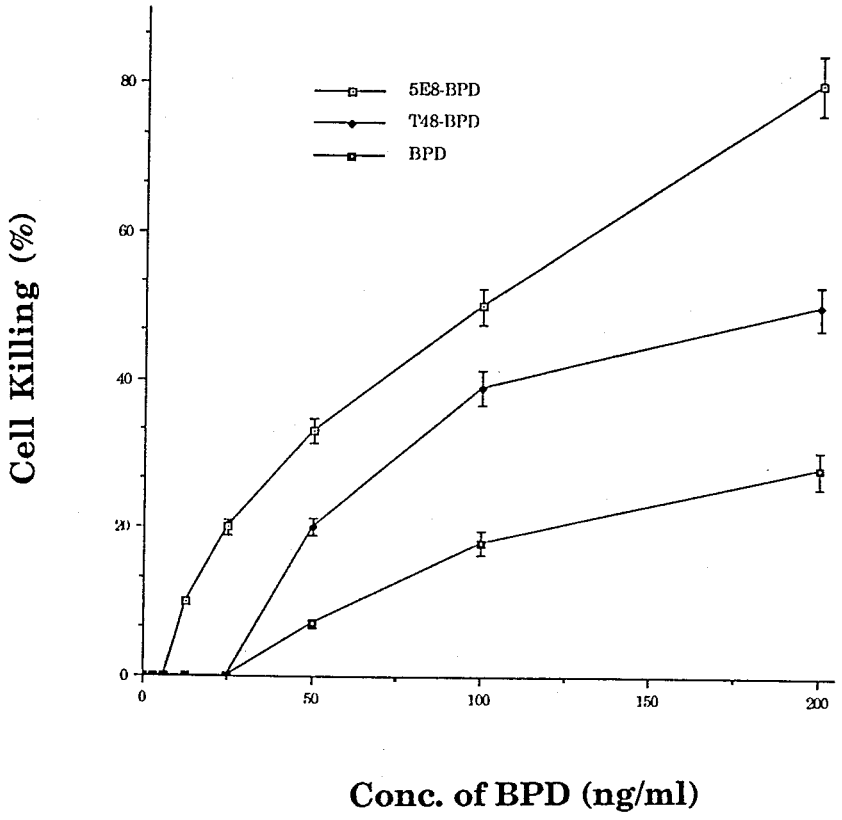

Figure 26. Cytotoxicity assay of MoAb-BPD conjugates on A549 cells at 4°C. BPD and the MoAb conjugates were diluted in DMEM with 10% FCS. Incubation of the photosensitizers with the cells was performed at 4°C and plates were exposed to 690 nm laser light on ice. Results are expressed as mean ± SD (bar).

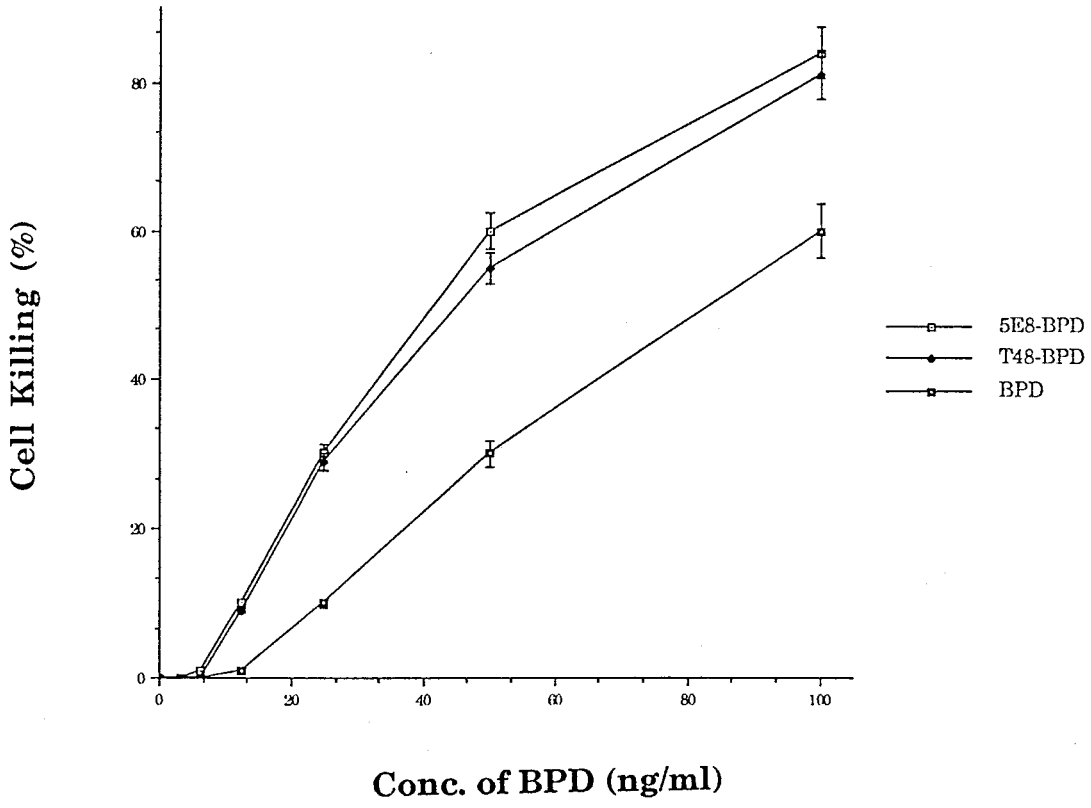

Figure 27. Cytotoxicity assay of MoAb-BPD conjugates on M-1 cells at 4°C. 5E8-M-PVA-BPD conjugate, T48-M-PVA-BPD and BPD were diluted in DMEM in presence of 10% FCS. Incubation of the PS with the cells was performed at 4°C and plates were exposed to 690 nm laser light for 1 h on ice. Results are expressed as mean ± SD (bar).

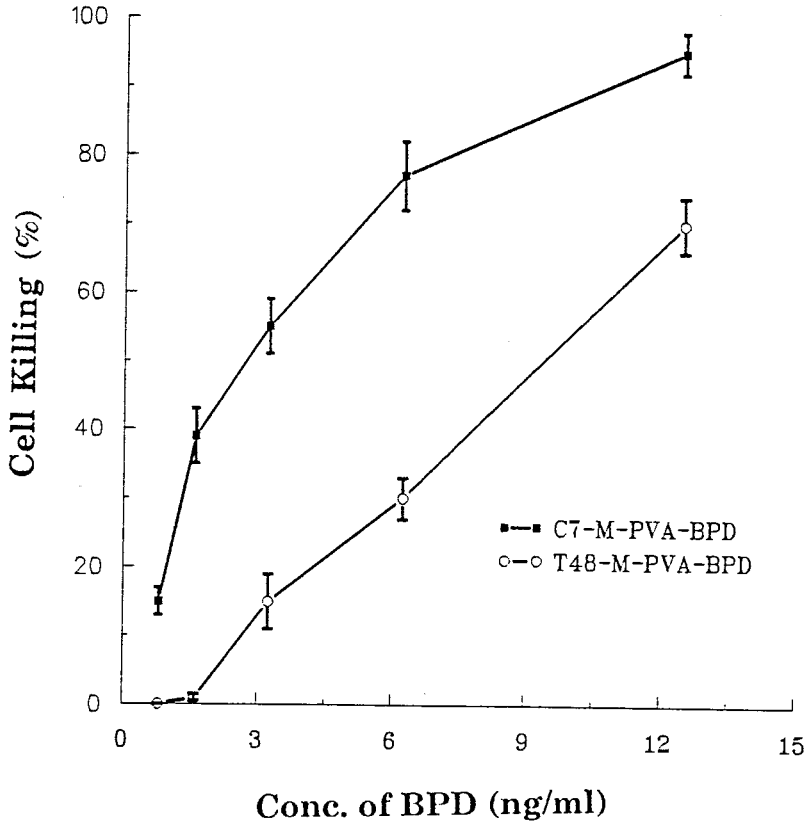

Figure 28. Cytotoxicity assay on GM3348B Fibroblasts. Cells were grown in 5% LPDS for 48 h before use. Two MoAb conjugates were diluted in DMEM containing 10% FCS. C7-M-PVA-BPD or the control was added and then cells were incubated at 37°C for 1 h. (Laser) Light exposure was performed at room temperature for 1 h. Results are expressed as mean ± SD (bar).

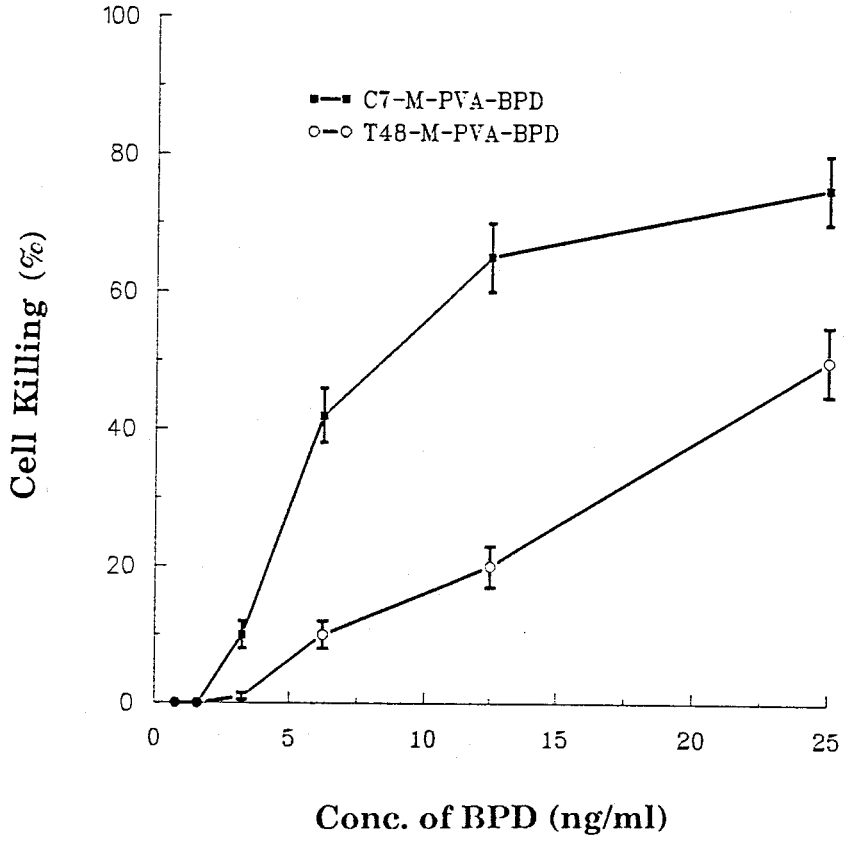

Figure 29. Cytotoxicity assay on GM3348B Fibroblasts at 4°C. Cells were grown in 5% LPDS for 48 h before use. Two MoAb conjugates were diluted in DMEM containing 10% FCS. C7 conjugate or the control was added and then cells were incubated at 4°C for 1 h. Laser light exposure was performed for 1 h on ice. Results are expressed as mean ± SD (bar)

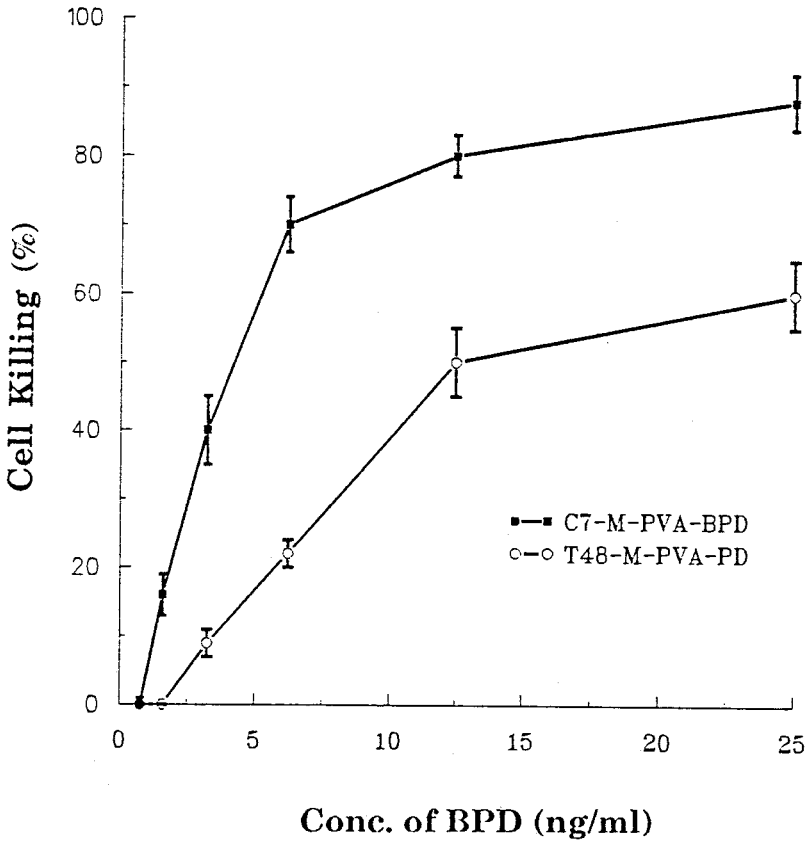

Figure 30. Cytotoxicity assay on GM2408B Fibroblasts at 37°C. Cells were grown in 5% LPDS for 48 h before use. Two MoAb conjugates were diluted in DMEM containing 10% FCS. C7 conjugate or the control was added and then cells were incubated at 37°C for 1 h. Laser light exposure was performed for 1 h at room temperature. Results are expressed as mean ± SD (bar).

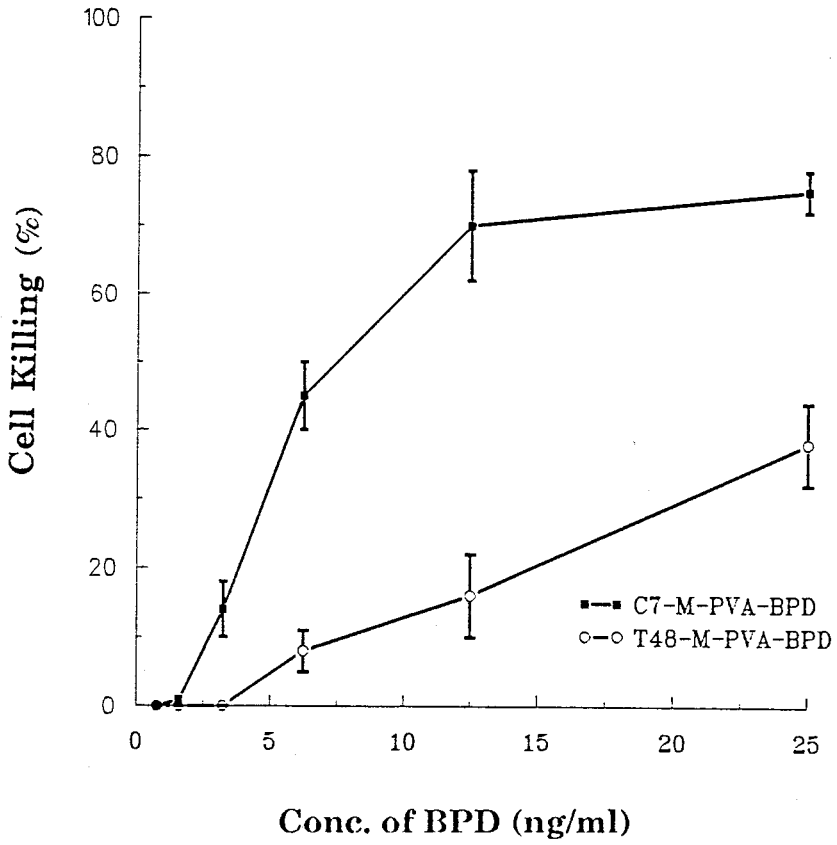

Figure 31. Cytotoxicity assay on GM2408B Fibroblasts at 4°C. Cells were grown in 5% LPDS for 48 h before use. Two MoAb conjugates were diluted in DMEM containing 10% FCS. C7 conjugate or the control was added and then cells were incubated at 4°C for 1 h. Laser light exposure was performed for 1 h on ice. Results are expressed as mean ± SD (bar).

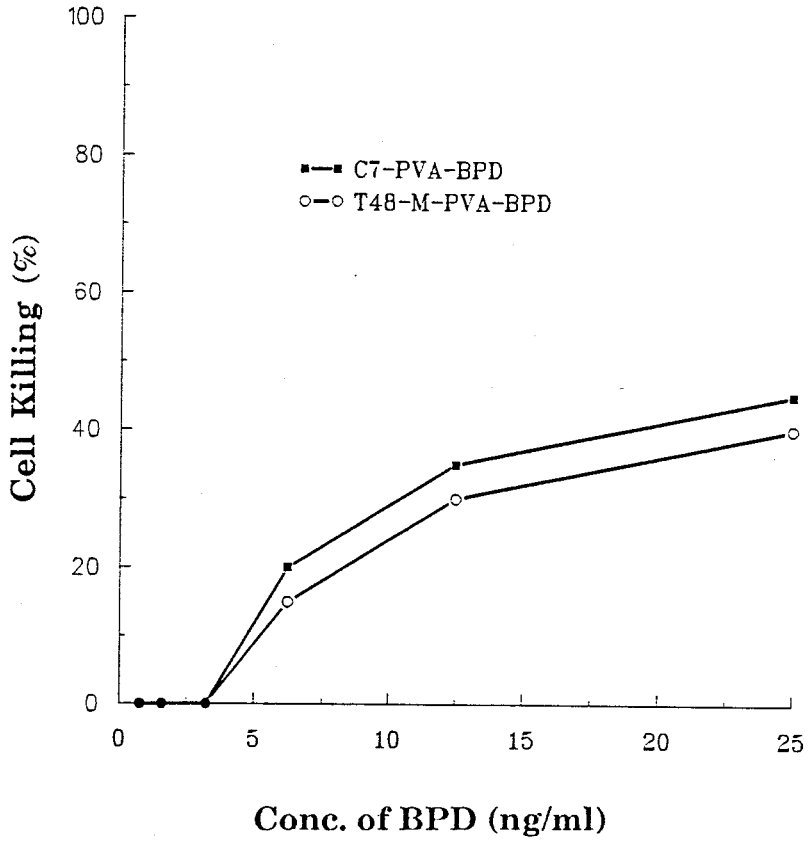

Figure 32. Cytotoxicity assay on GM2000E Fibroblasts at 37°C. Cells were grown in 5% LPDS for 48 h before use. Two MoAb conjugates were diluted in DMEM containing 10% FCS. C7 conjugate or the control was added and then cells were incubated at 37°C for 1 h. Laser light exposure was performed for 1 h at room temperature.

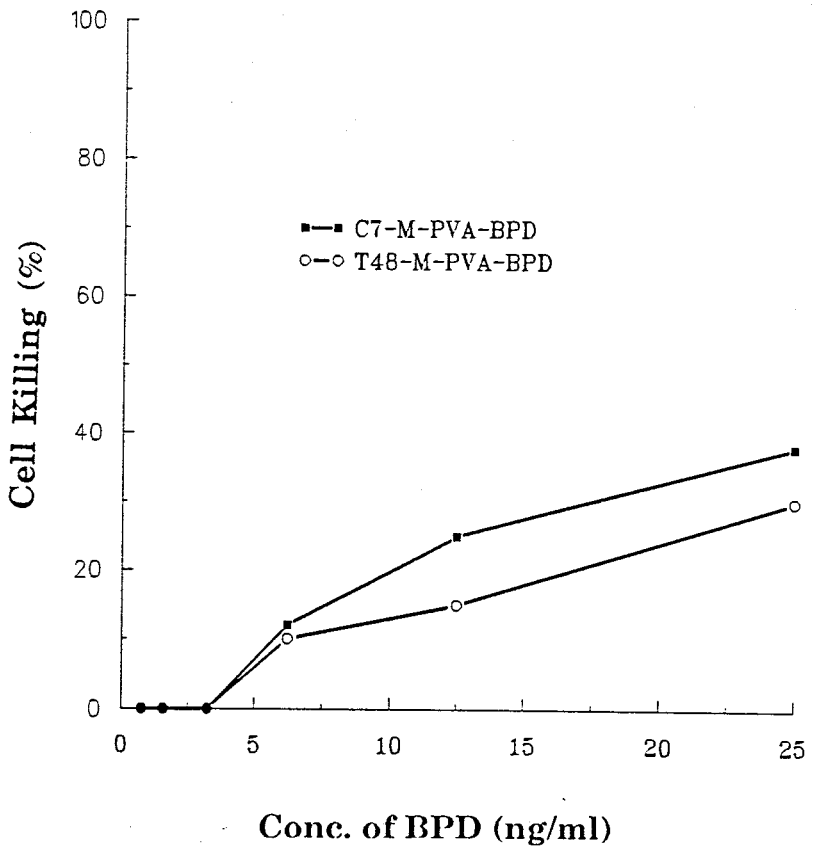

Figure 33. Cytotoxicity assay on GM2000E Fibroblasts at 4°C. Cells were grown in 5% LPDS for 48 h before use. Two MoAb conjugates were diluted in DMEM containing 10% FCS. C7 conjugate or the control was added and then cells were incubated at 4°C for 1 h. Laser light exposure was performed for 1 h on ice.

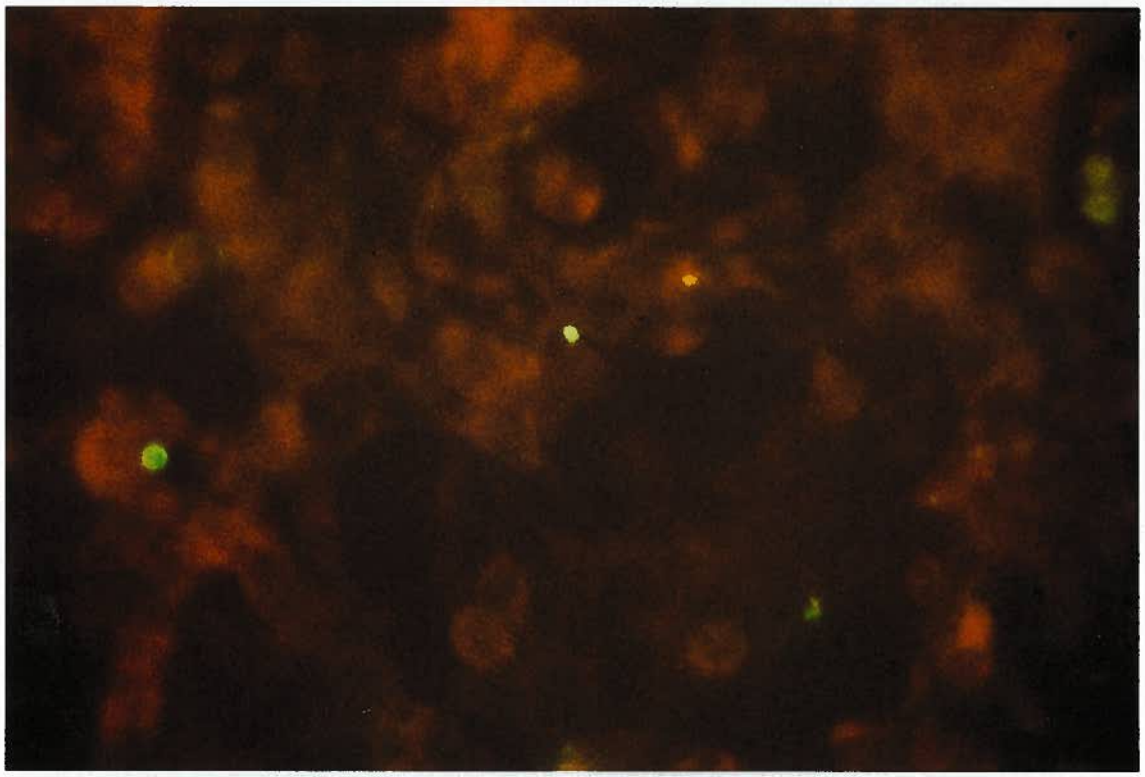

Figure 34. Immunofluorescent staining patterns of 5E8-M-PVA-BPD in A549 cells after incubation at 4°C for 1 h. Monolayers of A549 cells were grown on coverslips and incubated with 5E8-M-PVA-BPD at 4°C for 1 h. The coverslips were then washed, fixed, and processed for indirect immunofluorescent localization of surface conjugates.

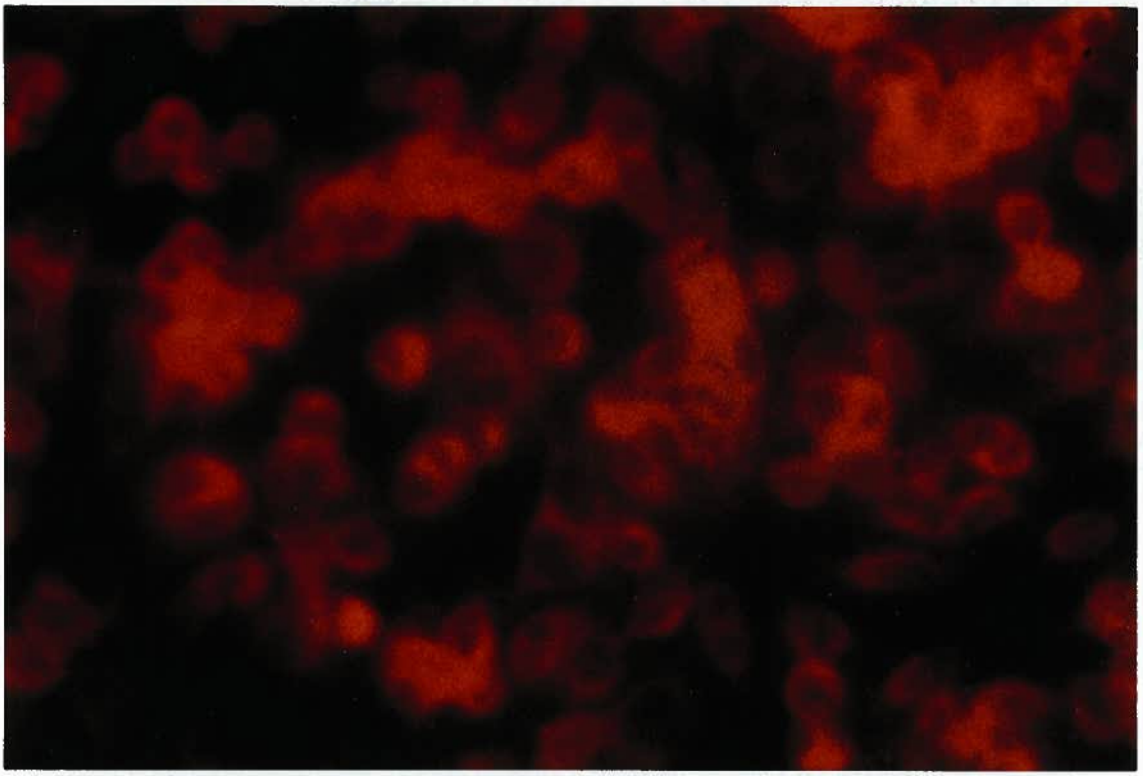

Figure 35. Immunofluorescent staining patterns of 5E8-M-PVA-BPD in A549 cells after incubation at 37°C for 1 h. Monolayers of A549 cells were grown on coverslips and incubated with 5E8-M-PVA-BPD at 37°C for 1 h. The coverslips were then washed, fixed, and processed for indirect immunofluorescent localization of internalized conjugates.

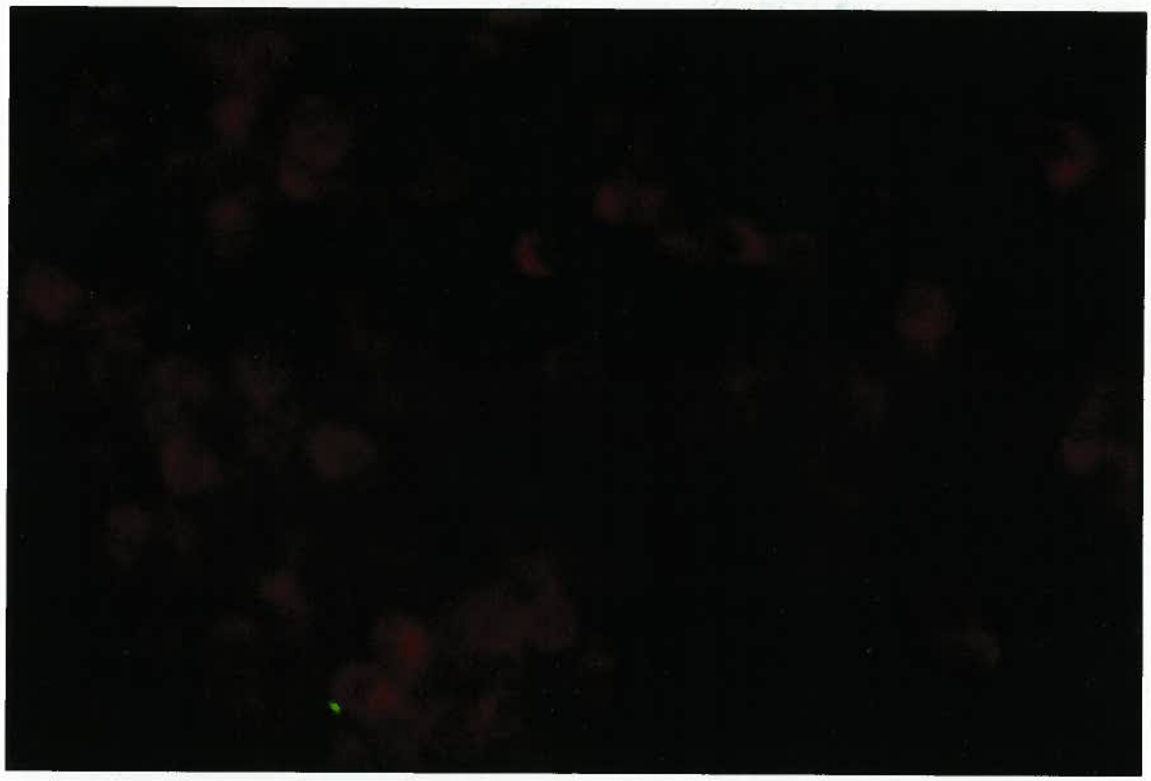

Figure 36. Immunofluorescent staining patterns of T48-M-PVA-BPD in A549 cells after incubation at 37°C for 1 h. Monolayers of A549 cells were grown on coverslips and incubated with T48-M-PVA-BPD at 37°C for 1 h. The coverslips were then washed, fixed, and processed for indirect immunofluorescent localization of surface conjugates.

Figure 37. Immunofluorescent staining patterns of BPD in A549 cells after incubation at 37°C for 1 h. Monolayers of A549 cells were grown on coverslips and incubated with BPD at 37°C for 1 h. The coverslips were then washed, fixed, and processed for indirect immunofluorescent localization of internalized PS.

CHAPTER VI. BIODISTRIBUTION OF A BENZOPORPHYRIN DERIVATIVE-MONOCLONAL ANTIBODY CONJUGATE IN A549 TUMOR BEARING NUDE MICE

Introduction

In previous chapters, we have demonstrated that the PS, BPD, can be covalently bound to MoAbs via a water soluble carrier (polyvinyl alcohol). These MoAb-PS conjugates have been tested in a number of in vitro experiments. It was first shown that the activity of both PS and MoAb was retained after the conjugation (chapter III). It was then demonstrated that a specific MoAb-PS conjugate, 5E8-M-PVA-BPD, caused ten times higher killing than that of control conjugates towards appropriate target cells. Furthermore, it was found that the internalized MoAb-BPD conjugates showed much greater cytotoxicity than the membrane bound materials. The ultimate goal of the project is to determine whether MoAb would be able to deliver PS to a tumor site in a specific manner in vivo. Currently, there are only three reports, in addition to one from this laboratory, regarding the biodistribution of MoAb-PS. In one report (96), the conjugate showed a strong time-dependent localization after intraperitoneal injection in nude mice with subcutaneously implanted human tumor. The distinct cellular localization only appeared 72 h after injection. These observations seemed consistent with our preliminary studies in vivo (68). In the other two reports (96, 97), the peak accumulation of the

specific conjugates in the tumor site occurred at 24 h. In the present study, we investigated the biodistribution of M-PVA-BPD-5E8 conjugates in nude mice bearing the A549 tumor and compared it to that of a control antibody-BPD conjugate and of free BPD. The results indicated that BPD remained bound to the 5E8 MoAb after i.v. injection and that 5E8 MoAb was able to deliver BPD to A549 tumor in a specific manner. In addition, we showed that the highest tumor accumulation appeared between 14 and 24 h. This seemed to be similar to the other two reports (96, 97).

Materials and Methods

Cell Lines

The A549 and the M-1 cell lines were described previously (chapters II and IV). Both cell lines form adherent monolayers in vitro, and were cultured in a 5% CO_2 humidified incubator. They were harvested, while still in logarithmic growth, using 10% trypsin in medium, washed and diluted in medium at the concentration required for injection into the mice.

Animals and Tumors

Male nude (nu/nu) mice (28-42 days old) were obtained from Charles River Canada, Inc. (St. Constant, Quebec, Canada). Mice were housed in plastic (polycarbonate) cages with microfilter tops kept in a Ventilated Animal Rack with a HEPA-filtered portable exhaust unit (Lab Products Inc., Maywood, NJ) and maintained under pathogen-limited conditions. Cages and bedding were autoclaved before use. Water was acidified to pH 2.8, and provided ad libitum. Male DBA/2 mice (Charles Rivers) were maintained in the animal facility under standard conditions.

The A549 tumors were inoculated into the flanks of nude mice by subcutaneous (s.c.) injection of 1×10^7 A549 cells, in 0.2 ml of medium, through a 26 gauge needle. The

tumor size was monitored, and the mice with tumor diameters greater than 0.5 cm (usually this takes six to eight weeks) were selected for the study.

The M-1 tumor model in DBA/2 mice has been described in detail elsewhere (50) and was used in this study as a control. Briefly, male, mature DBA/2 mice were injected s.c. with 1 x 10^5 M-1 tumor cells in the flank and used in the study when tumor diameter reached 0.5 cm.

Monoclonal Antibodies

Two MoAbs of the same subclass, 5E8 and T48 were used in this studies (chapters III-V). 5E8 reacts specifically with an antigen expressed on A549 cells. T48 was used as a non-specific control.

Photosensitizers

^{14}C-BPD. The ^{14}C-labeled BPD was synthesised by Dr. David Dolphin's group in the Department of Chemistry, University of British Columbia as described earlier (54). ^{14}C was incorporated in positions 2 and 3 of the cyclohexadiene ring. The batch was characterized by HPLC and liquid scintillation counting. The chemical purity was 96.4%, the radioactive purity was 92% and the specific activity was 91 μCi/mg. The compound was stored in DMSO at 7.2 mg/ml, frozen at -70°C. Dilutions were prepared immediately

before use in the experiments.

BPD-antibody conjugates. ^{14}C-labeled BPD was linked to the MoAbs (either 5E8 or T48) after pre-loading on to the carrier molecule, M-PVA, using a modified procedure described below. The molar ratio of ^{14}C-BPD to MoAb in the conjugates was 50-70:1. The conjugates were water soluble, and they were stored at 4°C in PBS before use, usually no more than 3 days following conjugation.

The absorption spectrum of BPD in the conjugates was not changed, therefore the characteristic absorbance peak for BPD at 690 nm was used as a measure of concentration of BPD in the conjugates. For comparisons between the conjugates and free BPD, the injected doses were calculated according to BPD concentration.

All stocks and tissue samples containing BPD were protected from light throughout the study.

Conjugation Procedures

The conjugation of BPD to antibody was carried out in a two-step procedure and has been described in detail in Chapters II and III. Slight modifications were made in conjugating ^{14}C-BPD. The modified PVA was loaded with ^{14}C-BPD using a standard carbodiimide reaction at a molar ratio 1:35. This M-PVA-^{14}C-BPD carrier was then linked to the 5E8

monoclonal antibody via the heterobifunctional cross linking reagent, SMBS. The SMBS activated antibody was mixed with the M-PVA-BPD-SH carrier system at a molar ratio of 1:2 (MoAb:PVA). The conjugated product was separated from the unconjugated materials by passage through a Sepharose CL-4B (Pharmacia LKB, Uppsala, Sweden) column as described previously. Spectrophotometric analysis of the purified conjugate indicated that the molar ratio of BPD to antibody was in the range of 50-70:1. These modifications in conjugation were used in order to increase loading of BPD onto the MoAb.

Distribution Studies

Twenty nine A549 tumor bearing nude mice, divided into 3 groups, were used in this study. Each mouse received an intravenous injection of either free or conjugated ^{14}C-BPD at a dose equivalent to 100 μg ^{14}C-BPD/mouse. Following the injection, animals were kept in the dark for 3 hours and sacrificed at various time points by asphyxiation in CO_2 under halothane anaesthesia. About 1 ml blood was drawn from the anaesthetized mice by cardiac puncture.

The first group (9 mice) received free ^{14}C-BPD and the mice (3 per point) were sacrificed at 3,14, and 24 h post injection. The second and the third groups (10 mice each) received ^{14}C-BPD-M-PVA-5E8 and ^{14}C-BPD-M-PVA-T48 respectively. Three mice in each group were sacrificed at 3 and 24 h post injection, and two mice at 14 and 48 h.

Six M-1 tumor bearing DBA/2 mice were injected with free ^{14}C-BPD at 100 μg/mouse and sacrificed (3 mice per time point) at 3 and 24 h post injection.

From each mouse, in addition to blood , samples from the following tissues were obtained, listed in alphabetical order: adrenal gland, bladder, bone, bone and marrow, brain, epididymis, fat, gall bladder, heart, small intestine, large intestine, kidney, liver, lung, lymph nodes, muscle, salivary gland, spleen, testes and tumor. Radioactivity content of tissues was determined.

The Determination of ^{14}C-BPD Content in Tissue Samples

Blood samples of 50 μl and about 100 mg tissue samples (wet weight) were prepared for liquid scintillation counting as described earlier (54). Briefly, tissue samples were weighed and solubilized in Protosol (NEN, Boston, MA). The solubilized samples were counted in Econofluor (NEN) in a Packard Tri-Carb Model 4550 liquid scintillation counter after 10 h adaptation in the dark. The counts per minute (CPM) were converted to disintegrations per minute (DPM) by means of an appropriate quench curve. DPM were subsequently converted to micrograms of ^{14}C-BPD and expressed as per gram of wet tissue, or per milliliter of blood.

Results

The biodistribution of ^{14}C-BPD injected intravenously into A549 tumor bearing nude mice and into M-1 tumor bearing DBA/2 mice was determined and compared between both mouse strains. The distribution of ^{14}C-BPD in most of the tissues was very similar in both strains. As expected, at 3 h post injection, tissues such as the liver, kidney and spleen contained high levels of radioactivity. Other tissues containing relatively high levels of radioactivity were the lung and adrenals. Brain, skin and muscle contained relatively low levels of radioactivity. For purposes of comparison between the two mouse species, the concentration of radioactivity in tissues was normalized to the concentration in blood at 3 h. The results showed that most tissues in both strains exhibited very similar levels of accumulation of ^{14}C-BPD with the exception of lymph nodes and tumors (Fig. 38). The lymph nodes in nude mice contained twice as much radioactivity as those in DBA/2 mice. In contrast, A549 tumors in nude mice accumulated about half of the amount accumulated by M-1 tumors in DBA/2 mice (Fig. 38A). The elimination of radioactivity from the blood and tissues after injection of free ^{14}C-BPD was similar in both species. The half-lives of ^{14}C-BPD in blood, shown in Table IX, indicated rapid elimination within the first 24 h post injection. The slightly longer half-life of free ^{14}C-BPD in DBA/2 mice compared to nudes could be attributed to the small differences between the doses (see Table IX). However, the conjugated ^{14}C-BPD had much longer half-lives as shown in Table IX. Radioactivity cleared from tissues in the same manner, and in both strains, tissue levels at 24 h post injection represented on average less than 20% of the levels at

3 h (results not shown).

The distribution of ^{14}C-BPD conjugated with either specific (5E8) or irrelevant (T48) antibody, after intravenous injection at 100 μg of ^{14}C-BPD/mouse to A549 tumor bearing nude mice was determined and compared to that of free ^{14}C-BPD. The results were evaluated with respect to the contribution of the antibody to tissue uptake, retention and elimination of radioactivity.

In comparison with free ^{14}C-BPD, the antibody conjugated ^{14}C-BPD cleared from blood more slowly, which resulted in significantly ($p < 0.01$) higher levels of radioactivity in blood at all time points tested (Fig. 39). There was no significant ($p < 0.3$) difference in the kinetics of elimination from blood when the two antibody conjugates were compared.

^{14}C-BPD conjugated to either of the antibodies distributed in tissues of A549 tumor bearing mice in a similar pattern to that of free ^{14}C-BPD. At 3 h post injection the gall bladder, liver, kidney, spleen, lung and adrenals contained more radioactivity than other tissues. However, the concentration of radioactivity in tissues, at this time, although comparable in many, was about twice as high in the adrenals, heart, kidney and liver, and about 10 times higher in the lung and spleen after injection of antibody-conjugated ^{14}C-BPD as compared to free ^{14}C-BPD. At the same time, however, little difference was seen between the two conjugates in terms of their accumulation in various tissues, including tumor (Figures 40, 43).

At 14 h post injection, all tissues tested from animals injected with antibody conjugates contained more radioactivity than those of animals receiving free ^{14}C-BPD. The difference was especially pronounced in the kidney, liver, lung, spleen and tumor, and remained so even after normalization of the results to the level of radioactivity in the blood at 14 h. The most striking difference was observed in the tumor and lung, with high accumulation of ^{14}C-BPD-M-PVA-5E8 in the A549 tumor and of ^{14}C-BPD-M-PVA-T48 in the lung (Figures 41, 43).

At 24 h, the distribution pattern was similar to that at 14 h in that the concentration of radioactivity in all tissues after injection of antibody-conjugated ^{14}C-BPD was higher than after injection of free ^{14}C-BPD, and the kidney, liver, lung and spleen contained higher levels of radioactivity than other tissues. As at 14 h, high levels of radioactivity were observed in the A549 tumor after injection of ^{14}C-BPD-M-PVA-5E8, and in the lung after injection of ^{14}C-BPD-M-PVA-T48 (Figures 42, 43). This picture was very similar at 48 h post injection of the radioactive materials, although the levels of radioactivity in all tissues were reduced (results not shown).

The main focus of this study was on the accumulation of the radioactivity in the tumor. The kinetics of tumor accumulation of free as well as T48 antibody-conjugated ^{14}C-BPD were the same as observed in other tissues, that is, the radioactivity accumulated in the A549 tumor and reached its highest concentration at 3 h post injection of the radioactive materials. The accumulation was followed by the elimination phase. The kinetics of

uptake and elimination of radioactivity delivered to the A549 tumor by ^{14}C-BPD-M-PVA-5E8 were different. The radioactivity reached its maximum in the tumor at 14 h post injection and then was eliminated at a slow rate, resulting in lower levels at 24 and 48 h (Fig. 43). While the ^{14}C-BPD-M-PVA-T48 was eliminated from the tumor at a rate similar to that in blood, the ^{14}C-BPD-M-PVA-T48 was eliminated much more slowly. As a result, at 48 h post injection of either ^{14}C-BPD-M-PVA-5E8 or ^{14}C-BPD-M-PVA-T48, the concentration of radioactivity in the A549 tumor represented 114% and 32% of the concentration in blood at 48 h, respectively.

The efficiency of delivery of ^{14}C-BPD to tumor is best represented by a ratio between the concentration of radioactivity in the A549 tumor as delivered by the specific 5E8 antibody to the concentration of radioactivity delivered either by the irrelevant T48 antibody or by free ^{14}C-BPD. These ratios were determined at various time points post injection. The ratio of ^{14}C-BPD-M-PVA-5E8 to free ^{14}C-BPD was between 1.74 (at 3 h) to 2.94 (at 24 h) and the ratio of ^{14}C-BPD-M-PVA-5E8 to ^{14}C-BPD-M-PVA-T48 was between 0.87 (at 3 h) to 4.2 (at 48 h) (Fig. 44).

At 14 h post injection of ^{14}C-BPD-M-PVA-5E8, when the blood level of radioactivity was high, the concentration of radioactivity in A549 tumor was higher than in tissues such as skin, muscle, brain and bladder, reaching tumor:tissue ratios of 1.69, 2.60, 16.24 and 2.14 respectively. At 24 h post injection of ^{14}C-BPD-M-PVA-5E8 the tumor:tissue ratios increased in all tissues.

Discussion

The work described here was carried out in order to determine whether a MoAb with specificity for a human squamous cell carcinoma antigen, when conjugated to the photosensitizer BPD, would enhance delivery of the photosensitizer to tumor cells in vivo. The model used involved the implantation of A549 cells subcutaneously into the backs of nude mice, followed by biodistribution studies in tumor bearing mice following i.v. administration of internally labelled ^{14}C-BPD, either as free photosensitizer or conjugated to a specific or control MoAb using a heterobifunctional linker between the MoAb and the water soluble carrier system of BPD covalently bound to modified PVA.

A considerable amount of work has been carried out on ^{14}C- and ^{3}H-BPD in terms of its distribution in DBA/2 mice bearing syngeneic tumors, either the P815 mastocytoma or the M-1 rhabdomyosarcoma (54, 55). Initial studies here involved evaluation and comparison of ^{14}C-BPD biodistribution in conventional tumor bearing mice (DBA/2 with M-1) and nude mice bearing A549 tumors. Results showed that with the exception of lymph nodes and tumor tissue, biodistribution levels between the two mouse strains at all time points tested did not differ significantly. In the case of lymph node tissue, in nude mice, the levels at 3 h post injection were twice those of DBA/2 mice. At the time of post mortem tissue collection it was noted that the lymph nodes of nude animals were considerably larger than those of the DBA/2. It is possible that the hypercellularity of the nude nodes caused the increased uptake of BPD. In the case of tumor tissue,

accumulation of BPD in A549 was less than half that in the M-1 tumor. In fact the tumor:skin or tumor:muscle ratios in the nude model failed to show favourable accumulation in tumor, unlike the DBA/2 tumor model (Table X). This poor accumulation of BPD in the A549 tumors shows a distinct difference between nude mouse models and syngeneic tumor models. It was noted that the A549 tumors grew very slowly in the nude mice, and tumors tended to be hard and poorly vascularized. It is probable that the relatively poor vascularity of A549 tumors accounted for the low levels of ^{14}C-BPD found in the tumors.

We have compared the biodistribution of the 5E8-M-PVA-BPD conjugate with both free BPD and an irrelevant control MoAb conjugate (T48-M-PVA-BPD) in A 549 bearing nude mice. When the two MoAb conjugates were compared to BPD, obvious differences were evident. First, blood clearance studies (Fig. 39) showed that free BPD was cleared far more rapidly than either conjugate; at 24 hours post injection blood levels for both conjugates were 10 fold higher than levels from BPD treated animals. This high retention level probably accounts for the higher levels seen in essentially all tissues at 3, 14 and 24 h post injection in mice injected with the conjugates in comparison to free BPD. These results indicated that the conjugates retained their integrity in vivo, since if BPD had become dissociated under these conditions, one would expect to see clearance rates equivalent to free BPD.

In terms of tissue distribution of the two conjugates, an anomalous result was observed

in that the control conjugate (T48) was retained at higher levels in the lung than the 5E8 conjugate. The difference became more apparent over time. There are two possible explanations for this. One, the T48-M-PVA-BPD preparation might be more readily phagocytosed than the 5E8 conjugate, owing possibly to undetected levels of micro aggregation. While we have no evidence to support this possibility, it is known that lung tissue would concentrate such aggregates. Two, T48-M-PVA-BPD might recognize some antigenic determinant in mouse lung tissue. This is thought to be unlikely because the kinetics of the clearance of T48 from the lung was essentially the same as the clearance from blood. If specific antigen recognition were a factor here, clearance kinetics should have resembled the clearance of 5E8-M-PVA-BPD from tumor tissue (discussed below).

The only tissue which did not exhibit clearance kinetics which followed blood clearance was A549 tumor tissue from mice injected with the 5E8-M-PVA-BPD conjugate. In these animals, radioactivity accumulated in tumor tissue for up to 14 h post injection despite the decrease of radioactivity in blood during this time (Fig. 43). These results are compatible with two recent reports in which MoAb-photosensitizer conjugates reached maximum levels in tumors at about 24 h post i.v. injection (97, 98). These results support the claim that 5E8-M-PVA-BPD conjugates maintain their selectivity in vivo, that the MoAb in question accumulates selectivity in A549 tumors, and that the photosensitizer remains associated with the MoAb.

Chapter Summary

Biodistribution of the photosensitizer benzoporphyrin derivative monoacid ring A (BPD) was compared in DBA/2 mice bearing the syngeneic M-1 tumor and nude mice bearing the A549 human squamous cell carcinoma. These studies, using internally labelled ^{14}C-BPD showed that in general, biodistribution between the two strains was equivalent with the exception of two tissues; lymph nodes (BPD levels were higher in nude mice) and tumor (BPD levels were lower in nude mice). Further studies were carried out in A549 tumor bearing nude mice in which the biodistribution of BPD conjugated to a monoclonal antibody (5E8) with specificity for an antigen on A549 cells was compared to a conjugate prepared with an irrelevant monoclonal antibody (T48). These studies showed that both conjugates had biodistribution characteristics which distinguished them from free BPD in that they remained in the circulation and most tissues for significantly ($p<0.01$) longer times than did free BPD. Also, with the exception of the 5E8-M-PVA-BPD conjugate and A549 tumor tissue, levels in all tissues were highest at the 3 hour time point following injection of conjugates. In the case of A549 tumor and the 5E8-M-PVA-BPD conjugate the highest concentration of ^{14}C labelled material was observed at the 14 hour time point following injection. The results reported herein show that the conjugates tested behaved differently from free BPD indicating that the materials did not become dissociated in vivo and that the specific conjugate (5E8-M-PVA-BPD) demonstrated specificity for the A549 tumor in terms of the kinetics of its accumulation in tumor tissue.

Table IX. Elimination of ^{14}C-BPD from blood of M-1 tumor bearing DBA/2 mice and A549 tumor bearing nude mice. Elimination half-lives were determined during various periods post intravenous injection of ^{14}C-BPD either free or conjugated to T48 or 5E8 MoAb. Calculations were based on data obtained in at least 3 mice.

Time	DBA/2 Mice*	Nude Mice**		
Post i.v.(h)	BPD	BPD	T48-BPD	5E8-BPD
0-3	40 min.	37 min.	43 min.	44 min.
3-24	7.7 h	5.9 h	12.2 h	12 h

* Dose:100 μg ^{14}C-BPD/mouse=4.0 mg/kg body weight

** Dose:100 μg ^{14}C-BPD/mouse=3.3 mg/kg body weight

Table X. Comparison of tumor:tissue ratios at 3h and 24 h after i.v. injection of ^{14}C-BPD at 100 μg/mouse, obtained in the tumor models: A549 tumor in nude mice and M-1 tumor in DBA/2 mice. Each value represents mean ± S.D.

Tissues	3h		24h	
	A549	M-1	A549	M-1
Adrenals	0.25±0.08	0.80±0.26	2.71±1.46	0.09±0.13
Bladder	1.37±0.23	3.25±0.91	3.96±2.26	2.90±0.26
Brain	10.60±5.30	32.78±6.82	15.5±0.5	103.1±60.2
Fat	0.52±0.12	1.87±0.27	3.81±0.74	5.62±0.45
Intestine	0.19±0.04	1.54±0.43	3.50±1.31	2.25±0.42
Muscle	1.45±0.34	3.82±0.61	5.10±0.31	12.95±2.81
Skin	1.0±0.01	5.93±1.55	1.18±0.55	2.94±0.19

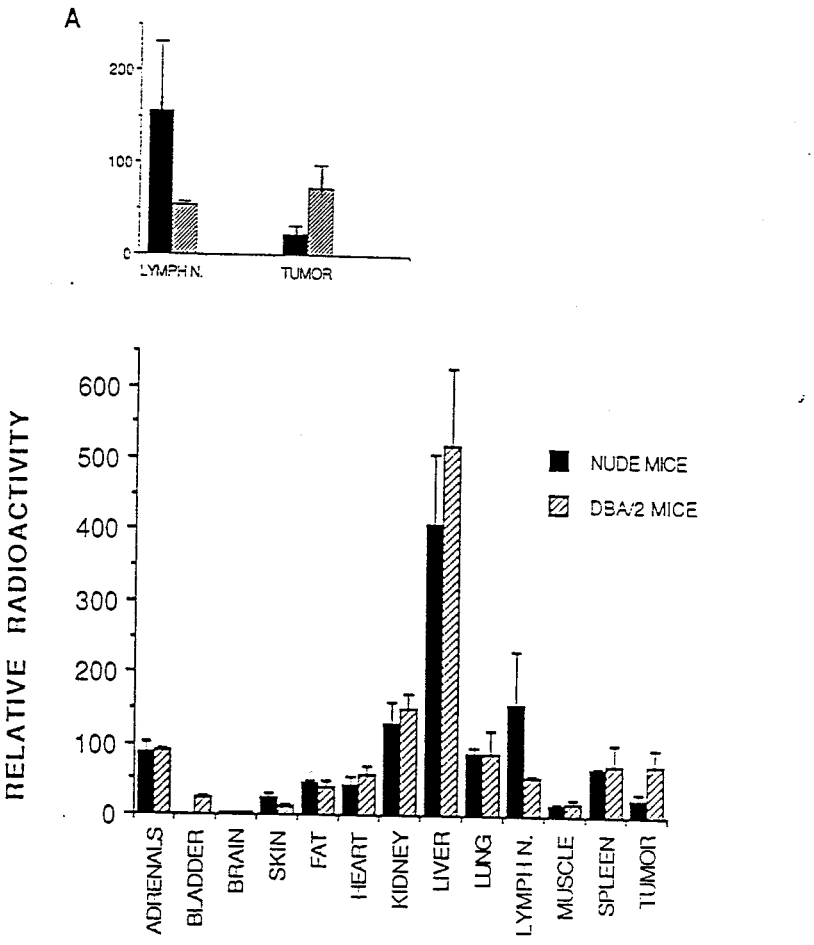

Figure 38. Distribution of radioactivity in tissues of M-1 tumor bearing DBA/2 mice and A549 tumor bearing nude mice at 3 h post intravenous injection of ^{14}C-BPD at a dose of 100 μg/mouse. The radioactivity in tissues (μg equivalent of ^{14}C-BPD/g wet tissue) was expressed as the percentage of the radioactivity in blood (μg equivalent of ^{14}C-BPD/ml blood) at 3 h post injection. Each value represents mean ± S.D. of data obtained in 3 mice. A. Close-up of the data obtained in lymph nodes and tumors.

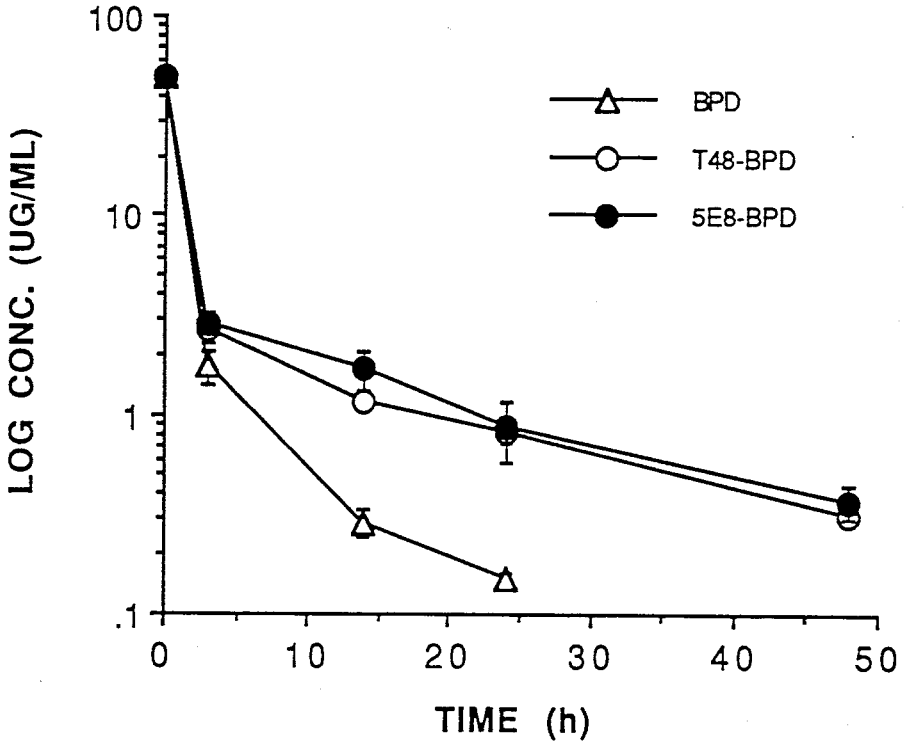

Figure 39. Elimination of radioactivity from blood of A549 tumor bearing nude mice following intravenous injection of ^{14}C-BPD (100 μg/mouse), administered either free or conjugated to T48 or 5E8 MoAb. Each point represents mean ± S.D. of data obtained in 2-3 mice.

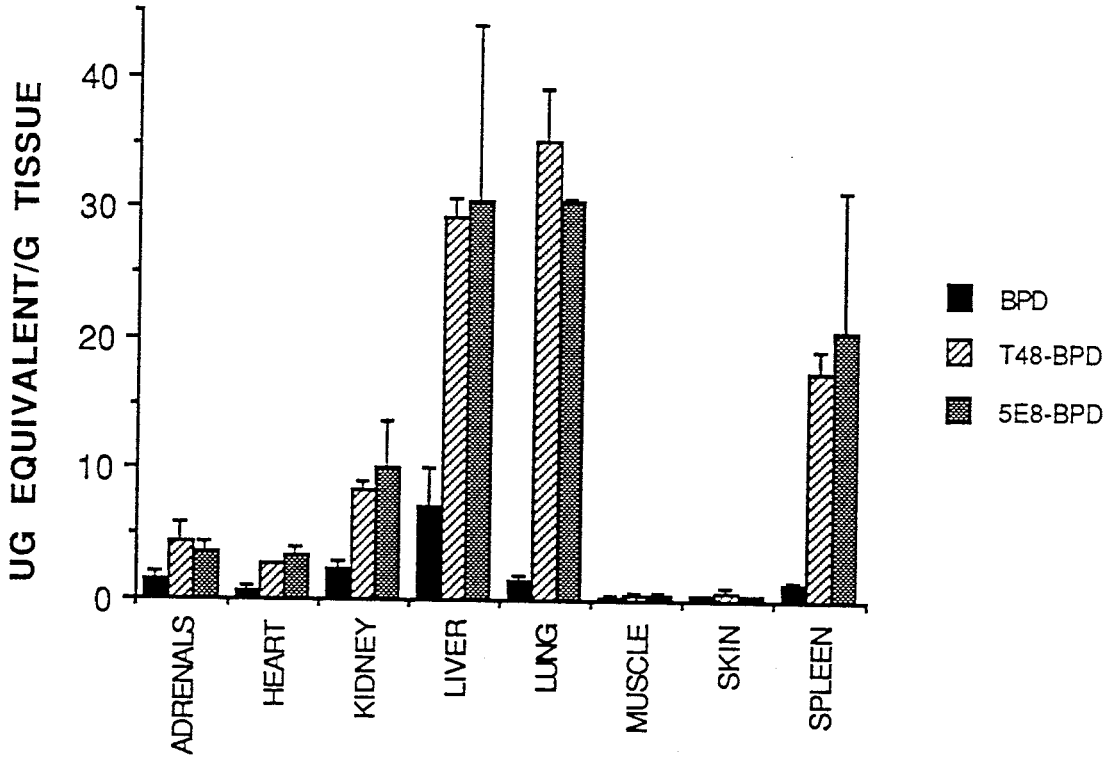

Figure 40. Distribution of radioactivity in tissues of A549 tumor bearing nude mice at 3 h post intravenous injection of ^{14}C-BPD (100 μg/mouse), administered either free or conjugated to T48 or 5E8 MoAb. Tissue concentration of radioactivity was expressed in μg equivalent of ^{14}C-BPD/g wet tissue. Each value represents mean ± S.D. of data obtained in 3 mice.

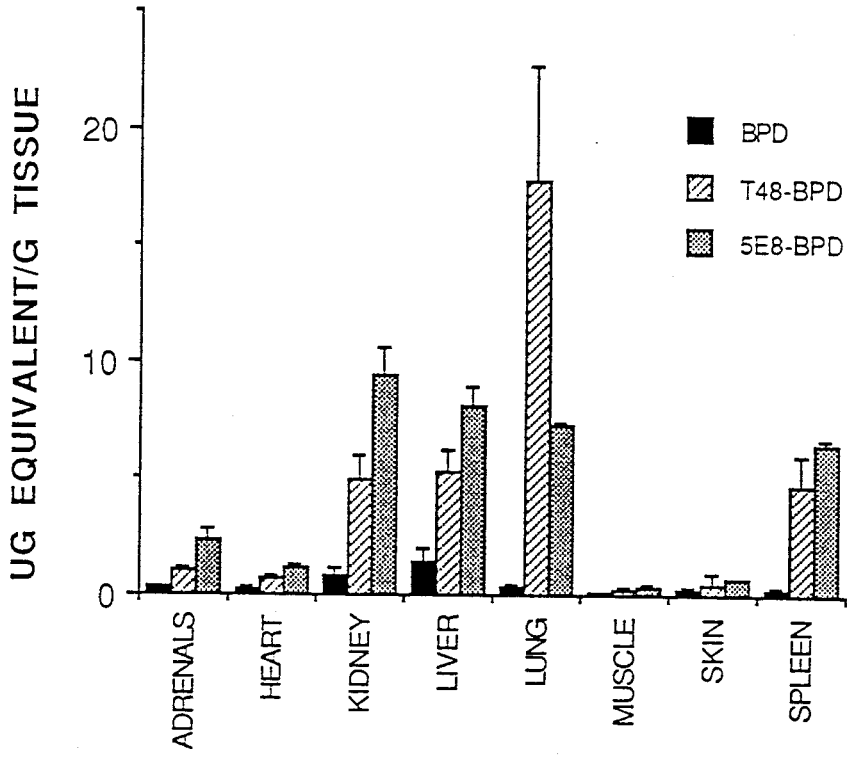

Figure 41. Distribution of radioactivity in tissues of A549 tumor bearing nude mice at 14 h post intravenous injection of ^{14}C-BPD (100 μg/mouse), administered either free or conjugated to T48 or 5E8 MoAb. Tissue concentration of radioactivity was expressed in μg equivalent of ^{14}C-BPD/g wet tissue. Each value represents mean ± S.D. of data obtained in 3 mice.

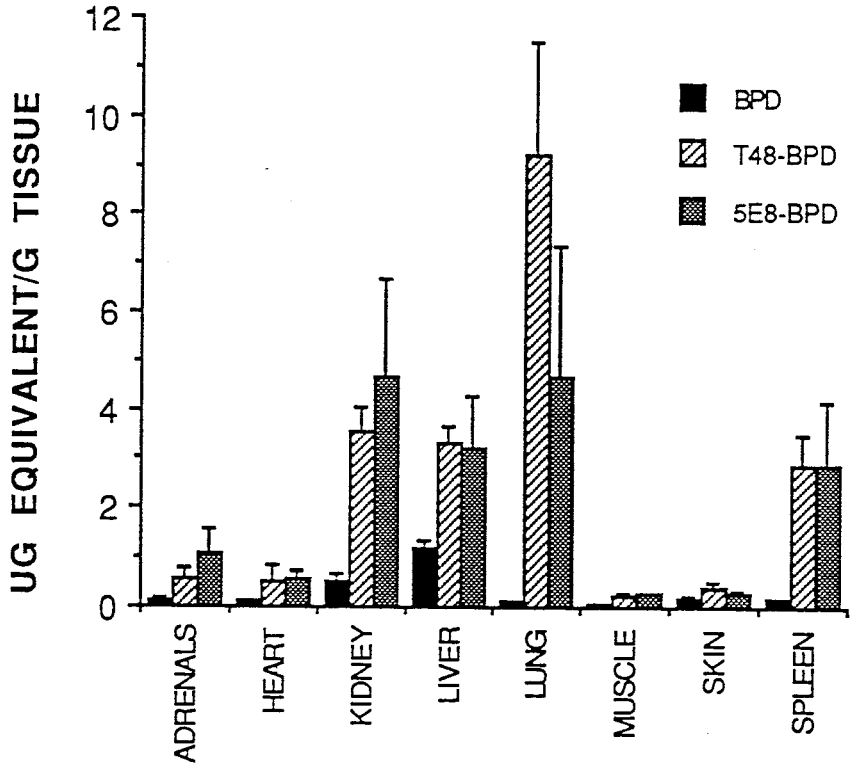

Figure 42. Distribution of radioactivity in tissues of A549 tumor bearing nude mice at 24 h post intravenous injection of ^{14}C-BPD (100 μg/mouse), administered either free or conjugated to T48 or 5E8 MoAb. Tissue concentration of radioactivity was expressed in μg equivalent of ^{14}C-BPD /g wet tissue. Each value represents mean ± S.D.of data obtained in 3 mice.

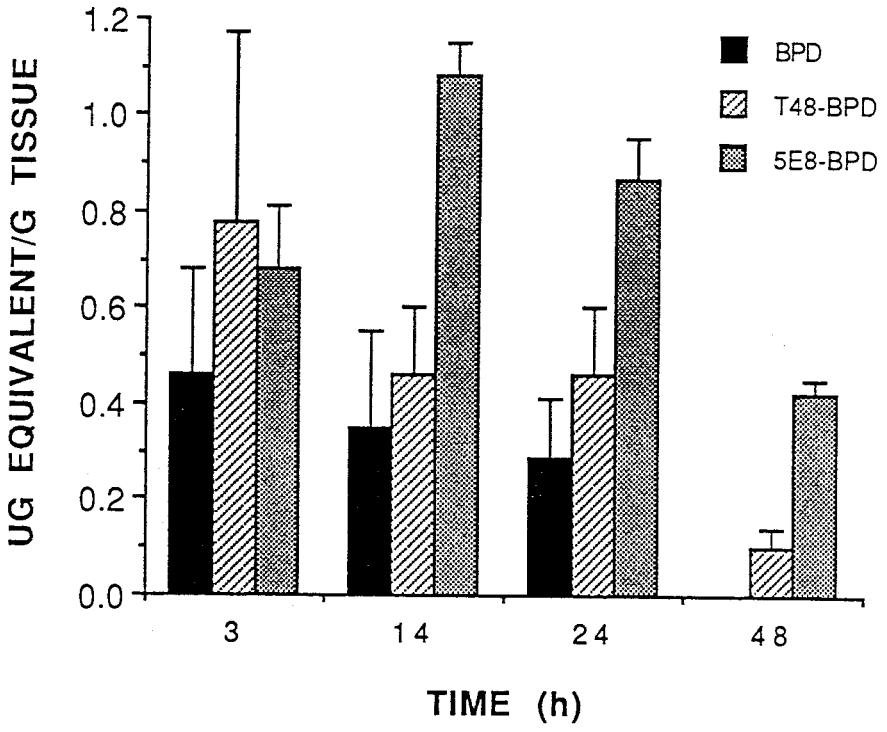

Figure 43. Concentration of radioactivity in tumor tissue following intravenous injection of either free or MoAb conjugated ^{14}C-BPD (100 μg/mouse) into A549 tumor bearing nude mice. The concentration ^{14}C-BPD (μg equivalent/g wet tissue) was determined at various time points post injection. Each value represents mean ± S.D of data obtained in 2-3 mice.

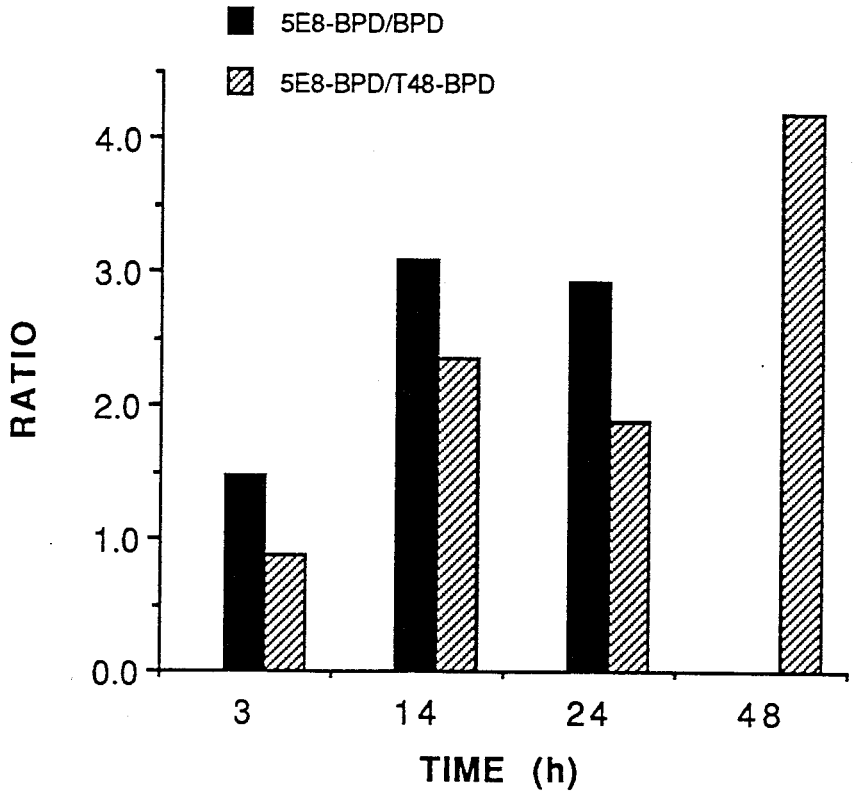

Figure 44. Tumor specific delivery of ^{14}C-BPD (dose:100 μg/mouse) to A549 tumor in nude mice, by a specific 5E8 MoAb was expressed as a ratio between the concentration of radioactivity in tumor tissue as delivered by 5E8-M-PVA-^{14}C-BPD and as delivered by either free ^{14}C-BPD or ^{14}C-BPD conjugated to T48. The ratios determined at various time points post injection represent the average values obtained in 2-3 mice.

CHAPTER VII. GENERAL DISCUSSION

A. Overview

The major objective of the research was to explore ways by which the selective delivery of photoactive drugs to identified targets could be achieved. PS are a group of chemicals which can be activated by light at a particular wavelength. Once activated, PS can either emit fluorescence which can be detected by laser-induced fluorescence endoscopy, or release singlet oxygen which are considered to be the major reaction product responsible for cell killing; or both. The theoretical basis of the treatment for cancers using PS relies on a dual selectivity - the selectivity of the PS to achieve higher concenrations in malignant compared with surrounding normal tissue, and the selectivity of applying light of a particular wavelength to the tumor site only. Efforts in search of a better PS with high photoreactivity at excitation wavelength above 600 nm and with high tumor selectivity continue. In an attempt to increase the selectivity of PS, we, as well as many other investigators, have investigated the use of monoclonal antibodies (MoAbs) as a delivery system. The obvious advantage of using antibody as a vector to deliver PS to tumors involves the inherent ligand-binding property of antibody. This added selectivity would be expected to increase the efficacy of photodynamic therapy (PDT). Antibody-targeted photodynamic killing may have advantages over conventional immunotherapy in which MoAbs are used as carriers of radioisotopes, drugs or toxins. These advantages include: 1) the enhanced dual selectivity of photodynamic antibody-mediated tumor killing would

eliminate the potential selectivity problems of immunotoxins accumulating in non-targeted organs such as the liver; 2) MoAb-PS need not be internalized in order to be effective because of the diffusion distance of singlet oxygen, and even MoAb-PS near the surface of tumor cells may be effective; and 3) because of singlet oxygen diffusion, antigen-negative tumor cells adjacent to cells which bind the MoAb-PS may still be killed.

One other important issue addressed in this research was to determine the photodynamic killing efficacy of membrane bound MoAb-PS conjugates in comparison to internalized materials using target cells. The resolution of this question would help us to understand better the mechanisms of photodynamic killing and relative sensitivities of various subcellular targets of PDT.

Since the main aim of the study was to enhance the selectivity of PDT using a MoAb mediated PS delivery system, the focus of this discussion will be centered on the procedure of conjugating PS to MoAb and the in vitro and in vivo analyses of the conjugates of this nature. The potential use in imaging via MoAb-PS in early diagnosis, and improved delivery of PS to targets using other delivery systems such as low density lipoprotein (LDL), liposomes, lymphokines, hormones, growth factors, microsphere and so on, will only be briefly discussed.

B. Conjugation

There is considerable ongoing research on linking anti-cancer drugs to monoclonal antibodies. The possible reactive groups on monoclonal antibodies for such a purpose include free carboxyl groups, amino groups, sulfhydryl groups or the carbohydrate (CHO) moieties on the Fc portion (129). Early work usually involved direct linkage between drug and one of these groups on MoAbs in the presence of linking agents to make the drug-MoAb complex. Among these linking agents, glutaraldehyde and carbodiimide have been the most commonly used. In the case of glutaraldehyde, the amino group of the drug is linked with an amino group on the antibody (130). The major problem associated with the use of this reagent is polymerization. To avoid polymerization, a two step reaction is recommended - first mix glutaraldehyde with one reactant, remove the excess glutaraldehyde, and then react with the second component. For EDCI, free amino and carboxyl groups are linked to form an amide bond. However, polymerization occurs during this reaction as well (131). A better method of coupling carboxyl-containing drugs to MoAb is the use of the active ester which is formed between the NHS (N-hydroxysuccinimide) and COOH groups. Reaction of the active ester with an amino group results in a stable amide linkage (132). Hydrazide and halocarbonyl are also commonly used for direct linkages (133, 134).

Ten years ago this laboratory started to explore a novel anti-cancer treatment - "photoimmunotherapy". This approach involved a combination of the phototoxic effects

of chemicals such as hematoporphyrins (Hp) and the target seeking ability of MoAb. About 60 Hp molecules were covalently bound to MoAbs using EDCI coupling. It was further demonstrated that conjugates of this nature increased the cytotoxicity of the PS both in vitro and in vivo (69, 70). It was found, however, that direct linking was not optimal since conjugation was random. Also, PS had a tendency to bind naturally to the hydrophobic area of the monoclonal antibody, making the actual quantification of loading extremely difficult. In addition, inactivation of at least some of the MoAb was a common occurrence particularly when a high level of loading was attempted. Later, using similar strategies, other investigators tried to protect MoAb activity by loading a limited number of PS molecules (less than 5) (71). That again would not be optimal, since the low level PS substituted MoAb-PS conjugates, if used in vivo, would not increase the amount of PS localized in the tumor in comparison to unconjugated PS. This is due to the fact that the PS represents only a small percentage of the molecular weight of the conjugate, about 1% for a MoAb-$(PS)_5$ conjugate, and the amount of injectable MoAb is limited by the possible saturation of antigenic determinants available on the tumor. To protect the antigen binding ability, and to load more PS to the MoAbs, an indirect approach of conjugation was investigated. In this approach, PS was first linked to an inert intermediate molecule, a carrier molecule which was then bound to the MoAb.

Several carrier molecules have been used. These include modified dextran, polyglutamic acid and polyvinyl alcohol. Dextran is a bacterial polysaccharide and can be derivatized in a variety of ways to introduce reactive groups and thereby be coupled to antibody (133).

It is water soluble and nontoxic. Polyglutamic acid (PGA) has also been utilized as an intermediary for carrying large amounts of drug. Two approaches have been used to couple drugs to MoAbs. First, PGA may be activated with a cross-linking agent such as carbodiimide and reacted with amino-functionalized drugs. The MoAb in this procedure is oxidized with sodium metaperiodate and reacted with the PGA-drug conjugate. The Schiff's base thus formed may be stabilized by reduction with sodium cyanoborohydride to yield the final MoAb-PGA-drug conjugate (74). A second procedure is to synthesize the PGA by polymerization of a suitably functionalized monomer. The latter method was used to introduce a thiol group onto PGA for coupling to MoAb in the final step (134). In addition to using an intermediatory molecule, these investigators attached the PS-carrier to the MoAb CHO, which is well away from the antigen binding sites. These modifications would protect the biological activity of antibodies. We have worked with polyvinyl alcohol (PVA) as a carrier (Chapter II). This molecule is relatively easily modified with hexanediamine to introduce free amino groups. It is hydrophilic and nontoxic. After modification, M-PVA was readily conjugated to BPD. The ratio between M-PVA and BPD could be easily altered by changing the molar ratio. The subsequent conjugate (M-PVA-BPD) was tested both chemically and biologically. Chemically, it was found that BPD covalently bound to M-PVA. Biologically, conjugated BPD showed similar, if not greater, cytotoxicity in in vitro experiments. The M-PVA-BPD was further linked to MoAb using a heterobifunctional reagent, SMBS, to form the MoAb-PS conjugate. Extensive characterizations on the MoAb-PS were performed. It was first purified by a sizing column (Sepharose CL-4B). Purified product was further subject to

SDS-PAGE analysis which provided evidence of covalent bonding between BPD and MoAb. The Ab binding activity was determined through ELISA which showed that essentially all the antigen binding activity was retained after conjugation. These results, along with reports from other groups on indirect approaches, have indicated that this method provided a good way of linking drugs with MoAbs. However, some concerns on the use of intermediatory molecules have been generated: 1) using an intermediatory molecule would increase the size of the immunoconjugate, which may result in less tumor specific binding in vivo, due to increased accumulation in the liver; and 2) the high ratio of dyes per antibody causes a high charge on the surface of the antibody, which may complicate its passage through the intravascular space to reach cells within solid tumors.

C. In vitro and in vivo Activities of MoAb-PS Conjugates

Early studies on photoxicity of an anti-M-1 rhabdomyosarcoma MoAb-Hp conjugate in this laboratory showed that this conjugate, in combination with light of the appropriate wavelength, could selectively kill tumor cells in vitro and inhibit the tumor growth in vivo. However, the conjugate was prepared via a direct linkage at a relatively high level of substitution (60:1, Hp:MoAb). As discussed earlier, most PS molecules are very hydrophobic and tend to interact with hydrophobic regions of MoAbs which may cause inactivation of the antigen binding activity or make reliable quantification of the number of PS molecules bound, very difficult. In addition, highly hydrophobic molecules tend to aggregate among themselves in aqueous solvents. Therefore the final preparation in these

early studies would not only contain Moab-PS conjugates but also some Hp aggregates and non-covalent mixtures of Hp and MoAbs. These mixtures could also interfere with the selectivity. In an attempt to protect the antigen binding activity of Abs, a report from Oseroff et al. described a MoAb-PS conjugate through a direct linkage with limited substitutions. Less than 5 PS molecules were attached to each MoAb molecule. They were able to demonstrate highly selective phototoxicity of this conjugate compared to controls. However, low substitution means that a large quantity of MoAb was required for in vitro assays (considering the difference of the M.W. between PS and MoAb) and would probably result in low tumor accumulation in vivo due to limited tumor surface antigens and steric hindrance. More recently, improved conjugation methods using indirect linking appears to render higher substitution with minimum interference of MoAb antigen binding activity. In our recent report, the MoAb 5E8 which is specific for a human lung squamous cell carcinoma (antigen expressed on the A549 tumor cell line) was conjugated to the photosensitizer BPD via a PVA carrier. In vitro studies showed that the 5E8-M-PVA-BPD conjugate caused 10 times higher cytotoxicity than control conjugate and 15 times more than BPD alone on A549 cells. When the conjugate was assessed and compared with a control conjugate (T48-M-PVA-BPD) on a irrelevant cell line (M-1), no significant difference in photodynamic killing was observed. This certainly demonstrated the selectivity of the specific MoAb-PS conjugate. Meanwhile, studies on cytotoxicity of MoAb-PS conjugates in vitro from other groups have been reported. In one report (72), efficient and selective cytotoxicity was observed using an anti-Leu-1 MoAb conjugated to chlorin e_6 (Ce_6) via a dextran intermediary. It was noted, however, that the control in this

study was not appropriate. Since the MoAb-Ce_6 was compared with cholrin e_6 monoethylene diamine monoamide (CMA), rather than Ce_6 itself. In fact, CMA was highly phototoxic to all cells at the concentrations used in that study. Several other reports from Hasan's group showed very promising results. In one study (74), PS CMA was bound via PGA to an anti-Leu-1 antibody. When anti-Leu-1 target cells, HPB-ALL T-leukemia cells treated with the conjugate were exposed to broad-band, long wavelength irradiation and cell survival evaluated by fluorescence microscopy, a radiant-exposure-dependent phototoxicity was observed. Controls were unaffected. In another study (79), CMA was conjugated to an anti-bladder carcinoma MoAb (3G2-C6) using PGA as an intermediary and the selective phototoxicity of these conjugates in vitro against target cells was demonstrated. More recently, as a result of a more sophisticated synthesis procedure using PGA and dextran, specific light-dependent and PS dose-dependent killing of target melanoma cells (84) and ovarian carcinoma cells has been reported.

In addition to the in vitro studies on phototoxicity of MoAb-PS, we also addressed question of cellular targets at a preliminary level. We have found, using two different MoAb-PS conjugate systems, that internalized MoAb-PS showed higher cytotoxicity than that of surface associated materials. Using 5E8-PS conjugates, we observed 10 fold greater cytotoxicity of internalized conjugate toward target cells than of materials associated with cell membrane. Similarly, the internalized C7-PS conjugates affected four times higher killing on the specific cell line than the membrane bound conjugates. However, our experiments were designed in such a way that they did not permit

quantitation of PS either outside or inside the cells under the experimental conditions, nor were intracellular targets identifiable. Future studies using radiolabeled conjugates and confocal microscopy would clarify these issues. The following possibilities may provide some explanations as to why internalized conjugates have better cytotoxicity than do surface associated conjugates.

1) the susceptibility of cell membrane versus intracellular organelles. Since the internalized conjugates and membrane bound conjugates are expected to act on different targets, one would expect different effects. Once internalized, the conjugates may be delivered to cytosol where they are dissociated/degraded. PS would probably then affiliate with some intracellular membrane structure, such as mitochondria due to the lipophilicity. When light activates the PS, it releases singlet oxygen which damages these membrane structures and causes the death of the cells. The greater killing effects induced by internalized conjugates, as shown in our experiments, could indicate that intracellular organelles are more susceptible to photodynamic killing than are cell membranes.

2) fluorescence quenching. One study has shown that the florescence intensity per PS (such as fluorescein) molecule diminishes with increases in the PS:MoAb molar ratio. Although the mechanism for this phenomenon is not clear, at a high PS:MoAb ratio, the close proximity of two or more PS molecules might lead to exciplet formation upon optical excitation. While using carrier to link the PS with MoAb, this will become more dominant since many PS may be distributed on a much smaller molecule than MoAb. In addition, the intracellular and extracellular environments are different and may cause a

different degree of quenching.

3) quantitative uptake of PS into cells. This is expected to play an important role in phototoxicity. In our studies, we have no way of telling the exact number of membrane bound versus internalized MoAb-PS conjugates, although fluorescence microscopy suggested that more PS was present in the cells which internalized the PS. There is no question that over time more PS would be associated with cells which internalize MoAb conjugates and this would enhance PDT. In addition to MoAb mediated PS delivery systems, many other delivery systems have been reported or are currently under investigation. These include LDL (120), liposomes (135), cytokines, hormones, growth factor (136), and microspheres (137) and so on. In the case of LDL and cytokines, it has been found that many tumors express high levels of LDL receptors and cytokine or hormone receptors (such as growth factor receptor). Targeting these receptors using LDL, cytokines or hormones conjugated to PS have proved to be very effective. Enhanced photo-cytotoxicity of PS via microsphere mediated delivery also has been reported. This was considered to be a consequence of the high intracellular PS concentration attained by endocytosis of the conjugates and their particular sites of intracellular localization. Currently, our laboratory is investigating CD4 as a carrier for HIV infected T cells and IL-2 as a carrier for activated T cells in rheumatoid arthritis. Preliminary results from these studies have shown some promising potential in these types of targetted delivery.

The <u>in vitro</u> studies reported here have demonstrated the feasibility of using a MoAb-PS

conjugate in selective cytotoxicity towards appropriate target cells. However, only a few reports are available on the fate of these conjugates in vivo. In one early report, the MoAb-PS conjugate showed a strong time-dependent localization after intraperitoneal injection into nude mice with subcutaneously implanted human tumors (96). Distinct cellular localization only appeared 72 h after injection. These observations appear to be consistent with our preliminary studies in vivo (69). More recently, two other reports on biodistribution of MoAb-PS showed that the peak accumulation of specific conjugates in the tumor site occurred at 24 h. These results are similar to our most recent study with the 5E8-M-PVA-BPD conjugate in a tumor bearing nude mouse model (Chapter VI) where we showed the highest tumor accumulation to be between 14 and 24 h. Further studies on the efficacy of the MoAb-PS conjugate in eliminating the target in vivo are required. The improvement of the delivery of PS to tumor sites via a MoAb mediated system would also increase the contrast between tumor and surrounding normal tissue. This feature could also be used for imaging to detect small lesions. Many studies have been reported in this area and the detection of accessible tumors by laser-induced fluorescence depends upon 1) PS used; 2) the contrast between abnormal and normal tissues; 3) the concentration of PS in tumor and 4) optical properties of the tumor as well as the surrounding tissues. The major problems associated with in vivo applications of MoAb-PS are 1) the large size of the conjugate makes passing through vascular barrier difficult; 2) rapid clearance of conjugates by reticuloendothelial system; and 3) development of human anti-mouse antibodies (HAMA). These in vivo limitations of conjugates may be reduced or eliminated in extracorporeal treatments such as for the

eradication of viruses (hepatitis C from blood supplies intended for transfusion) and possibly for the selective killing of tumor cells in bone marrow of patients with leukemia and other systemic cancers who are undergoing autologous bone marrow transplant using PS designed to absorb light that is transmitted by blood.

In summary, photoimmumotherapy has provided another alternative for the cancer treatment and diagnosis. Our data have suggested that the approach merits further investigation. Future direction in this area will include improving the synthesis, purification, and characterization of conjugates and optimizing light dosimetry and delivery in appropriate animal models.

REFERENCES

1. Jesionek, A. and Tappeiner, V.H. (1903) Zur Behandlung der Hautcarcinomi mit Fluorescienden Stoffen. Med. Bochenschr. 47:2042

2. Hausmann, W. (1911) Die sensibilisierende Wirkung des Hamatoporphyrins. Biochem. Z. 30:276

3. Auler, H. and Banzer, G. (1942) Untersuchengen uber due Rolle der Porphyrine bei geschqulstkranken Menschen und Tieren. Z. Krebsforsch. 53:65-68

4. Lipson, RL, Baldes, EJ and Olsen, AM. (1961) The use of a derivative of hematoporphyrin in tumor detection. JNCI 26:1-8

5. Lipson, MS, Gray, MT and Baldes, EJ. (1966) Haematoporphyrin derivative for detection and management of cancer. Proceedings of the 9th international cancer congress. 393

6. Dougherty, TJ, Gridey, GB and Fiel, R. (1975) Photoradiation therapy II. Cure of animal tumors with haematoporphyrin and light. JNCI 55:115-119

7. Dougherty, TJ, Kaufman, JE, Goldfarb, A. (1978) Photoradiation therapy for the treatment of malignant tumors. Cancer Res. 38:2628-35

8. Dougherty, TJ. (1984) Photodynamic therapy (PDT) of malignant tumors. (1984) CRC Crit. Rev. Oncol./Hematol. 2:83-116

9. Dougherty, TJ. (1985) Photodynamic therapy. In: Jori G. and Perria CA (eds) Photodynamic therapy of tumors and other diseases. Padova: Ediaioni Libreria Progetto. 267-279

10. Moan, J. and Christensen, T. (1980) Porphyrins as tumor localizing agents and their possible use in photochemotherapy of cancer. A review. Tumor Res. 15:1-10

11. El-Far, MA and Pimstone, NR. (1983) Tumor localization of uroporpyrin isomers I and II and their correlation to albumin and serum protein binding. Cell Biochem. Funct. 1:156-160

12. Kessel, D. and Dougherty, TJ (eds) (1983) Porphyrin photosensitization (Adv. Exptl. Med. Biol. Vol. 160). New York: Plenum

13. Christensen, T., Wahl, A. and Smedshammer, L. (1984) Effects of haematoporphyrin derivative and light in combination with hyperthermia on cells in culture. Br. J. Cancer 50:85-92

14. Andreoni, A. and Cubeddu, R. (eds) (1984) Porphyrins in tumor phototherapy. New York:Plenum

15. Doiron, DR and Gomer, CJ. (eds) (1984) Porphyrin localization and treatment of tumors. New York:Alan R Liss

16. Kessel, D. (1984) Porphyrin localization: a new modality for detection and therapy of tumors. Biochm. Pharmacol. 33:1389-93

17. Kessel, D. (ed) (1985) Methods in porphyrin photosensitization. New York: plenum

18. Jori, G and Perria, CA (eds) (1985) Photodynamic therapy of tumors and other diseases. Padova:Edizioni Libreria Progetto

19. Wilson, BC and Jeeves, WP (1987) Photodynamic therapy of cancer. in Photomedicine, Ben-Hur and Rosenthal (eds) CRC

20. Manyak, M.J., Russo, A., Smith, P. and Glastein, E. (1988) Photodynamic therapy. J. Clin. Oncol. 6:380-391

21. Spikes, J.D. (1984) In Porphyrin Location and Treatment of Tumors (Doiron, D.R.,and Gomer, Ch., Eds). Alan R. Liss, Inc., New York, pp.19-39

22. Morgan, A.R. and Selman, S.H. (1988) New photosensitizers for photodynamic therapy of tumors. Drugs of the future. (13)12:1073-1082.

23. Foote, CS. (1984) Mechanisms of photooxydation. in Porphyrin Localization and Treatment of Tumors Dorrion, DR and Gomer, CJ (eds) 301-334 AR Liss, New York

24. Foote, CS (1981) Photooxidation of model biological compounds. In Rodgers MAJ, Powers, EL (eds): "Oxygen and Oxy-Radicals in Chemistry and Biology" New York: Academic Press, p 425.

25. Cortese, DA., Kinsey, JH., Woolner, LB, Payne, WS., Sanderson, DR. and Fontana, RS. (1979) Clinical application of a new endoscopic technique for detection of in situ bronchial carcinoma. Mayo Clin. Proc. 54:635-642

26. Dougherty, TJ. (1982) Photoradiation therapy-clinical and drug advances. In: Kessel, D. and Dougherty, TJ. (eds) Porphyrin Photosensitization, pp 3-13. New York:Plenum Publishing Corp.

27. Dougherty, TJ. (1982) Variability in hematoporphyrin derivative preparations. Cancer Res. 42:1188

28. Dougherty, TJ., Kaufman, LG., Boyle, JH. Weishaupt, KR. and Goldfarb, A. (1979) Photoradiation therapy for the treatment of recurrent breast cancer. JNCI 62:231-237

29. Forbes, IJ., Cowled, PA., Leong, ASY., Ward, AD., Black, RB., Blake, A. and Jacka, FJ. (1980) Phototherapy of human tumors using haematoporphyrin derivative. Med. J. Aust. 2:489-492

30. Kato, H. Tahara, M. Hayashi, N. Limura, I. Matsushima, Y. Saito, T. and Hayata, Y. (1980) Basic studies of diagnosis and treatment of cancer by photoirradiation. Proc. Jpn. Cancer Assoc. 39:312

31. Kessel, D. and Chou, T-H. (1983) Tumor-localizing components of the porphyrin preparation hematoporphyrin derivative. Cancer Res. 43:1994-1999

32. Dorion, DR. and Gomer, CJ. (1984) Introduction, in Dorion, DR and Gomer, CJ. (eds):Porphyrin Localization and Treatment of Tumors. New York, Liss,

33. Dougherty, TJ. (1987) Studies on the structure of porphyrins contained in Photofrin II. Photochem Photobiol. 46:569-573

34. Marcus, SL and Dugan, M. (1992) Global status clinical photodynamic therapy: The registration process for a new therapy. Lasers in Surgery and Medicine. (in press)

35. Pandey, RP., Majchrzycki, DF. Smith, KM. and Dougherty TJ. (1989) Chemistry of photofrin II and some new photosensitizers. SPIE 1065:164-174

36. Evenson, JF., Sommer, C., Rimington, C. and Moan, J. (1987) Photodynamic therapy of C^3H mouse mammary carcinoma with hematoporphyrin di-ethers as sensitizers. Br. J. Cancer 55:483-486

37. Berenbaum, MC., Akande, SL., Bonnett, H. and Winfield, UJ. (1986) Mesotetra(hydroxyphenyl)-porphyrins, a new class of potent tumor photosensitizers with favourable selectivity. Br.J. Cancer 54:717-725

38. Bogel, E. Kocher, M. and Lex, J. (1986) Porphycene-a novel porphin isomer. Angew, Chem. Int. Ed. Engl. 25:257-258

39. Gosmann, M. and Frank, B. (1986) Synthesis of a four fold expanded porphyrin weight an extremely high diamagnetic ring current system. Angew. Chem. Int. Ed. Engl. 25:1100-1101

40. Sessler, JL. Johnson, MR. and Lynch, V. (1987) Synthesis and crystal structure of a novel tripyrrane containing porphyrinogen like macrocycle. J. Org. Chem. 52:4394-4397

41. Reddi, E., Lo Castro, G. and Jori, G. (1986) Preliminary studies on the use of Zn phthalocyanines in photodynamic therapy. Abstract from porphyrin photosensitization workshop, Los Angeles, June 26-27

42. Firey, PS. and Rodgers, MA. (1987) Photoproperties of a silicon naphthalocyanine, a potential photosensitizer for photodynamic therapy. Photochem. Photobiol. 45:587-594

43. Morgan, AR., Garbo, GM., Keck, RW. and Selman, SH. (1988) New photosensitizers for photodynamic therapy, combined effect of metallopurpurin derivatives and light on transplantable bladder tumors. Cancer Res. 48:194-198

44. Morgan, AR., Rampersaud, A., Keck, RW. and Delman, SH. (1987) Verdins: new photosensitizers for photodynamic therapy. Photochem. Photobiol. 46:441-446

45. Grigg, R., Johnson, AW. and Sweeney, A. (1968) J. Chem. Soc. Chem. Commun. 697

46. Morgan, AR., Pangka, VS. and Dolphin D. (1984) Ready syntheses of benzoporphyrins via Diels-Alder reaction with protoporphyrin IX. J. Chem. Soc. Chem. Commun. 1047-1048

47. Kinello, PK. and Dolphin, D. (1980) Reactions of protoporphyrin with tetracyanoethylene. J. Org. Chem. 45:5196-5204

48. Kessel, D. and Dutton, CJ. (1984) Photodynamic effects; porphyrins vs chlorins. Photochem Photobiol. 40:403-405

49. Roberts, WG., Shiau, FY., Nelson, JS., Smith, KM. and Berns, MW. (1988) in vitro characterization of monoaspartyl chlorin-e6 and diaspartyl chlorin-e6 for photodynamic therapy. JNCI 80:330-336

50. Beems, EM., Bubbelman, TMAR, Lugtenburg, J., Best, JAV., Smeets, MFMA and Bodgheim, JPJ. (1987) Photosensitizing properties of bacteriochlorophyllin-a and bacteriochlorin-a. Photochem. Photobiol. 46:639-643

51. Foley, JW., Cincotta, L. and Cincotta, AH. (1987) Structure and properties of novel benzo[a]phenoxazinium photochemotherapeutic agents. SPIE New directions in photodynamic therapy. 847:90-95

52. Richter, AM., Kelly, B., Chow, J. & 4 others. (1987) Preliminary studies on more effective photoxic agent than hematoporphyrin. JNCI 79:1327-1332

53. Richter, A.M., Sternberg,E., Waterfield, E., Dolphin, D. and Levy, J.G. (1988) Characterization of benzoporphyrin derivative, a new photosensitizer. Proc.SPIE 997:132-138

54. Richter, AM., Cerruti-Sola, S. Sterngerg, ED, Dolphin, D. and Levy, JG. (1990) Biodistribution of tritiated benzoporphyrin derivative, a new potent photosensitizer, in normal and tumor-bearing mice. J. Photochem. Photobiol. B5:231-234

55. Richter, AM., Waterfield, E., Jain, AK. Allison, B., Sternberg, ED, Dolphin, D. and Levy, JG. (1991) Photosensitising potency of structural analogues of benzoporphyrin derivative in a mouse tumor model. Br. J. Cancer 63:87-93

56. Gomer, CJ., Bucker, N., Ferrario, A., Wong, S. (1989) Properties and Application of Photodynamic Therapy. Radiation Research 120:1-18

57. Spikes, JD. (1989) Photosensitization. in:The science of photobiology (2nd ed) by Smith, KC. (ed) Plenum Publishing Co.

58. Schenck, GO. Bechker, H-D. and Krauch, CH. (1963) Mit Benzpphenon photosensibilisierte autoxidation von sek. Alkoholen und Aethern. Darstellung von Hydreoperoxyden. Chem. Ber. 96:509

59. Gomer, CJ., Rucher, N. Ferrario, A. and Wong, A. (1989) Properties and Aplications of photodynamic therapy. Radia. Res. 120:1-18

60. Spike, JD (1981) The sensitized photooxidation of biomolecules. In Rogers MAJ and Powers EL (eds): "Oxygen and Oxy-Radicals in Chemistry and Biology", New York: Academic Press, p 421.

61. Wilson, BC., and Patterson, MS. (1986) The physics of photodynamic therapy. Phys. Med. Biol. 31:327-360

62. Wilson, BC. and Jeeves, WP. (1987) Photodynamic therapy of cancer. In:Photomedicine (E. Ben-Hur and Rosenthal, eds) Vol II, pp 127-177 CRC Press, Boca Raton, Fl

63. Fuller, TA. (1983) Fundamentals of lasers in surgery and medicine, in Dixon, JA (ed): Surgical application of lasers. Chicago, Yearbook, 11-28

64. Coulter, A. (1990) The Status of Photodynamic therapy research: an overview of current and future cancer clinical treatments. J. Clin. Laser Med. Surg. August:2-11

65. Manyak, M. (1990) Photodynamic therapy: present concepts and future applications. Cancer J. Vol 3, 2:104-109

66. Shumaker., BP., Lutz, MD., Haas, GP. et al. (1986) Practical clinical use of laser photodynamic therapy in the treatment of bladder carcinoma in situ. Lasers Medi. Sci. 1:257-261

67. Nseyo, UO., Whalen, RK., Duncan, MR., et al. (1989) Urinary cytokines following photodynamic therapy for bladder cancer. Laser Res Med Dent Surg (in Press)

68. Kato, H. Konaka, D., Kawate, N. (1986) Five-year disease-free survival for lung cancer patient treated only by photodynamic therapy. Chest 90:768-770

69. Mew, D. Wat, CK., Towers, GHN. and Levy, JG. (1983) Photoimmunotherapy:treatment of animal tumors with tumor-specific monoclonal antibody-hematoporphyrin conjugates. J. Immunol. 130:1473-1477

70. Mew, D., Lum, V., Wat, CK., Touwers, GHN. Sun, CH., Walter, RJ., Wright, M.W., Berns, MW. and Levy, JG. (1985) Ability of specific monoclonal antibodies and conventional antisera conjugated to hematoporphyrin to label and kill selected cell lines subsequent to light activation. Cancer Res. 45:4380-4386

71. Oseroff, A.R., Wimberly, J., Lee, C., Alvarez, V. and Parrish, J.A. (1985) J. Invest. Dermatol. 84:335 (Abstr)

72. Oseroff, AR., Ohuoha, D., Hasan, T., Bommer, JC. and Yarmush, ML. (1986) Antibody-targeted photolysis:selective photodestruction of human T-cell leukemia cells using monoclonal antibody chlorin e6 conjugates. Proc Natl Acad Sci USA 83:8744-8748

73. Sreele, KJ., Liu, D., Stammers, AT., Whitney, S., Levy, JG. (1988) Suppressor deletion therapy:selective elimination of T suppressor cells in vivo using a hematoporphyrin conjugated monoclonal antibody permits animals to reject syngeneic tuomr cells. Cancer Immunol Immunother. 26: 125-131

74. Hasan, T., Lin, A., Yarmush, S., Oseroff, AR. and Yarmush, M. (1989) Monoclonal antibody-chromophore conjugates as selective phototoxins. J Controlled Release 10:107-117

75. Hasan, T. Lin, CW. and Lin, A. (1989) Laser-induced selective cytotoxicity using monoclonal antibody-chromophore conjugates. Pro. Clin. Bio. Res. 288:471-477

76. Hasan, T., Chen, N., Anderson, T., Deak, MR., Kinden, K., Gransterin, R., Zurawski, VR. and Fotte, T. (1989) Immunologic targeting of cancer cells. Fundamentals of photodynamic therapy. Proc. SPIE (1065)11:80-86

77. Radestraw, SL., Tompkins, RG., Yarmush, ML. (1990) Antibody-targeted photolysis:in vitro studies with Sn(IV) chlorin e6 covalently bound to monoclonal antibodies using a modified dextran carrier. Proc. Natl. Acad. Sci. USA 87:4217-4221

78. Rakestraw, S., Tompkins, RG. and Yarmush, ML. (1990) Preparation and characterization of immunoconjugates for antibody-targeted photolysis. Bioconjugate Chem. 1:212-221

79. Hasan, T. (1990) Targeting of cancer cells with molecular delivery systems. Proc SPIE 1203:136-143

80. Jiang, FN, Jiang, S., Liu, D., Richter, A. and Levy, JG. (1990) Development of technology for linin g photosensitizers to a model monoclonal antibody. J. Immunol. Methods 134:139-149

81. Jiang, FN, Liu, D., Neyndorff, H., Chester, M., Jiang, S. and Levy, JG. (1991) Photodynamic killing of human squamous cell carcinoma cells using a monoclonal antibody-photosensitizer conjugate. JNCI (83)17:1218-1225

82. Jiang, FN, Allison, B., Liu, D. and Levy, JG. (1991) Enhanced photodynamic killing of target cells by either monoclonal antibody or low density lipoprotein medicated delivery systems. J Controlled Release (in press)

83. Jiang, FN, Richter, AM., Jain, A., Smits, C and Levy, JG. (1991) Biodistribution of a benzoporphyrin derivative-monoclonal antibody conjugate in A549 tumor bearing nude mice. J. Immunol. submitted

84. Goff, B., Bamberg, M. and Hasan. T. (1991) Photoimmunotherapy of human ovarian carcinoma cells ex vivo. Cancer Res. 51:4762-4807

85. Hasan, T. (1991) Photosensitizer delivery mediated by macromelecular carrier systems. in Dougherty, TJ. and Henderson, B. (eds) Photodynamic therapy:basic principles and clinical applications. Marcel Dekker, inc. New York

86. Ehrlich, P. (1906) Collected studies on immunity. New York John Wiley and Sons.

87. Kohler, G. and Milstein, C. (1975) Continuous cultures of fused cells secreting antibody of predefined specificity. Nature (London) 256:495-497

88. Vitetta, E.S., Fulton, R.J., May, R.D., Till, M. and Uhr, J.W. (1987) Redesigning nature's poisons to create anti-tumor reagents. Science 238:1098-1104

89. Waldmann, T.A. (1991) Monoclonal antibodies in diagnosis and therapy. Science 252:1657-1662

90. Pastan, I., Willingham, M.C. and FitzGerald, D.J.P. (1986) Immunotoxins. Cell. 47:641-648

91. Pietersz, G. (1990) The linkage of cytotoxic drugs to monoclonal antibodies for the treatment of cancer. Bioconj. Chem. 2:89-95

92. Steele, K.J., Liu, D., Davis, N., Deal, H. and Levy, J.G. (1989) The preparation and application of porphyrin-monoclonal antibodies for cancer therapy. SPIE 1065:73-79

93. Allison, B., Richter, A., Jiang, F., Jiang, S., Liu, D. and Levy, J.G. (1990) Approaches to improved delivery of photosensitizers. Proc. SPIE in press.

94. Hasan, T. (1988) Selective phototoxicity using monoclonal antibody-chromophore conjugates. SPIE 997:42-47

95. Devanathan, S., Dahl, T.A., Midden, W.R. and Neckers, D.C. (1990) Readily available fluroscein isothiocyanate-conjugated antibodies can be easily converted into targeted phototoxic agents for antibacterial, antiviral, and anticancer therapy. Proc. Natl. Acad. Sci. USA 87:2980-2984

96. Hasan, T. (1990) Targeting of cancer cells with molecular delivery systems. Proc. SPIE 1203:136-143

97. Pelegrin, A., Folli, S., Buchegger, F., Mach, J., Wagnieres, G. and van den Bergh, H. (1991) Antibody-fluorescein conjugates for photoimmunodiagnosis of human colon carcinoma in nude mice. Cancer 67:2529-2537

98. Dawson, J.W., J. Morgan, J. Barr, B.R. Davidson, A.J. MacRobert, F. Savage, C. Dean, and P.B. Boulos. (1991) Targeted photosensitisation of colorectal and ovarian cancers: enhanced tumor selectivity and cytotoxicity of a new antibody-photosensitizer conjugate. Photochem Photobiol 53 suppl:25s Abstr.

99. Sands, H. (1990) Experimental studies of radioimmunodetection of cancer: An overview. Cancer Res (suppl) 50:820s-827s

100. Sehon, A.H. (1982) Suppression of IgE antibodies with conjugates of haptens or allergens and synthetic hydrophillic polymers. Ann. N.Y. Acad. Sci. 392:45-70a

101. Pangka, V.S., Morgan, A.R. and Dolphin, D. (1986) Diels-Alder reactions of protoporphyrin XI dimethyl ester with electron-deficient alkynes. J. Org. Chem. 51:1094-1100

102. Ngo, T.T. (1986) Facile activation of sepharose hydroxyl groups by 2-fluoro-1methylpyridinium toluene-4-sulfonate: preparation of affinity and covalent chromatographic matrices. Biotechnology,4 Feb.

103. Mosmann, T. (1983) Rapid colorimetric assay for cellular growth and survival:application to proliferation and cytotoxicity. J. Immunol. Methods 65:55-63

104. Richter, A.M., Waterfield, E., Jain, A.K., Sternberg, E.D., Dolphin, D. and Levy, J.G. (1990) in vitro evaluation of phototoxic properties of four structurally related bengoporphrin derivatives. Photochem. Photobiol. 52:495-500.

105. Peppas, N.A. and Stauffer, S.R. (1991) Reinforced uncrosslinked poly(vinyl alcohol) gels produced by cyclic freezing-thawing process: a short review. J. Controlled Release 16:305-310

106. DiLuccio, R.C., Hussain, M.A., CoffinBeach, D., Torosian, G. Shefter, E. and Hurwitz, A.R. (1989) Polyvinyl alcohol-Methyl acrylate copolymers as a sustained-release oral delivery system. Pharmaceutical Res. 10:844-847

107. Davis, N., Liu, D., Richter, A., Jain, A., Jiang, S., Jiang, F.N. and Levy, J.G. (1992) Modified polyvinyl alcohol-benzoporphyrin derivative as phototoxic agents. J. Photochem. Photobiol. submitted

108. Oakley, B.R., Kirsch, D.R. and Morris, N.R. (1980) A simplified sensitive silver stain for detecting proteins in polyacrylamide gels. Anal. Biochem. 105:361-363

109. Lowry, O.H., Rosebrough, N.J., Farr, A.L. and Randall, R.J. (1951) Protein measurement with the Folin phenol reagent. J.Biol.Chem. 193:265-275

110. Saji, S., Zylstra, S., Scheapt, B.S., Ghosh, S.K., Jou, Y.H., Takita, H., and Bankert, R.B. (1989) Monoclonal antibodies specific for two different histological types of human lung carcinoma. Hybridoma 3:119-129.

111. Zylstra, S., Chen, F.A., Ghosh, S.K., Repasky, E.A., Rao, U., Takita, H. and Bankert, R.B. (1986) Membrane-associated glycoprotein (gp160) identified on human lung tumors by a monoclonal antibody. Cancer Res. 46:6446-6451.

112. Yokota, S., Mayhew, E., Chen, F-A and Bankert, R.B. Immunospecific targeting of drug containing liposomes to a murine B-cell line and human lung tumor. Sixth International Congress on Immunology, Abstracts, 1986; 4.23.37, p. 551. Ottawa, Canada, National Research Council Canada.

113. Chen, F.A., Repasky, E.A., Takita, H., Schepart, B.S. and Bankert, R.B. (1989) Cell surface glycoprotein associated with human lung tumors that is similar to but distinct from epidermal growth factor receptor. Cancer Res. 49:3642

114. Chen, F.A., Repasky, E.A. and Bankert, R.B. (1991) Human lung tumor-associated antigen identified as an extracellular matrix adhesion molecule. J.Exp. Med.

115. Richter, A., Cerruti-Sola, S., Sternberg, E., Dolphin, D., and Levy, J.G. Biodistribution of tritiated benzoporphyrin derivative, a new potent photosensitizer in normal and tumor bearing mice. J. Photochem. Photobiol. 5:231-244.

116. Yutaka, K. Counting acrylamide gel slices. LSC Application Notes #1-30:24.

117. Glassy, M.C., and Surh, C.D. (1988) Immunodetection of cell-bound antigens using both mouse and human monoclonal antibodies. J. Immunol. Methods. 81:115-122

118. Zar, J.H. (ed) (1984) In: Biostatistical analysis. Prentice-Hall Inc. Englewood Cliffs, NJ

119. Hayslett, H.T. (ed) (1972) In: Statistics made simple. W.H.Allen and Co. Ltd. London, England

120. Allison, B., Pritchard, P.H., Richter, A.M. and Levy, J.G. (1990) The plasma distribution of benzoporphyrin derivative and the effects of plasma lipoproteins on its biodistribution. Photochem. Photobiol. 52:501-507.

121. Shen, G.L., Li, J.L., Ghetie, V., May, R.D., Till, M., Brown, A.N., Relf, M., Knowles, P., Uhr, M.W., Janossy, G., Vitetta, E.S., and Thorpe, P.E. 1988 Evaluation of four CD 22 antibodies as ricin A chain-containing immunotoxins for the in vivo therapy of human B-cell leukemias an lymphomas. Int. J. Cancer 42:792-797

122. Olsens, S., and Sandvig, K. 1988 Hoe protein toxins enter and kill cells. In:A.E. Frankel (ed). Immunotoxins, pp. 39-73. Dordrecht, kluwer Academic Publishers.

123. Sandvig, K., and Olsnes, S. (1982) Entry of the toxic proteins abrin, modeccin ricin and diphtheria toxin into cells. II. Effect of pH metabolic inhibitors and ionophores and evidence for toxin penetration form endocytotic vesicles. J.Biol. Chem. 257:7504-7513

124. Olsens, S., Sandvig, K., Petersen, O.W. and Van Deurs, B. (1988) Immunotoxinsentry into cells and mechanisms of action. Immunol. Today 110:291-295

125. Preijers, F.W.M.B. Tax W.J.M. (1988) Relationship between internalization and cytotoxicity of ricin A-chain immunotoxins. Br. J. Haematology 70:289-294

126. Lindig, B.A. and rodgers, M.A.J. (1981) Rate parameter for the quenching of singlet oxygen by water soluble and lipid soluble substrates in aqueous and micellar systems. Photochem. Photobiol. 33:716-720

127. Oseroff, A.R. Ara, G., Ohuoha, D., Aprille, J., Bommer, J.C., Yarmush, M.L. and Cincotta, L. (1987) Strategies for selective cancer photochemotherapy: antibody-targeted and selective carcinoma cell photolysis. Photochem. Photobiol. 46:83-96

128. Beisegel, U., Schnieider, W.J., goldstein, J.L., Anderson, R.G., Brown, M.S. (1981) Monoclonal antibodies to the low density lipoprotein receptors as probes for study of receptor-mediated endocytosis and the genetics of family hypercholesterolmia. J. Biological Chemistry. (256)22:11923-11931

129. Goldberg, EP (ed) (1983) Target Drugs. Vol. 2. Wiley and Sons, New York

130. Peters, K and Richards, FM. (1977) Chemical cross-linking: Reagents and problems in studies of membrane structure. Annu. Rev. Biochem. 46:523-551

131. Timkorich, R. (1977) Polymerization side reactions during protein modification with carbodiimide. Biochem. Biophys. Res. Commun. 74:1463-1468

132. Kanellos, J., Pietersz, GA., and Mckenzie, IFC. (1985) Studies of methotrexate-monoclonal antibody conjugates for immunotherapy. JNCI 75:319-332

133. Ghose, T., Blair, AH, Kralovec, J., Uadia, PO. and Mammen, M. (1988) Synthesis and testing of antibody-antifolate conjugates for drug targeting. In: Targeted Diagnosis and Therapy (Rodwell, JD., ed.) Vol.1. pp 88-122, Marcell Dekker, New York

134. Kato, Y., Umemoto, N., Kayama, Y., Fukushima, H., Takeda, Y., Hara, T. and Tsukada, Y. (1984) A novel method of conjugation of daunomycin with antibody with a poly-L-glutamic acid derivative as intermediate drug carrier. An anti-a-fetoprotein antibody-daunomycin conjugate. J. Med. Chem. 27:1602-1607

135. Hope, M.J., Bally, M.B., Mayer, L.D., Janoff., AS. and Cullis, PR. (1986) Chem. Phys. Lipids 40:127-144

136. Struthers, JE and Newman, EL. (1990) Aconjugate between haematoporphyrin and EGF as a potential tumor-targetted photosensitizer. Third Biennial Meeting of the International Photodynamic Association, Buffalo, N.Y. Abstr.,p.9

137. Bachor, R., Shea, C., Gillies and Hasan, T. (1991) Photosensitized destruction of human bladder carcinoma cells treated with chlorin e_6-conjugated microspheres. Proc. Natl. Acad. Sci. USA 88:1580-1584